Title
Interactions of diasteriomeric tripeptides of Lys-5-fluoro-Trp-Lys with native and apurinic DNA

Author
Shine, Nancy R.

Publication Date
1984

Peer reviewed|Thesis/dissertation

INTERACTIONS OF DIASTERIOMERIC TRIPEPTIDES OF LYS-5-FLUORO-TRP-LYS WITH NATIVE AND APURINIC DNA

by

NANCY R. SHINE

DISSERTATION

Submitted in partial satisfaction of the requirements for the degree of

DOCTOR OF PHILOSOPHY

in

PHARMACEUTICAL CHEMISTRY

in the

GRADUATE DIVISION

of the

UNIVERSITY OF CALIFORNIA

San Francisco

[redacted]

Date University Librarian

Degree Conferred: . . . . . .

ABSTRACT

The nucleic acid binding properties of the fluorine-labeled diasteriomeric tripeptides, lysyl-5-fluoro-*l*-tryptophyl-lysine and lysyl-5-fluoro-*d*-tryptophyl-lysine, are investigated using ^{19}F NMR, fluorescence spectroscopy, and thermal denaturation.

The ^{19}F NMR studies of these model peptides demonstrate that each forms a distinct complex with double-stranded DNA. The ^{19}F chemical shift and relaxation measurements indicate that the aromatic indole ring of the tripeptide Lys-*l*-Trp-Lys is involved in a stacking interaction when bound to double-stranded DNA. The data are consistent with the idea that the tryptophyl ring is not intercalated in the classical sense, but partially inserted between the bases of one strand of the double helix. Changing the chirality of the aromatic residue modifies the mode of binding. Although Lys-*d*-Trp-Lys participates in the same number of electrostatic bonds (two) and exhibits the same affinity for double-stranded DNA, the *d*-Trp peptide-DNA complex is easily discriminated by ^{19}F NMR. The *d*-Trp indole ring does not appear to associate with the DNA bases.

These studies are extended to include the complexes formed with DNA modified to contain apurinic sites. When 5% of the purine bases are removed from native DNA, differences in the ^{19}F NMR chemical shift and linewidth measurements suggest that both peptides, Lys-*l*-Trp-Lys and Lys-*d*-Trp-Lys, form complexes with depurinated DNA which are distinct from those formed with native DNA. In addition, comparison of the fluorine chemical shift for the depurinated complexes indicate that the fluorine nuclei of the two diasteriomers reside in different local environ-

ments. The differential linebroadening demonstrates that the motional properties of these peptides within or between their binding sites on apurinic DNA are also significantly different. Both diasteriomeric tripeptides promote cleavage of plasmid DNA containing apurinic sites. No measurable difference in the rate at which nicks are introduced is observed. These results indicate that neither the precise positioning of the tryptophyl indole ring nor significant changes in its mobility are crucial to the nicking activity.

Thomas L. James

ACKNOWLEDGEMENTS

I would like to thank my advisor, Tom James, for his support and encouragement during the course of my thesis work. I also wish to thank Richard Shafer for many helpful discussions and suggestions and his continued interest during these investigations. I would like to express my gratitude to Martin Shetlar for his advice and assistance and for making his instrumentation available to me. The work of Vladimir Basus in patiently keeping the XL-100 spectrometer in operating condition was most deeply appreciated. I would like to thank Alain Delbarre for his critical review of the proposed project and valuable suggestions, assistance and encouragement during the course of this work. I also wish to express my appreciation to Kenway Hoey from whom I learned peptide synthesis, Elisha Berman for helpful discussions concerning the chromatography, Michelle Broido for help with the 2-D studies of the tripeptide, Micheal Moseley and Greg Young for additional aid with the XL-100, Ed Bubienko for helpful discussions and especially for performing the gel electrophoresis of the plasmid DNA, Max Keniry for careful review of and advice concerning parts of this manuscript, Linda Shoer for help with a number of the illustrations in this thesis, and Peter Desmeules for graciously supplying the Versatec on which the final copy of this thesis was printed. I also wish to thank Jim Stoner for valuable technical advice and for generously allowing the use of his laboratory equipment as well as for his patience and support during the course of these studies. The encouragement and support of Linda Shoer and Steven Johnson were deeply appreciated.

This work was supported in part by NIH Training Grant GM 07175.

CONTENTS

CHAPTER I

INTRODUCTION

INTRODUCTION

Over the past decade, considerable attention has been focused on the selective associations between specific proteins and nucleic acids (1,review). These protein-nucleic acid complexes play an essential role in a number of fundamental cellular processes such as the replication, transcription and repair of DNA, the translation of messenger RNA, and regulation of gene expression. These proteins may recognize a nucleic acid structure or a distinctive sequence of bases.

In order to identify the molecular mechanisms by which proteins discriminate preferred binding sites, a detailed knowledge of the precise functional groups of both macromolecules involved in direct interactions, is required. The types of interactions that may be responsible for complex formation include: electrostatic interactions, hydrogen bonding, stacking and hydrophobic interactions. For example, the amino acids containing positively charged side chains, such as lysine, arginine, and histidine, are easily accomodated on the surface of a protein, due to their hydrophilic nature; consequently, ion pairs can be formed with the negatively charged phosphates of the DNA backbone. A number of amino acids including glutamine, asparagine, and arginine, as well as the amide group of the peptide bond, possess hydrogen bond donor and acceptor groups capable of interacting with corresponding groups on the nucleic acid bases, sugars, and phosphates. The planar aromatic amino acids, tryptophan, tyrosine, and phenylalanine, can contribute to complex formation by stacking between the nucleic acid bases. The aliphatic amino acid side chains can participate in protein-nucleic acid associations by hydrophobic interactions with the bases.

In order to characterize the types of interactions that contribute to complex formation as well as to provide evidence for the particular amino acids involved in the binding to DNA, small oligopeptides have been used as model systems (2,review). A number of physicochemical investigations have focused on the binding of the tripeptide, lysyl-tryptophyl-lysine (fig. 1) to various polynucleotides (3-15). This tripeptide has three positive charges, one on the α-amino group of the N-terminal residue, and one on each of the ε-amino groups of the lysine side chains. These positive charges can form ion pairs with the negatively charged phosphates of the polynucleotides. These electrostatic interactions increase the affinity of this tripeptide for polynucleotides thus allowing study of interactions of the aromatic amino acid, tryptophan, with nucleic acids. Of particular interest is whether the aromatic amino acids of proteins can contribute to the stability of protein-nucleic acid complexes by stacking between the bases.

In the presence of various polynucleotides, changes in the fluorescence (3-13) and the ^{1}H NMR (13,14) of the tripeptide-tryptophan as well as the circular dichroism (5,6,7,15) and ^{1}H NMR (13,14) of the polynucleotides are observed. These changes can be reversed by the addition of salt (4,13,14) indicating that the binding of the tripeptide to polynucleotides is very sensitive to the ionic strength of the medium. This provides direct evidence for the contribution of electrostatic interactions to complex formation. For each Lys-Trp-Lys molecule, the number of ion pairs formed for the complex with single-stranded poly(rA) has been calculated to be 3 as determined by the method of Record (16). The magnitude of change observed by all these methods (fluorescence, ^{1}H NMR, and CD) is decreased by the neutralization of the N-terminal amino group of the

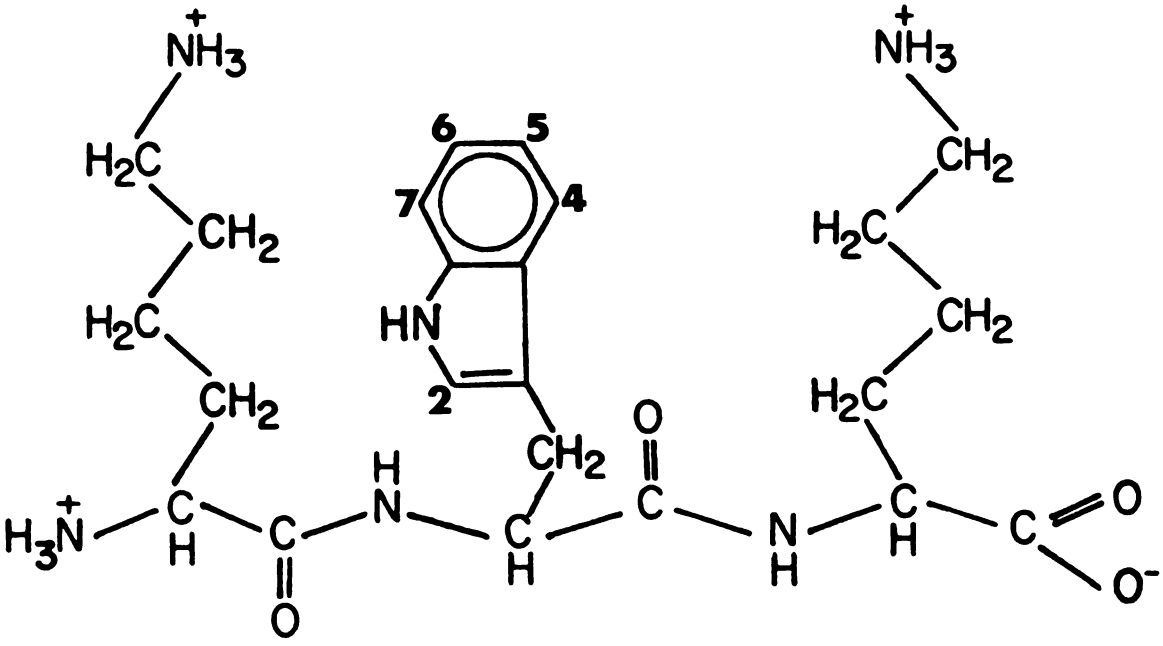

fig. 1: Structure of the tripeptide lysyl-tryptophyl-lysine.

peptide, indicating that this group is responsible for one of the electrostatic interactions.

In addition to electrostatic interactions, there is also evidence that the indole ring participates in stacking interactions with the nucleic acid bases. First, in the proton NMR study of the complexes with native DNA and single-stranded poly(rA) (14), an upfield shift of both the tryptophan indole and $CH_2(\beta)$ proton resonances was observed. The direction of the shifts is consistent with that expected from the ring current effects that would be experienced by the tryptophan if it were in close proximity to the bases. Although there is no high resolution spectrum for the DNA in this study, for poly(rA), the H_8, H_2, and H_1, protons are affected as expected for the stacking of adenine with the aromatic tryptophan ring. Second, a phosphorescence study (17) done with Lys-Trp-Lys - poly(rA) complex (77°K) showed a very efficient energy transfer at the triplet level from the polynucleotide bases to the tryptophan residue. Energy transfer between the stacked bases of poly(A) alone is very efficient at the triplet level. If a tryptophan is inserted between the bases it could act as an energy trap. It was found that the tryptophan trapped the excitation energy of approximately 60 adenine bases. This triplet energy transfer occurs by an electron exchange mechanism where a good orbital overlap of donor and acceptor electron clouds is necessary. Third, electric dichroism studies (9), again of the poly(rA) complex, indicate that the tryptophan residue is preferentially oriented in the plane of the adenine bases, suggesting stacking. Fourth, the intrinsic fluorescence of the indole ring is quenched in the presence of various polynucleotides (18). That stacking leads to quenching of tryptophan fluorescence has been shown in fluorescence studies of frozen aqueous mixtures of tryptophan

and various nucleosides (19). The quenching of both compounds and the appearance of a new fluorescence emission band at a longer wavelength is consistent with the formation of charge transfer complexes. The indole ring can serve as electron donor and the bases as acceptors. The quantum yield of the complex is reduced and would not be observed at room temperature. Several other mechanisms for quenching of the indole ring are possible. For example, hydrogen bonding of the indole NH group to various acceptor sites on the nucleotides could lead to a decrease in the fluorescence emission due to ring deprotonation in the excited state. Also energy transfer between the purine and pyrimidine bases and the tryptophan would result in a quenching of the observed fluorescence. However, recent studies have concluded that these are unlikely interpretations (20,21).

Fluorescence decay studies have shown that the fluorescence lifetime of the tripeptide Lys-Trp-Lys does not change significantly upon binding to nucleic acids even though the fluorescence intensity is markedly reduced in the bound state (4,11,12). On the basis of these data, a two-step model (fig. 2) for the binding to both single-stranded and double-stranded polynucleotides has been proposed. According to this model, the first association involves only the electrostatic interaction of the basic amino acid residues with the backbone phosphates. This complex has the same fluorescence characteristics as the free peptide. The second process includes a direct stacking between the tryptophan and nucleic acid bases. Here the fluorescence is presumed to be totally quenched. Analysis of the fluorescence data assuming two complexes leads to values for the binding parameters that are in good agreement with those determined from CD measurements (5,6,7,15). Also, it has been shown that for native DNA and

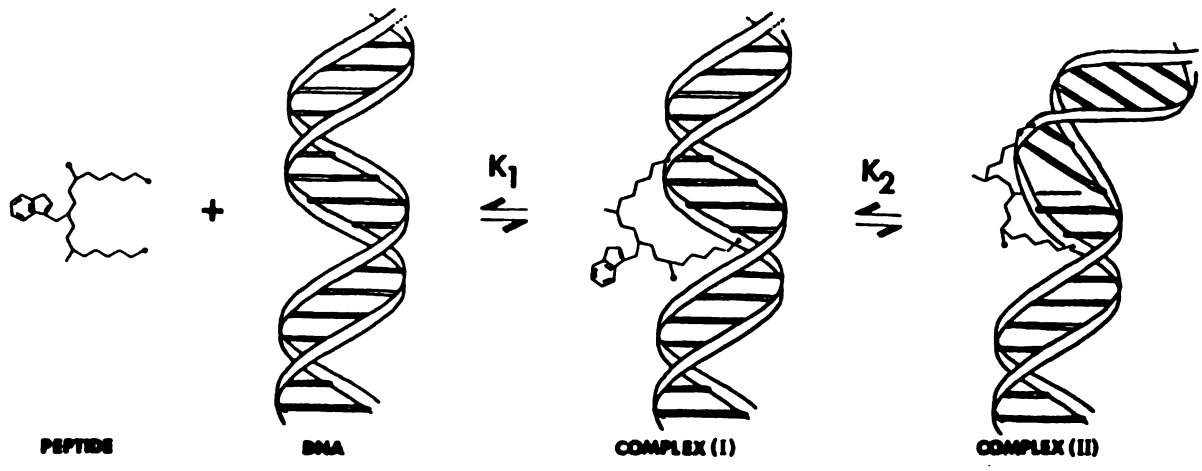

fig. 2: Schematic drawing illustrating the two-step model proposed by Helene (2) for the binding of Lys-*l*-Trp-Lys to DNA. Both complexes (I) and (II) involve electrostatic interactions. Complex (II) includes an additional stacking interaction between the aromatic tryptophyl ring and the nucleic acid bases. According to this model, a bending of the DNA helix is induced by stacking.

poly(rA), K_1 values, which reflect the electrostatic contribution, decrease as the ionic strength increases, while K_2 is unaffected. This is consistent with the behavior predicted by the two-step model. This sequential two-step mechanism is also supported by kinetic experiments (9,10). The complexes formed with poly(rA) (9) and DNA (10) were studied using the electric field jump method. Two separate relaxation processes were distinguished using fluorescence detection. The relaxation time constants are consistent with a mechanism involving a fast diffusion-controlled bimolecular step followed by a slow intramolecular transition. For the complex with poly(rA), the slow step has a forward rate (1.5×10^5 sec^{-1}) which is less than that for the formation of base stacks in the polymer alone (4.6×10^6 sec^{-1}). Since the insertion of the tryptophan would not be expected to be faster than the rearrangement of the adenine bases, the observed kinetics are consistent with the idea that the slow step entails a stacking interaction between tryptophan and adenine. For the complex with DNA, the forward rate of the second process is faster for short (500 base pair) DNA (8.3×10^4 sec^{-1}) than for the longer (30,000 base pair) DNA (6.4×10^3 sec^{-1}). One explanation offered by the authors is that this step is again due to an insertion of the tryptophan ring and that the rate of insertion is associated with the degree of flexibility of the helix.

That the stacked complex may involve a kinking of the DNA helix has been proposed previously for oligopeptides containing aromatic amino acids (22,23,24,25). This "partial insertion" model suggests that the aromatic amino acid is stacked between two consecutive bases on the same DNA strand and that the insertion of the aromatic residue would result in a slight bending of the helix (see fig. 2). This model differs from

that found for the classical intercalators which involves the unstacking of two base pairs with concommitant unwinding of the DNA helix (28). The "partial insertion" model is consistent with viscosity data available for the DNA complexes formed by several oligopeptides containing aromatic amino acids (22,23,24,25). Whereas there is a dramatic increase in viscosity when intercalation occurs attributed to the increase in length of the helix (26,27,28), a substantial decrease in viscosity is found with these peptides bound to DNA. This can be explained if stacking of the aromatic amino acid requires a bend or kink in the helix thus decreasing the overall length of the molecule.

The binding parameters for a number of different tripeptide polynucleotide complexes have been obtained using fluorescence titrations (3-7). Analysis of the quenching data according to the two-step model discussed above (see fig. 2) gives a value for K_2, which represents the ratio of stacked to unstacked complexes. When the K_2 values are compared, it appears that stacking is favored in single-stranded nucleic acids. This observation lead to subsequent binding studies to examine the ability of the tripeptide to probe for single-stranded regions in several modified DNA's. The peptide was found to bind more strongly to double-stranded DNA which had been altered by UV irradiation (3,5) or by 2-(N-acetoxyacetylamino)fluorene (29). Both of these modifications create locally destabilized regions. As a result of these findings it has been proposed that proteins, in particular those involved in repair of damaged DNA, may use their aromatic amino acids to locate and/or anchor the protein at the damaged sight. The preferential stacking to single-stranded structures could provide the specificity of recognition necessary.

Removal of damaged purines and pyrimidines by enzymes known collectively as N-glycosylases is known to occur in vivo and is the first step in the excision repair of certain forms of damaged DNA. The apurinic or apyrimidinic site is then recognized by a specific endonuclease (Ap endonucleases) which subsequently cleaves at this site (31,review). Recently, the binding of Lys-Trp-Lys to DNA containing apurinic sites has been investigated (30). For this model peptide, a K_2 value of approximately 200 was estimated assuming that each apurinic site provided only one strong binding site. This is a dramatic increase over that found for native DNA (K_2 = 0.3) and suggests that this tripeptide can also discriminate between native and apurinic sites in double stranded DNA. The size of the cavity left by removal of a purine should easily accomodate the indole ring. The tryptophan may simply substitute for the missing base.

Besides the strong binding of Lys-Trp-Lys to DNA containing apurinic sites, further experimentation showed that this tripeptide also induces cleavage of the phosphate backbone (32,33,34). When apurinic sites were introduced into either plasmid pBR322 (32) or phage PM2 DNA (33,34), conversion of the supercoiled form to the relaxed form upon incubation with this tripeptide provided evidence for the nicking activity. Thus this simple tripeptide not only appears to locate apurinic sites as is done by the apurinic endonucleases but also mimics the catalytic activity of these repair enzymes.

That amines, lysine in particular, are capable of promoting cleavage of apurinic DNA is well documented (35). This suggests that the the ε-amino or the N-terminal amino group of this tripeptide may be responsible for chain breakage. There is also evidence suggesting that in the case of this tripeptide the aromatic residue may play an important role. First,

when the ability of the tripeptide to facilitate cleavage is compared to that of lysine alone under the same conditions, no nicking activity is observed for lysine at concentrations 2000-fold greater than that of the tripeptide (34). Second, for similar tripeptides where the aromatic residue has been substituted by either alanine, glycine, or lysine, a significant reduction in nicking activity is observed (33,34). Lys-Tyr-Lys, however, has the same activity as the tryptophan tripeptide. Third, it has been reported that the tetrapeptides, Lys-Gly-Trp-Lys and Lys-Trp-Gly-Lys are less active in the cleavage of apurinic DNA, suggesting that the sequence of the tripeptide placing the tryptophan between two lysines is important (32). From these data, it has been proposed that the tryptophan of Lys-Trp-Lys binds at the apurinic site and positions the lysyl amino group(s) in close proximity to the reactive group at the apurinic site (33).

Further details on the mechanism of strand breakage by this peptide have been investigated. At a depurinated site in DNA, the furanose form of the ribosyl moiety is in equilibrium with its free aldehyde form (fig. 3) (36,37). As proposed for the cross-linking of histones to apurinic DNA (38), these aldehyde groups may react with the lysyl amino groups of the peptide to produce a Schiff base. If the phosphodiester bond cleavage occurs by β-elimination, as in alkaline solution (35), it would be catalyzed by this Schiff base. Alternately, β-elimination could also be catalyzed by lysine proton abstraction at the C-2 position, i.e., the position α to the aldehyde. For Lys-Trp-Lys, it appears that the nicking of the DNA backbone does involve β-elimination (34,39). Reduction of the aldehyde by sodium borohydride prior to incubation with the peptide prevented subsequent cleavage by this peptide (see fig. 3) (39). Also, examination of the termini created by chain breakage supports β-elimination as the predominant

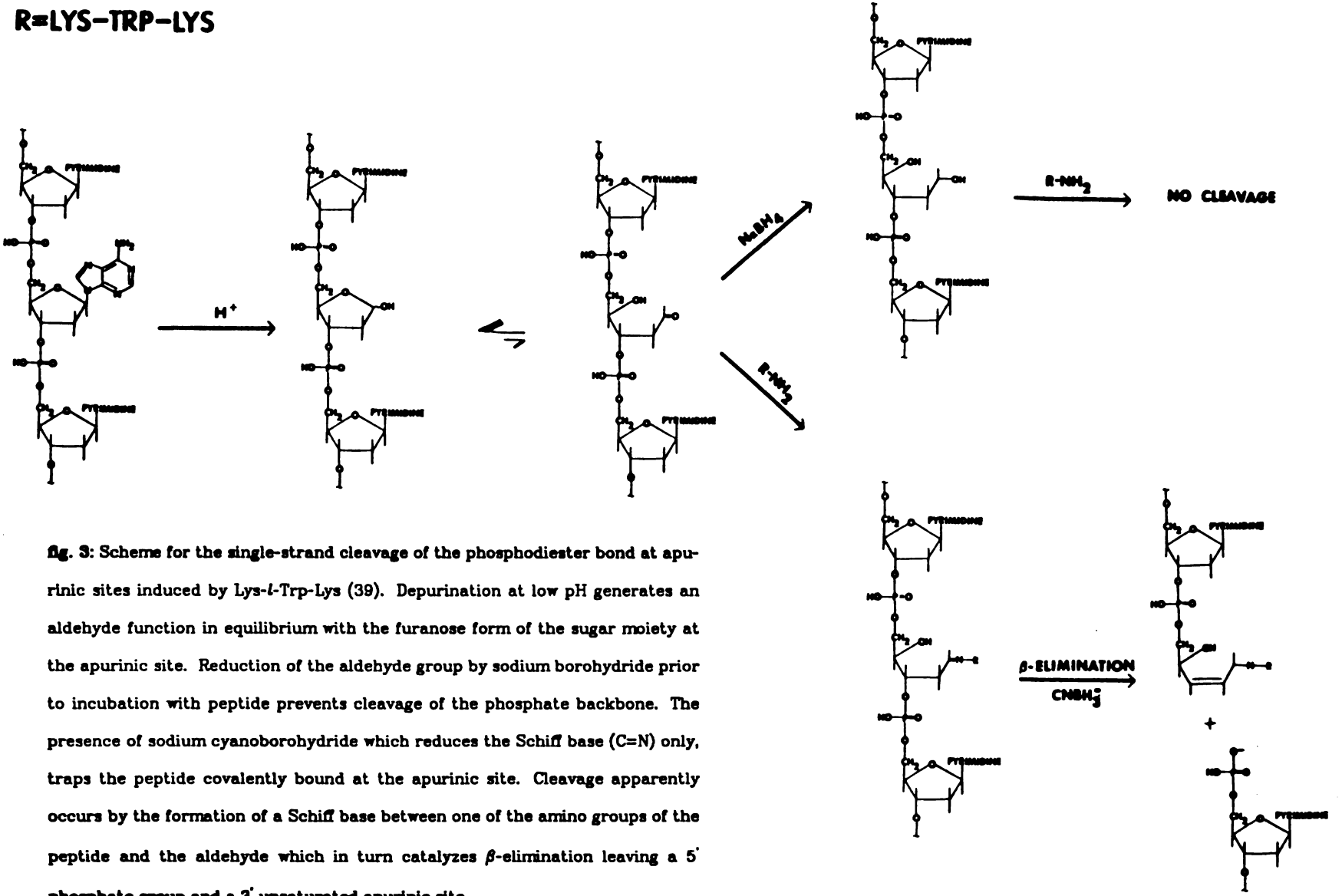

fig. 3: Scheme for the single-strand cleavage of the phosphodiester bond at apurinic sites induced by Lys-*l*-Trp-Lys (39). Depurination at low pH generates an aldehyde function in equilibrium with the furanose form of the sugar moiety at the apurinic site. Reduction of the aldehyde group by sodium borohydride prior to incubation with peptide prevents cleavage of the phosphate backbone. The presence of sodium cyanoborohydride which reduces the Schiff base (C=N) only, traps the peptide covalently bound at the apurinic site. Cleavage apparently occurs by the formation of a Schiff base between one of the amino groups of the peptide and the aldehyde which in turn catalyzes β-elimination leaving a 5' phosphate group and a 3' unsaturated apurinic site.

mechanism (34). A 5'-phosphoryl nucleotide on the 3' side of the apurinic sugar residue, as found with alkaline hydrolysis, is expected (fig. 4). For tripeptide-nicked DNA molecules, less than 10% of the termini could be directly phosphorylated with polynucleotide kinase using γ-^{32}P ATP. Thus the 5' termini have phosphate residues; conversion to substrate by treatment with alkaline phosphatase and subsequent incorporation of ^{32}P-labelled termini confirmed this result. The 3' terminus was not examined in this study. It should be noted that cleavage on the 5' side of the apurinic site also generates a 5'-phosphoryl group. However, there is evidence that polynucleotide kinase will not label this base-free deoxyribose phosphate after phosphatase treatment (40).

It also appears that for this tripeptide, the cleavage mechanism may involve Schiff base formation (39). When cyanoborohydride is present during incubation of the DNA with tripeptide, some of the peptide is recovered covalently bound to the DNA (see fig. 3). Cyanoborohydride will reduce only the C=N bond. Isolation of a covalently bound peptide suggests that a Schiff base between one of the amino groups of the peptide and an aldehyde group of the DNA was reduced. As noted above, the tripeptide where tyrosine has been substituted for tryptophan, is as active in the cleavage of apurinic sites. However, when the N-terminal of the tyrosine peptide is acetylated, the activity is significantly reduced (41). This result suggests that the N-terminal amino group may be involved in complex formation or cleavage.

Of the several AP endonucleases that have been isolated and characterized, several create termini consistent with that found for Lys-Trp-Lys. These repair endonucleases have been divided into two classes based on the site at which nicking occurs (fig. 4) (42). For Class I endonucleases

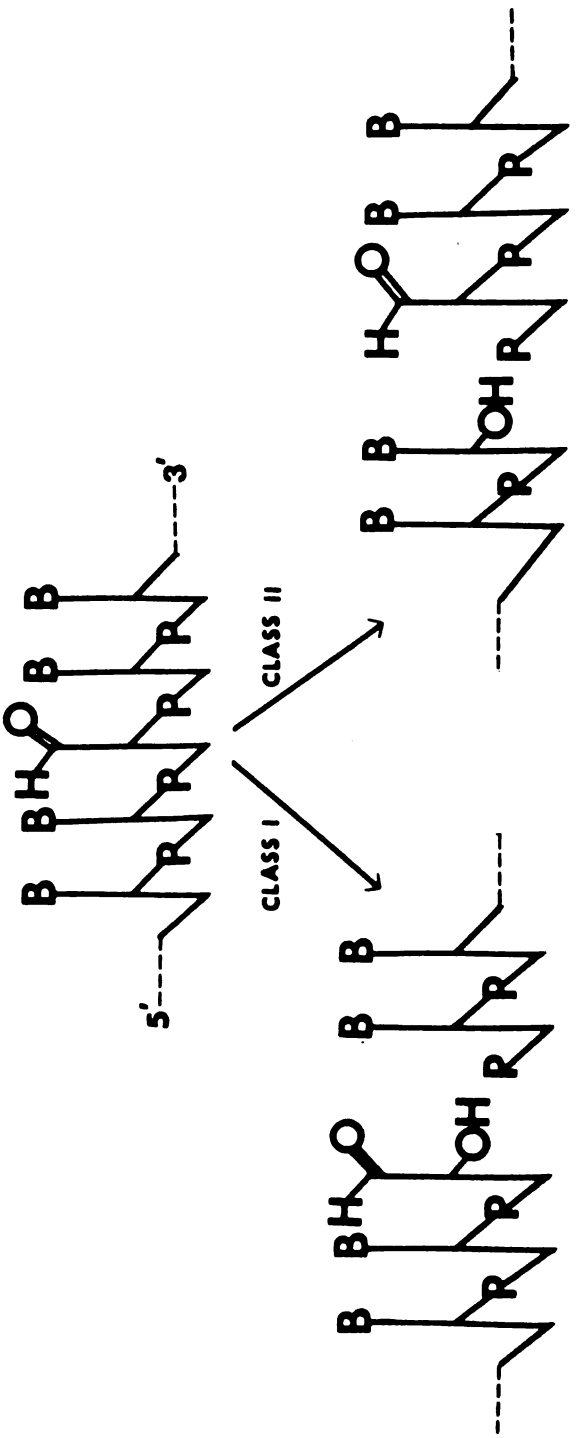

fig. 4: The mechanistic classes of Ap endonucleases (42).

incision occurs at the 3' side of the apurinic sugar and leaves a 5'-phosphoryl nucleotide. Hydrolysis of the phosphodiester bond at this point has been found for E.coli endonuclease III, the Ap endonuclease associated with T4 UV endonuclease, and human fibroblast Ap endonuclease I. Class II enzymes produce a 3'-hydroxyl nucleotide and 5' termini containing a 5'-phosphoryl deoxyribose. Human placental Ap endonuclease, E. coli endonuclease IV and VI, and human fibroblast AP endonuclease II belong to this class. The tripeptide degrades partially depurinated DNA as found for the Class I endonucleases. This tripeptide could serve as a good model for the study of this cleavage mechanism at apurinic sites.

The binding of diasteriomeric peptides containing aromatic amino acids to DNA has also been studied (24,25). Gabbay et al. have examined the complex formed with DNA by the dipeptide Lys-*l*-Phe(NH_2) and compared it to that formed by its diasteriomer, Lys-*d*-Phe(NH_2). These two peptides have different effects on the DNA structure upon binding. The decrease in both the relative specific viscosity and relative reduced dichroism of DNA solutions induced by both peptides is more pronounced for the complex with the *l*-Phe peptide. In addition, the flow dichroism effects observed for the *d*-Phe peptide are not significantly different than those observed for 1,5-diaminopentane; the latter compound was used as an analog of lysine alone. The ^1H NMR data also indicate that distinct complexes are formed. The protons of the *l*-Phe ring show two broad resonances which are shifted upfield from the single resonance observed for the free peptide. Only slight changes in chemical shift and line broadening are observed for the *d*-Phe peptide complex. The data are consistent with the idea that for the *l*-Phe-containing peptide, the

aromatic ring is partially inserted between the bases. This is not observed for the *d*-Phe peptide. Previous studies (23) by this same group indicated that the modified aromatic amino acids, *d*-Phe-amide and *l*-Phe-amide, did not exhibit different behaviours with respect to DNA binding. These data then form the basis for the proposal that the positive groups on the lysine residue of the dipeptides are stereospecifically bound to the DNA (fig. 5), thus dictating the direction that the aromatic ring would point; either in towards the helix or out away from the helix axis (25).

It is reasonable to assume that the diasteriomer of Lys-*l*-Trp-Lys may also form a distinct complex with DNA, in particular that the aromatic ring may point in the opposite direction. Since the molecules are the same except for the chirality of the tryptophan moiety, comparison of the data should help define their respective DNA complexes more precisely. Also, if the tryptophan ring plays an important role in the cleavage of apurinic DNA, significant differences with the *d*-Trp-containing peptide should be observed.

In summary, the published data for Lys-Trp-Lys strongly suggest that the tryptophan moiety can stack with nucleic acid bases in native DNA and, in the complex with apurinic DNA, can substitute for the missing purine base. Of the various techniques that have been employed for the study of this model system, ^{1}H NMR has provided the most direct evidence for stacking interactions. Upfield shifts of the aromatic proton resonances suggests an interaction of the aromatic ring of the amino acid with the DNA bases. However, as with all model systems, these results may not extrapolate to real biological systems and the interpretation of proton NMR studies of larger protein-DNA systems can be limited due to the overlap of peaks in the area of interest, difficulties in peak assignments,

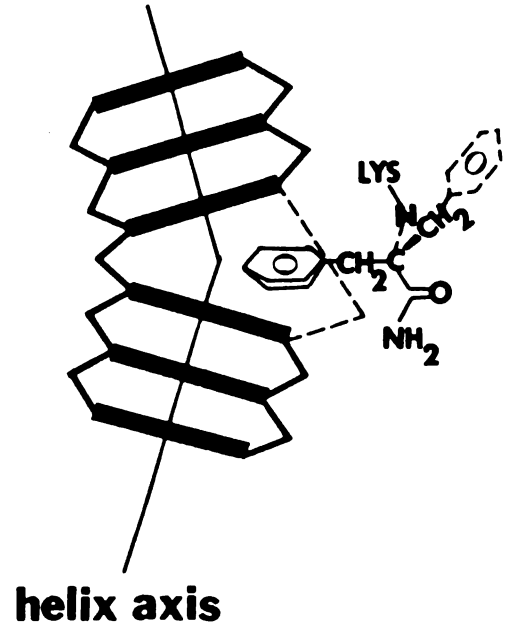

fig. 5: Schematic illustration of a segment of the DNA helix depicting the partial insertion of the aromatic ring of Lys-*l*-Phe-amide as proposed by Gabbay et. al. (25). Stereospecific binding of the charged groups would position the *d*-Phe ring to point away from the helix axis as shown (dashed ring).

and substantial increases in the linewidth on complex formation.

An alternative method is to use specifically-labelled amino acids. Fluorine-labelled amino acids have been successfully incorporated into bacterial proteins (43,44). Subsequently these labelled proteins have been studied in the presence of various polynucleotides (45-50). These studies have allowed the identification of specific residues involved in interactions with the polynucleotides on the basis of changes in the ^{19}F NMR chemical shift and/or relaxation parameters. However, the precise type of interaction, for example stacking of the aromatic amino acid, can not be identified because changes observed in ^{19}F NMR have not been characterized to correlate precisely with environmental changes of the fluorine nucleus as is the case of proton NMR.

In the present study, we have used ^{19}F NMR to investigate both diasteriomers of lysyl-5-fluorotryptophyl-lysine, one containing *l*-tryptophan and the other *d*-tryptophan, when complexed to native and apurinic DNA. The ^{19}F NMR studies allow us to specifically monitor the fluorine-labelled aromatic indole ring of the tryptophan residue. Noncovalent interactions between the tryptophan and DNA can be examined without interferring peaks due to the solvent or the macromolecule. The fluorine chemical shift is highly sensitive to changes in the environment of the fluorine nucleus. In addition, the fluorine relaxation parameters can be used to compare the relative mobilities of the tryptophan ring in the two diasteriomers. As far as the interactions with DNA are concerned, the fluorine has a Van der Waals radius similar to that of hydrogen so it is not expected that the interactions with DNA will be effected by the fluorine label. Also, fluorine has 83% the sensitivity of proton NMR.

Analysis of the ^{19}F NMR of these complexes can be applied to more complicated systems. The present study provides further information on the correlation between changes observed in the ^{19}F NMR parameters and the environment of fluorine-labelled amino acids.

The synthesis of the tripeptides, preparation of the DNA's, and the methods employed to study the peptide-nucleic acid complexes are described in Chapter II. The results of the ^{19}F NMR studies for these model peptides (Lys-*l*-Trp-Lys and Lys-*d*-Trp-Lys) when complexed to native DNA are presented and discussed in Chapter III. Fluorescence and thermal denaturation studies were used to complement and aid in the interpretation of the ^{19}F NMR data. These studies were then extended to include the complexes formed with DNA modified to contain apurinic sites. The ability of both of these tripeptides to cleave DNA at apurinic sites was also examined. The studies of the apurinic DNA complexes are presented in Chapter IV.

References

1. **Helene, C. and Lancelot, G.,** Interactions between Functional Groups in Protein-Nucleic Acid Associations, *Progr. Biophys. molec. Biol.*, *39*, 1-68, (1982).

2. **Helene, C. and Maurizot, J. C.,** Interactions of Oligopeptides with Nucleic Acids, *CRC Critical Rev. Biochem.*, *10*, 213-258, (1981).

3. **Toulme, J. J., Charlier, M. and Helene, C.,** Specific Recognition of Single-Stranded Regions in Untraviolet-irradiated and Heat-denatured DNA by Tryptophan-containing Peptides, *Proc. Nat. Acad. Sci. USA*, *71*, 3185-3188, (1974).

4. **Durand, M., Maurizot, J. C., Borazan, H. N. and Helene, C.,** Interactions of Aromatic Residues of Proteins with Nucleic Acids. Fluorescence Studies of the Binding of Oligopeptides Containing Tryptophan and Tyrosine Residues to Polynucleotides, *Biochemistry*, *14*, 563-570, (1975).

5. **Toulme, J. J. and Helene, C.,** Specific Recognition of Single-Stranded Nucleic Acids. Interaction of Tryptophan-containing Peptides with Native, Denatured and Ultraviolet-irradiated DNA, *J. Biol. Chem.*, *252*, 244-249, (1977).

6. **Maurizot, J. C., Boubault, G. and Helene, C.,** Interaction between the Peptide Lysyl-Tryptophanyl-Lysine and Copolynucleotides of Adenine and Uracil: Selectivity of Interaction, *FEBS Lett.*, *88*, 33-40, (1978).

7. **Maurizot, J. C., Boubault, G. and Helene, C.,** Interaction of Aromatic Residues of Proteins with Nucleic Acids. Binding of Oligopeptides to Copolynucleotides of Adenine and Cytosine, *Biochemistry*, *17*, 2096-2101, (1978).

8. **Helene, C., Toulme, J. J. and Le Doan, T.,** A Spectroscopic Probe of Stacking Interactions between Nucleic Acid Bases and Tryptophan Residues of Proteins, *Nucl. Acids Res.*, *7*, 1945-1953, (1979).

9. **Porschke, D.,** Structure and Dynamics of a Tryptophane Peptide-Polynucleotide Complex, *Nucl. Acids Res.*, *8*, 1591-1612, (1980).

10. **Porschke, D. and Ronnenberg, J.,** The Reaction of Aromatic Peptides with Double Helical DNA. Quantitative Characterization of a Two Step Reaction Scheme, *Biophys. Chem.*, *13*, 283-290, (1981).

11. **Montenay-Garestier, T., Brochon, J. C. and Helene, C.,** Complex Formation between Tryptophan-Containing Peptides and Nucleic Acids: Fluorescence Decay Studies using Synchrotron Radiation, *Intern. J. Quant. Chem.*, *20*, 41-48, (1981).

12. **Montenay-Garestier, T., Fidy, J., Brochon, J. C. and Helene, C.,** Dynamics of Peptide-nucleic Acid Complexes. Fluorescence Polarization Studies, *Biochimie*, *63*, 937-940, (1981).

13. **Helene, C. and Dimicoli, J. L.,** Interaction of Oligopeptides containing Aromatic Amino Acids with Nucleic Acids. Fluorescence and Proton Magnetic Resonance Studies, *FEBS Lett.*, *26*, 6-10, (1972).

14. **Dimicoli, J. L. and Helene, C.,** Interactions of Aromatic Residues of Proteins with Nucleic Acids. I. Proton Magnetic Resonance Studies of the Binding of Tryptophan-containing Peptides to Poly(adenylic acid) and Deoxyribonucleic Acid, *Biochemistry*, *13*, 714-723, (1974).

15. **Durand, M., Maurizot, J. C., Borazan, H. N. and Helene, C.,** Interaction of Aromatic Residues of Proteins with Nucleic Acids. Circular Dichroism Studies of the Binding of Oligopeptides to Poly(adenylic acid), *Biochemistry*, *14*, 563-570, (1975).

16. **Record, T. M., Lohman, T. M. and de Haseth, P.,** Ion Effects on Ligand-Nucleic Acid Interactions, *J. Mol. Biol., 107*, 145-158, (1976).

17. **Helene, C.,** Energy Transfer between Nucleic Acid Bases and Tryptophan in Aggregates and in Oligopeptide-Nucleic Acid Complexes, *Photochem. Photobiol., 18*, 255-262, (1973).

18. **Helene, C.,** Mechanisms of Quenching of Aromatic Amino Acid Fluorescence in Protein-Nucleic Acid Complexes, *In Excited States in Organic Chemistry and Biochemistry*, (eds. B. Pullman and N. Goldblum), Reidel Press, 65-78, (1977).

19. **Montenay-Gatestier, T. and Helene, C.,** Reflectance and Luminescence Studies of Molecular Complex Formation between Tryptophan and Nucleic Acid Components in Frozen Aqueous Solutions, *Biochemistry, 10*, 300-306, (1971).

20. **Alev-Behmoaras, T., Toulme, J. J. and Helene, C.,** Effect of Phosphate Ions on the Fluorescence of Tryptophan Derivatives, *Biochimie, 61*, 957-960, (1979).

21. **Montenay-Garestier, T.,** Singlet Energy Transfer between Aromatic Amino Acids and Nucleic Acid Bases. Theoretical Calculations, *Photochem. Photobiol., 22*, 3-6, (1975).

22. **Gabbay, E. J., Sanford, K. and Baxter, C. S.,** Specific Interaction of Peptides with Nucleic Acids, *Biochemistry, 11*, 3429-3435, (1972).

23. **Gabbay, E. J., Sanford, K., Baxter, C. S. and Kapicak, L.,** Specific Interaction of Peptides with Nucleic Acids. Evidence for a "Selective Bookmark" Recognition Hypothesis, *Biochemistry, 12*, 4021-4029, (1973).

24. **Adawadkar, P., Wilson, W. D., Brey, W. and Gabbay, E. J.,** Stereospecific Interaction of Dipeptide Amides with DNA. Evidence for Partial

Intercalation and Bending of the Helix, *J. Am. Chem. Soc.*, *97*, 1959-1961, (1975).

25. **Gabbay, E. J., Adawadkar, P. D. and Wilson, W. D.**, Stereospecific Binding of Diastereomeric Peptides to Salmon Sperm DNA, *Biochemistry*, *15*, 146-151, (1976).

26. **Drummond, D. S., Pritchard, N. J., Simpson-Gildemeister, V. F. W. and Peacocke, A. R.**, Interaction of Aminoacridines with Deoxyribonucleic Acid: Viscosity of the Complexes, *Biopolymers*, *1*, 971-987, (1966).

27. **Cohen, G. and Eisenberg, H. K.**, Viscosity and Sedimentation Study of Sonicated DNA-Proflavine Complexes, *Biopolymers*, *8*, 45-55, (1969).

28. **Lerman, L. S.**, Structural Considerations in the Interaction of DNA and Acridines, *J. Mol. Biol.*, *3*, 18-30, (1961).

29. **Toulme, F., Helene, C., Fuchs, R. P. P. and Duane, M.**, Binding of a Tryptophan-containing Peptide (Lysyltryptophyllysine) to Deoxyribonucleic Acid Modified by 2-(N-Acetozyacetylamino)fluorene, *Biochemistry*, *19*, 870-875, (1980).

30. **Behmoaras, T., Toulme, J. J. and Helene, C.**, Specific Recognition of Apurinic Sites in DNA by a Tryptophan-containing Peptide, *Proc. Nat. Acad. Sci. USA*, *78*, 926-930, (1981).

31. **Lindahl, T.**, DNA Glycosylases, Endonucleases for Apurinic/Apyrimidinic Sites, and Base Excision-Repair, *Progr. Nucleic Acid Res. molec. Biol.*, *22*, 135-192, (1979).

32. **Behmoaras, T., Toulme, J. J. and Helene, C.**, Reconnaissance it coupure des sites apuriniques dans l'ADN par le tripeptide lysyl-tryptophyl-lysine, *C. R. Acad. Sc. Paris*, *293*, 5-8, (1981).

33. **Behmoaras, T., Toulme, J. J. and Helene, C.,** A Tryptophan-containing Peptide Recognizes and Cleaves DNA at Apurinic Sites, *Nature*, *292*, 858-859, (1981).

34. **Pierre, J. and Laval, J.,** Specific Nicking of DNA at Apurinic Sites by Peptides Containing Aromatic Residues, *J. Biol. Chem.*, *256*, 10217-10220, (1981).

35. **Lindahl, T. and Andersson, A.,** Rate of Chain Breakage at Apurinic Sites in Double-Stranded Deoxyribonucleic Acid, *Biochemistry*, *11*, 3618-3623, (1972).

36. **Tamm, C., Hodes, M. E. and Chargaff, E.,** The Formation of Apurinic Acid from the Deoxyribonucleic Acid of Calf Thymus, *J. Biol. Chem.*, *195*, 49-63, (1952).

37. **Coombs, M. M. and Livingston, D. C.,** Reaction of Apurinic Acid with Aldehyde Reagents, *Biochim. Biophys. Acta*, *174*, 161-173, (1969).

38. **Kochetkov, N. K., Budovsky, E. I., Sverdlov, E. D., Symvkova, N. A., Turchinsky, M. F. and Shibaev, V. N.,** *In Organic Chemistry of Nucleic Acids*, (Plenum, New York), Part B, 512-514, (1972).

39. **Helene, C., Toulme, J. J., Behmoaras, T. and Cazenave, C.,** Mechanisms for the Recognition of Chemically-modified DNA by Peptides and Proteins, *Biochimie*, *64*, 697-705, (1982).

40. **Linsley, W. S., Penhoet, E. E. and Linn, S.,** Human Endonuclease Specific for Apurinic/Apyrimidinic Sites in DNA, *J. Biol. Chem.*, *252*, 1235-1242, (1977).

41. **Helene, C., Toulme, J. J. and Montenay-Garestier, T.,** Recognition of Natural and Chemically-damaged Nucleic Acids by Peptides and Proteins, *In Topics in Nucleic Acid Structure; Part 2*, (ed. S. Neidle), 229-285, (1982).

42. **Mosbaugh, D. W. and Linn, S.**, Further Characterization of Human Fibroblast Apurinic/Apyrimidinic DNA Endonucleases, *J. Biol. Chem.*, *255*, 11743-11752, (1980).

43. **Sykes, B. D. and Weiner, J. H.**, *In Magnetic Resonance in Biology*, (ed. J. S. Cohen), Wiley-Interscience, 171-197, (1980).

44. **Gerig, J. T.**, Applications of Fluorine NMR in Biochemistry, *In Biomedical Aspects of Fluorine Chemistry*, 163-189, (1983).

45. **Coleman, J. E. and Armitage, I. M.**, Tyrosyl-Base-Phenylalanyl Intercalation in Gene 5 Protein-DNA Complexes: Proton Nuclear Magnetic Resonance of Selectively Deuterated Gene 5 Protein, *Biochemistry*, *17*, 5038-5045, (1978).

46. **Coleman, J. E., Anderson, R. A., Ratcliffe, R. G. and Armitage, I. M.**, Structure of Gene 5 Protein-Oligodeoxynucleotide Complexes as Determined by ^{1}H, ^{19}F, and ^{31}P Nuclear Magnetic Resonance, *Biochemistry*, *15*, 5419-5430, (1976).

47. **O'Connor, T. P. and Coleman, J. E.**, Phosphorus-31 and Fluorine-19 Nuclear Magnetic Resonance of Gene 5 Protein-Oligonucleotide Complexes, *Biochemistry*, *21*, 848-854, (1982).

48. **Ardnt, K., Nick, H., Boschelli, F. and Lu, Ponzy**, Repressor-Operator Interaction in the *lac* Operon III. Nuclear Magnetic Resonance Observations with Altered Amino-terminal DNA Binding Domains, *J. Mol. Biol.*, *161*, 439-457, (1982).

49. **Boschelli, F., Jarema, M. A. and Lu, P.**, Inducer and Anti-Inducer Interactions with the *lac* Repressor Seen by Nuclear Magnetic Resonance Changes at Tyrosines and Tryptophans, *J. Biol. Chem.*, *256*, 11595-11599, (1981).

50. **Nick, H., Arndt, K., Boschelli, F., Jarema, M.A., Lillis, M., Sommer, H. and Lu, P.,** Repressor-Operator Interaction in the *lac* Operon II. Observations at the Tyrosines and Tryptophans, *J. Mol. Biol.*, *161*, 417-438, (1982).

CHAPTER II

METHODOLOGY

MATERIALS

Tripeptide Synthesis. Synthesis of lysyl-5-fluoro-*dl*-tryptophyl-lysine was performed by the solid phase method (1,2) on Boc-L-Lys(Cl-Z)-O-Resin (Peninsula, Labs., 2113R). The coupling of both Boc-5-fluoro-*dl*-tryptophan (Fluka Chemical Corp., 47570) and subsequently, Boc-Lys(Cl-Z)·TBA (Peninsula, Labs., 2113) was performed by means of their symmetrical anhydrides (3). A schematic presentation of the peptide synthesis is shown in fig. 1.

A. *Preparation of Boc-5-fluoro-dl-tryptophan.* The tertbutyloxycarbonyl (Boc)[1] derivative of 5-fluoro-*dl*-tryptophan was prepared by reaction with BOC-ON (Aldrich, 19,337-2). The amino acid (2.798g, 12.6 mmoles) was reacted with 1.1 equivalents of BOC-ON (3.42g, 13.9 mmoles) and 1.5 equivalents of triethylamine (2.7 mL) in the presence of water/dioxane 1:1 (v/v) for 4 hrs at room temperature. The excess BOC-ON was extracted with ether (2x25 mL) after the addition of 20 mL H_2O. The aqueous phase was cooled in an ice-H_2O bath, acidified to pH 3.0 with 1.0N HCl and the product extracted with ethyl acetate, dried over $MgSO_4$ and subsequently evaporated. The N^{α}-Boc amino acid was crystalized from ethyl acetate at 4°C. On TLC ($CHCl_3$:acetic acid, 15:1) the product gave one spot (ninhydrin and Cl_2 detection) with an R_f value of 0.25. mp = 156 - 158°C.

[1]ABBREVIATIONS: DCC, N,N'-dicyclohexylcarbodiimide; DCU, N,N' dicyclohexylurea; Boc, t-butyloxycarbonyl; CBZ, benzyloxycarbonyl; TFA, trifluoroacetic acid; CMC, carboxymethylcellulose; HPLC, high-pressure liquid chromatography; COSY, 2-dimensional correlated spectroscopy; NOESY, 2-dimensional nuclear Overhauser enhancement spectroscopy; Trp, tryptophan; CT DNA, calf thymus deoxyribonucleic acid; EDTA, ethylene diamine tetraacetic acid; SIS, solvent-induced shift; T1IR, T_1 by inversion-recovery; NOE, nuclear Overhauser effect; TBE, Tris-Borate-EDTA buffer.

fig. 1: Scheme for solid-phase synthesis of lysyl-5-fluoro-*dl*-tryptophyl-lysine. Step numbers refer to those given in Table I.

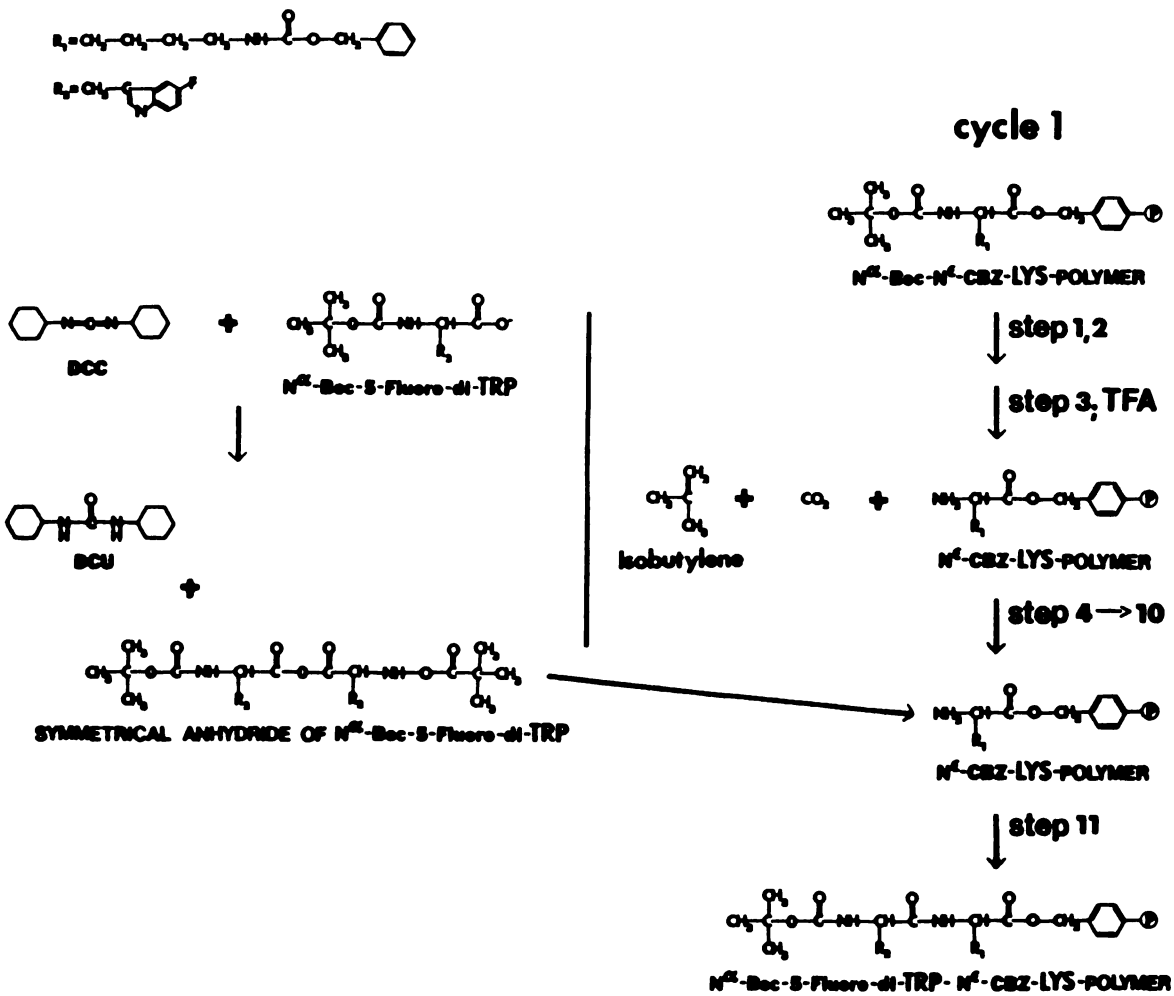

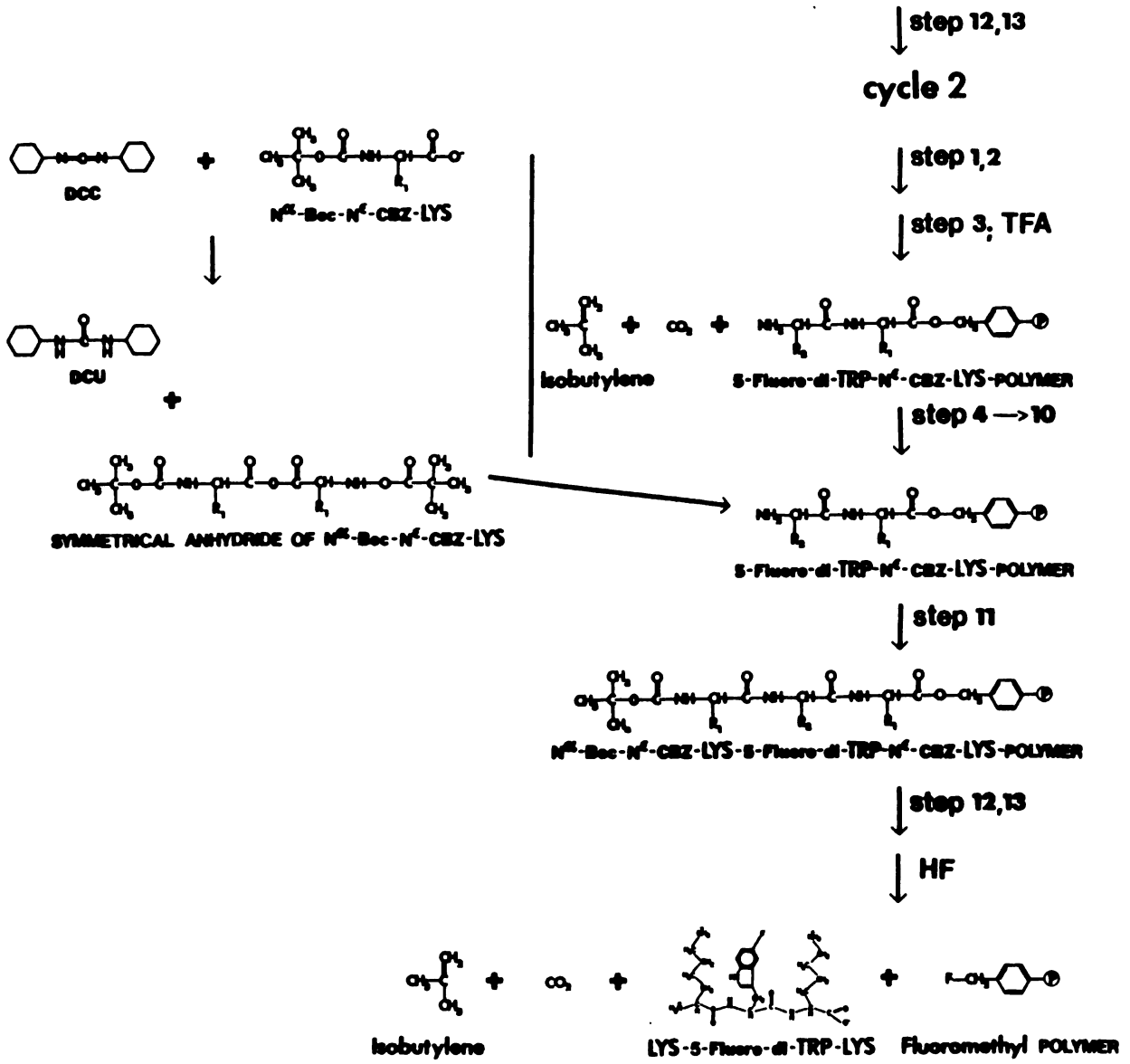
step 12,13
cycle 2
step 1,2
step 3; TFA
DCC
Nα-Boc-Nε-CBZ-LYS
DCU
Isobutylene
5-Fluoro-dl-TRP-Nε-CBZ-LYS-POLYMER
step 4 —>10
SYMMETRICAL ANHYDRIDE OF Nα-Boc-Nε-CBZ-LYS
5-Fluoro-dl-TRP-Nε-CBZ-LYS-POLYMER
step 11
Nα-Boc-Nε-CBZ-LYS-5-Fluoro-dl-TRP-Nε-CBZ-LYS-POLYMER
step 12,13
HF
Isobutylene
LYS-5-Fluoro-dl-TRP-LYS
Fluoromethyl POLYMER

B. *Preparation of the Free Acid of Boc-Lys(Cl-Z)·TBA.* To a chilled (ice-H_2O bath) solution of the protected amino acid (5.56g, 11.4 mmoles) in ethyl acetate (56 mL), 14 mL of 1.0N H_2SO_4 was added. Stirring in the ice-H_2O bath was continued until all material was dissolved. The mixture was then transferred to a separatory funnel and the lower aqueous phase discarded. The upper layer (ethyl acetate) was washed with cold H_2O (2x30 mL) then with 1.0N H_2SO_4 (1x4 mL) followed by additional cold H_2O (5x30 mL). The ethyl acetate layer was then dried over anhydrous $MgSO_4$. On TLC ($CHCl_3$:acetic acid, 15:1) the major spot (ninhydrin and Cl_2 positive) had an R_f of 0.53. The $MgSO_4$ was filtered and the ethyl acetate solution evaporated to an oil which was diluted appropriately for use in the synthesis.

C. *Preparation of the Symmetrical Anhydrides of Boc-5-fluoro-dl-tryptophan and Boc-Lys(Cl-Z)·TBA.* The symmetrical anhydrides of both of the Boc-protected amino acids were prepared immediately prior to their respective coupling reactions. For each Boc-amino acid an excess of 4.2 meq over the amount of resin-bound lysine (0.372 meq/g) was used. Because the tryptophan derivative was highly insoluble in CH_2Cl_2, it was initially dissolved in 10 mL of dimethylformamide to which 10 mL of CH_2Cl_2 was then added. For the Boc-Lysine derivative, an appropriate dilution of the oil (see section B.) was made so that the correct amount was dissolved in a final volume of 20 mL CH_2Cl_2. This solution was cooled to 0°C in an ice-H_2O bath. To form the symmetrical anhydride, 2 meq of N,N-dicyclohexylcarbodiimide (DCC) was added and the solution stirred at 0°C for 15 min. The N,N-dicyclohexylurea (DCU) was removed by filtration and the solution added to the reaction vessel at step 11 (Table I).

D. *Peptide Synthesis*. The schedule for the coupling of the symmetrical anhydrides of the protected tryptophan and lysine derivatives respectively, are given in Table 1. The imbibe of the resin (3.61g, load = 1.34 mmoles lysine) was determined to be approximately 14 mL, so 30 mL washes were used. Solutions expressed as percentages were v/v ratios. After all couplings were complete the protected-peptide resin was washed with 2x30 mL of 95% ethanol, removed from the reaction vessel and dried under reduced pressure over P_2O_5.

Cleavage of the peptide from the resin and removal of the protecting groups was accomplished by stirring the resin (2 g) in the presence of 4.0 mL anisole and 30 mL HF for 1 hr at 0°. 13 mL of 50% cold acetic acid was added to the reaction vessel and 5 washes with 25 mL each of pet ether were done to remove most of the anisole. The solution was then filtered and loaded immediately on a Sephadex G-10 (34 x 2.5 cm) column in 0.5 N acetic acid. The acending fractions of the major peak were pooled and lyophilized.

The crude tripeptide mixture obtained was purified by application to a 51 x 2.5 cm column of carboxymethylcellulose (CMC, Schleicher and Schuell, Inc.) which had been previously equilibrated in 0.01 M ammonium acetate, pH 4.7. The elution was performed using a salt and pH gradient formed by introducing a solution of 0.2 M ammonium acetate, pH 6.7 through a 500 mL stoppered mixing chamber containing the starting buffer. 10 mL fractions were collected at a flow rate of 60 mL per hr. The major absorbance at 280nm appeared to consist of two slightly resolved peaks (fig. 2). Accordingly, the ascending and descending portions were pooled separately and lyophilized.

TABLE I. Schedule for anhydride coupling (one cycle).

Step	Reagent	Amount (mL)	Mixing Time (min)
1	CH_2Cl_2	4 x 30	1
2	55% trifluoroacetic acid/CH_2Cl_2	1 x 30	1
3	55% trifluoroacetic acid/CH_2Cl_2	1 x 30	15
4	CH_2Cl_2	2 x 30	1
5	25% dioxane/CH_2Cl_2	2 x 30	1
6	CH_2Cl_2	2 x 30	1
7	5% diethylamine/CH_2Cl_2	1 x 30	1
8	CH_2Cl_2	2 x 30	1
9	5% diethylamine/CH_2Cl_2	1 x 30	1
10	CH_2Cl_2	4 x 30	1
11	symmetrical anhydride		60
12	CH_2Cl_2	3 x 30	1
13	33% ethanol/CH_2Cl_2	2 x 30	1

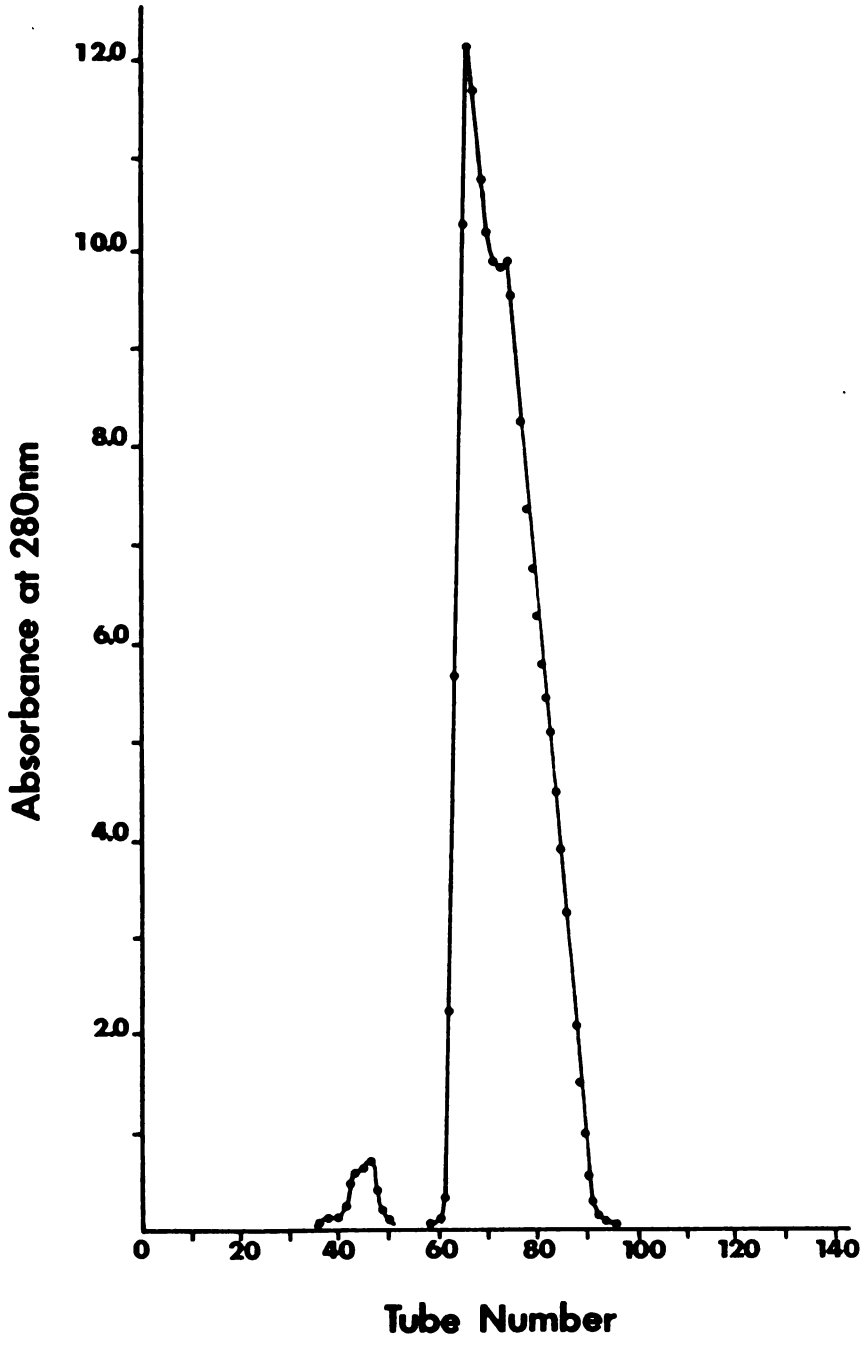

fig. 2: Chromatogram of the crude tripeptide mixture obtained from ion exchange chromatography using CM cellulose. The sample (252 mg) was loaded on a column (53 x 2.5 cm) equilibrated with 0.01 M ammonium acetate, pH 4.75. A gradient with respect to salt and pH was formed by introducing a solution of 0.2 M ammonium acetate, pH 6.7 through a 500 mL mixing chamber containing the starting buffer, immediately after application of the sample. 10 mL fractions were collected at a flow rate of 60 mL/hr. Tube numbers 61 → 70 and 71 → 90 were pooled separately and lyophilized.

Separation of the Diasteriomeric Tripeptides. The fractions obtained from the initial CMC purification were rechromatographed on the same resin. Approximately 20 mg of tripeptide were loaded on a column of 52 x 2.5 cm pre-equilibrated with 0.01 M ammonium acetate, pH 4.75. A shallower salt gradient formed from a solution of 0.1 M ammonium acetate, pH 4.9, introduced into a mixing chamber of 2 L was used for elution. 10 mL-fractions were collected at a flow rate of 60 mL per hr. The elution profile (fig. 3) from the ascending portion of the initial CMC column monitored at 280nm shows two well-separated tryptophan-containing peaks. Peaks A and B were pooled and lyophilized.

Separation of these diasteriomeric tripeptides was also possible by HPLC using a Whatman partisil-10 ODS-3 4.5 x 200 mm column. A Beckman liquid chromatograph (Model 334) equipped with Model 421 CRT microprocessor- controller, Model 110A pump, Model 210 sample injector, and a Gilson variable wavelength detector operating at 280 nm was used. The chromatogram obtained with 2.0% isopropanol in 0.1% TFA run isocratically at 2.0 mL per min is shown in fig. 4. All samples from CMC were subsequently checked for purity on HPLC.

Characterization of the Tripeptides. In order to insure that both peaks contained a tripeptide, the lyophylized material was redissolved in D_2O, pH 7.4, and analyzed using ^1H NMR. The 240 MHz spectra (fig. 5) of both samples contained three α–CH proton resonances which is consistent with the presence of a tripeptide. In addition, peak integration also conformed to that expected for these tripeptides. Comparison of these spectra with those obtained for free lysine, allows the assignment of the upfield multiplets. These resonances arise from the β, γ, and δ protons of the lysine sidechain. For this tripeptide, there are twelve such

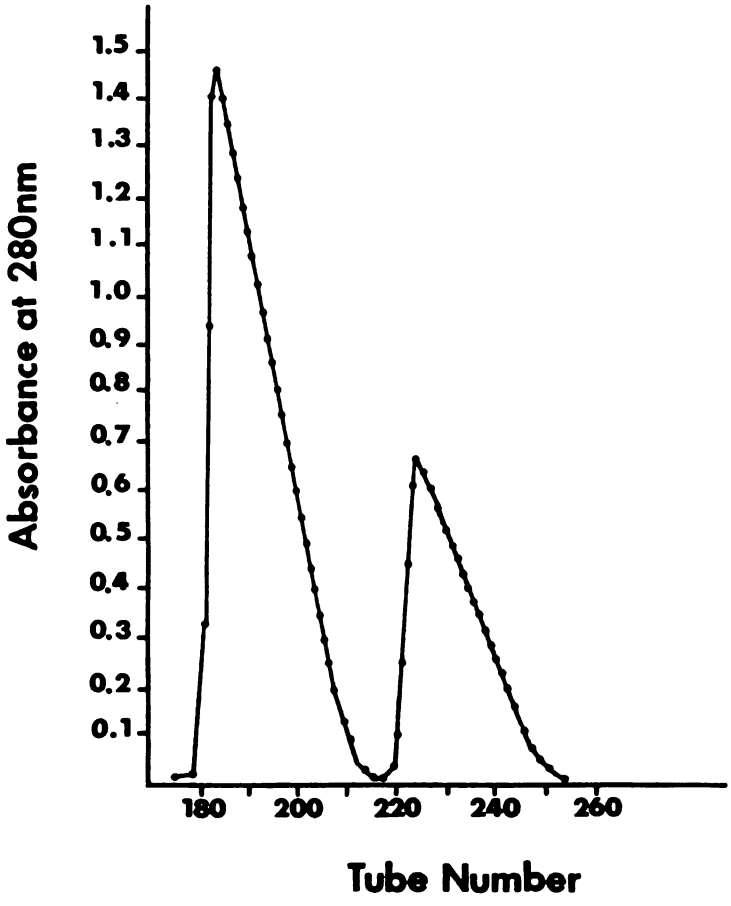

fig. 3: Rechromatography of 20 mg of the ascending portion (tube nos. 61 → 70) obtained from the initial CMC column (fig. 2). The column (52 x 2.5 cm) was equilibrated in the same starting buffer. A shallower salt gradient formed by introducing 0.1 M ammonium acetate, pH 4.75 through a 2 L mixing chamber was used for elution. Fractions (10 mL/tube) were collected at a flow rate of 60 mL/hr.

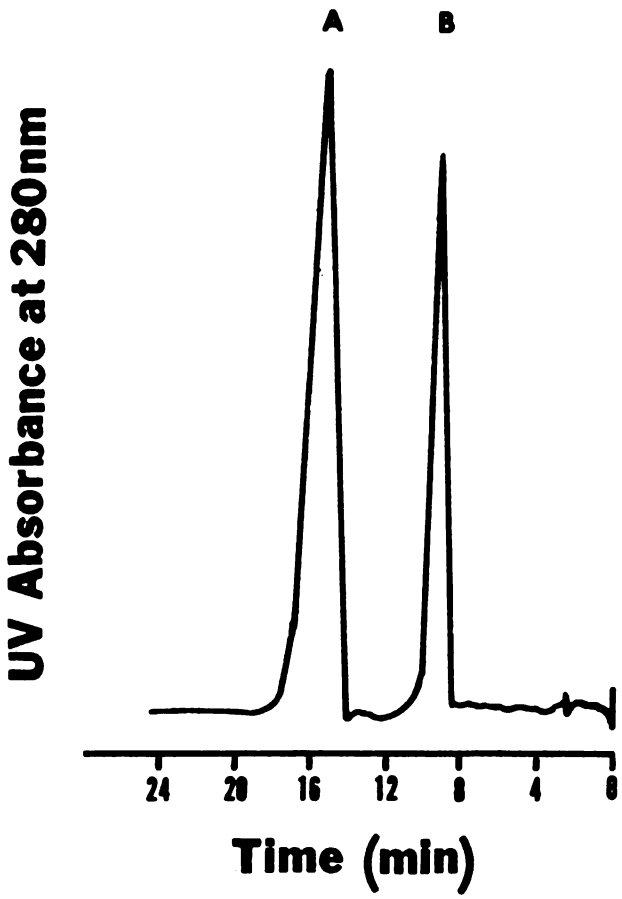

fig. 4: High-pressure liquid chromatographic separation of the tripeptide diasteriomers on a Whatman partisil-10 ODS-3 column by isocratic elution with 2.0% isopropanol in 0.1% TFA. The flow rate was 2.0 mL/min. Retention times were 10 and 14.8 min for CMC-B and CMC-A, respectively.

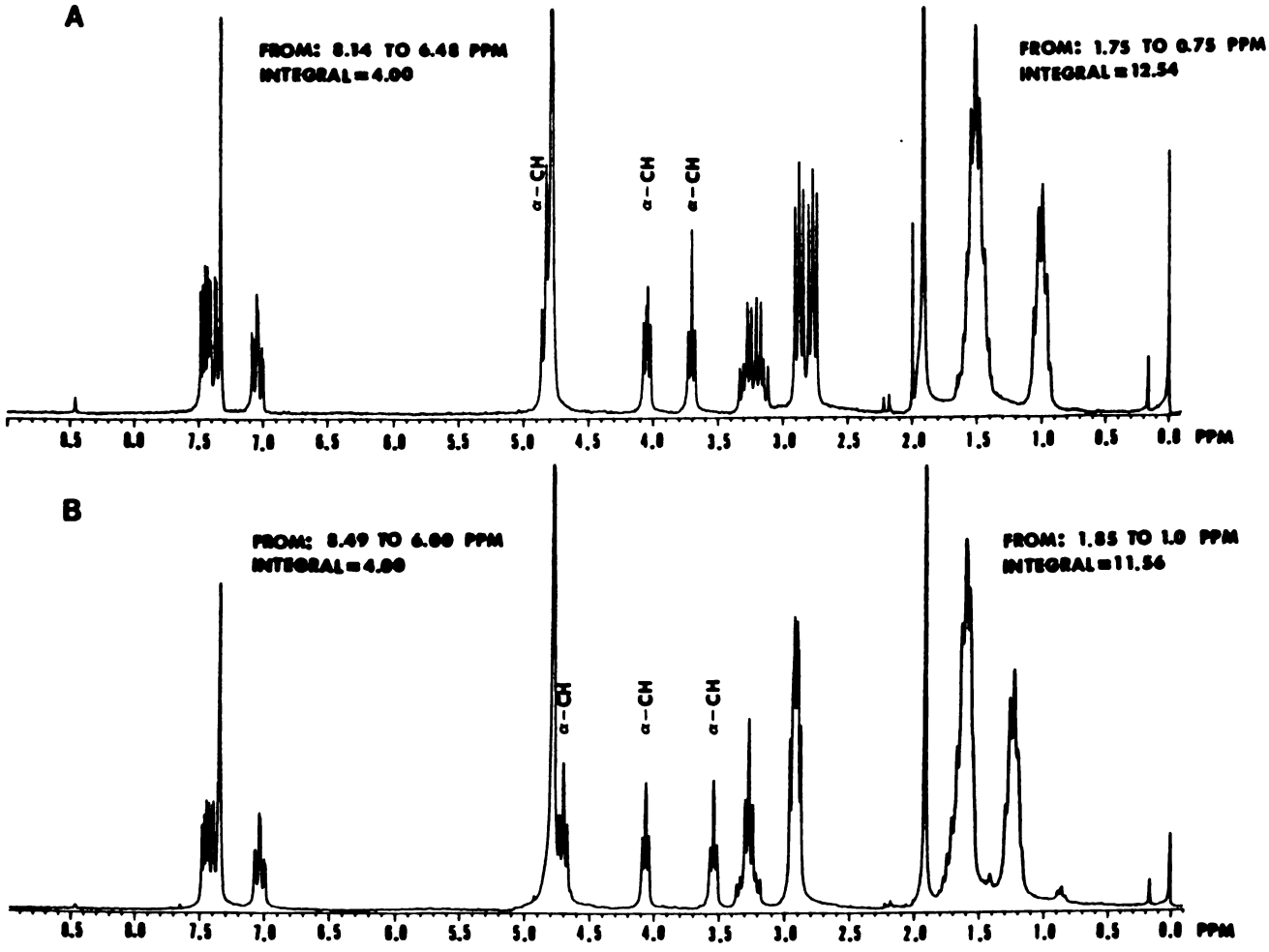

fig. 5: 240 MHz proton spectra of peak A (top) and peak B (bottom) from the CMC column after rechromatography (fig. 3).

sidechain protons; six per lysine. If the integral of the aromatic region is set to four (positions 2, 4, 6, and 7 of the indole ring) then the upfield peaks integrate to approximately twelve, as expected for these tripeptides.

The peaks present in the proton spectra of each of the tripeptides were subsequently assigned (fig. 6) from the results of 2D COSY and NOESY experiments as well as pH titration curves.

The chirality of the tryptophan residue in each tripeptide was determined by subjecting aliquots of both peaks A and B (fig. 3) to an enzymatic digest using α-chymotrypsin. 160 μg of peptide dissolved in 1.0 mL of 0.05 M sodium phosphate buffer, pH 7.3, was incubated with 100 μg of enzyme (Boehringer Mannheim) at 37°C. Four additional aliquots of enzyme (100 μg each) were added over a 43 hr period to insure complete digestion. The resulting digest products were analyzed by thin-layer electrophoresis (fig. 7) on Cellulose Acetate (Kodak) in 0.1 M ammonium bicarbonate, pH 9.2 at 300 V for 1.5 hrs. A single ninhydrin positive spot was observed for the sample originating from peak A. For peak B, a spot comigrating with that of free lysine was observed. Since α-chymotrypsin is expected to cleave only the *l*-Trp-containing peptide on the C-side of the aromatic residue selectively, peak B contains *l*-Trp while peak A contains the *d*-Trp-containing peptide.

Sonicated DNA. Calf thymus (CT) DNA (Sigma) was dissolved (1 mg/mL) in a 0.05 M phosphate buffer, pH 7.0, containing 0.1 M NaCl. The sample was cooled in a methanol-ice water bath and sonicated using a Heat Systems W-225R sonicator with a 10 mm probe at a power level of 5 and a 50% pulse cycle for 1.25 hrs. The sample was filtered through a 0.45 μm Millipore filter and precipitated with 2.5 volumes of 95% ethanol at

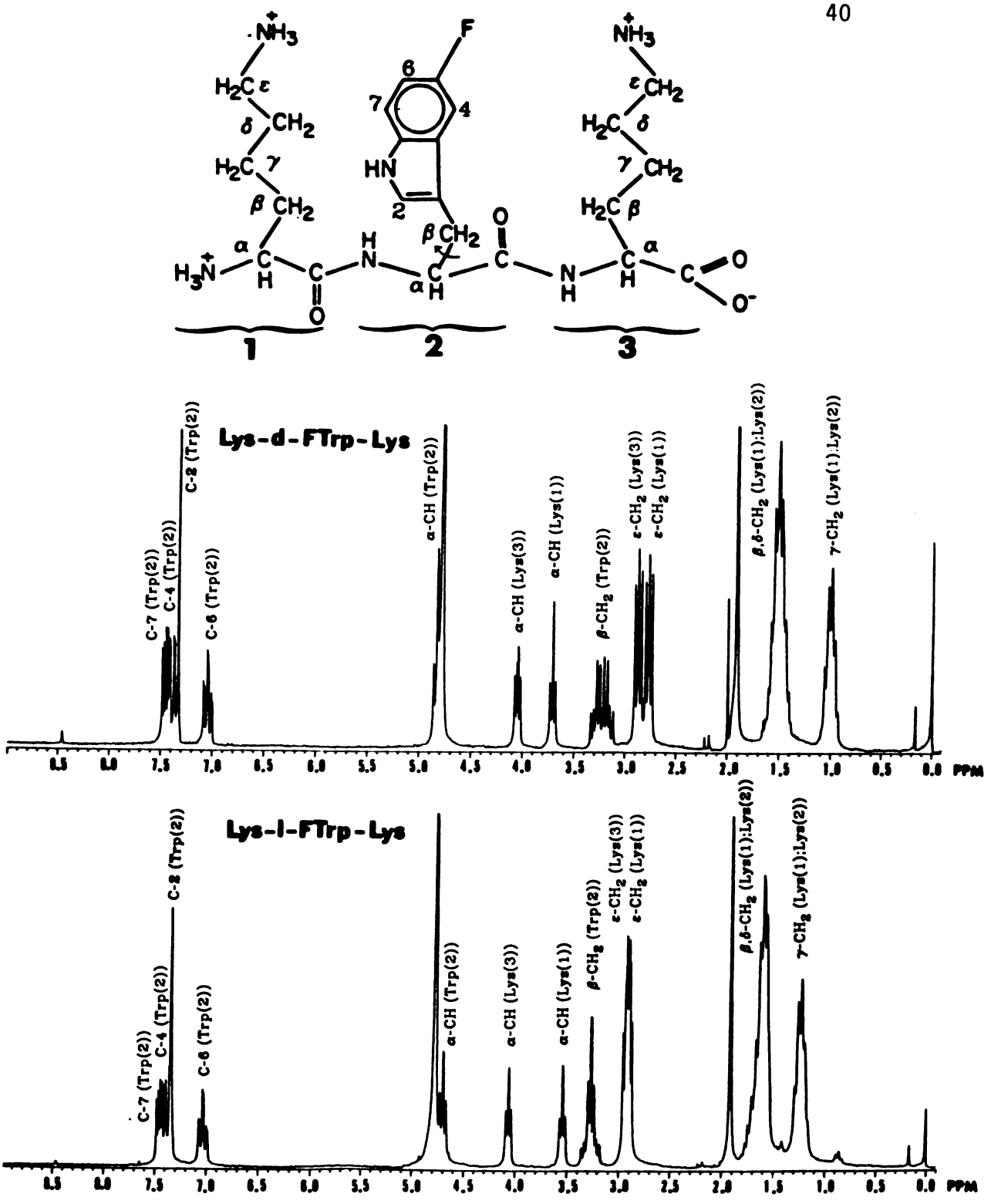

fig. 6: 240 MHz proton spectra (as shown in fig. 5) indicating the peak assignments obtained from 2D COSY and NOESY data. The α-amino and α-carboxyl terminal protons were assigned on the basis of pH titration data.

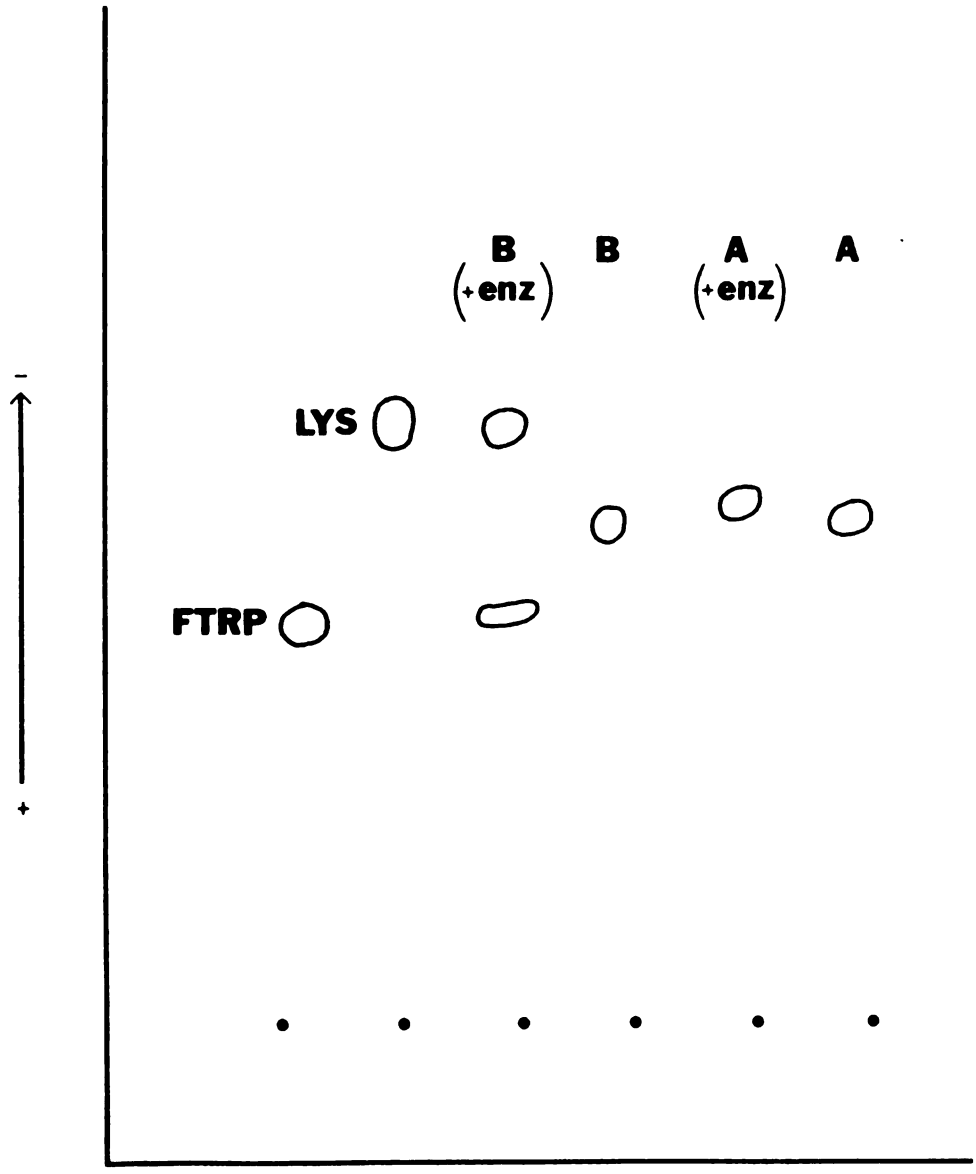

fig. 7: Analysis by thin-layer electrophoresis (Cellulose Acetate, 0.1 M ammonium bicarbonate, pH 9.2, 300 V, 1.5 hrs) of the chymotryptic digest products obtained from aliquots of peak A and peak B (fig. 3). The circles indicate the ninhydrin positive spots; • denotes the origins.

0°C. After centrifugation, the DNA pellet was redissolved in 10 mM sodium cacodylate, 10 mM NaCl, 1 mM EDTA, pH 6.0 and dialyzed extensively against this buffer. Final concentration of the sample was accomplished using a negative pressure micro-dialysis concentrator (Micro-ProDiCon, Bio-Molecular Dynamics). The sonicated fragments were checked for size distribution by electrophoresis on 8% polyacrylamide gels. The majority of the fragments migrated in the molecular weight range of 150-300 base pairs, using ϕX174-HaeIII fragments (BRL) as markers.

Preparation of DNA containing Apurinic Sites. Quantitatively depurinated DNA was obtained following the procedure of Lindahl and Nyberg (4). They found that the rate of release of purines proceeded at an initial rate of 3.8×10^{-7} sec^{-1} when [^{14}C] purine labeled B. subtilis DNA was incubated in 0.1 M NaCl, 0.01 M sodium phosphate, 0.01 M sodium citrate, pH 5.0, at 70°C.

A. *Introduction of Apurinic Sites into Sonicated DNA.* Calf thymus DNA was sonicated as described above except that the sonication was continued for 4 hrs at a power level of 6 and a high salt buffer (1.0 M NaCl, 10 mM sodium cacodylate, 1 mM EDTA, pH 7.0) was used in order to obtain smaller fragments with a more uniform size distribution. The average molecular weight of the fragments obtained was 135 base pairs as determined by polyacrylamide gel electrophoresis. Using the rate constant reported, approximately 4% depurination should be achieved in 29 hrs using the same conditions.

The sonicated calf thymus DNA was initially dialyzed extensively against 0.1 M NaCl, 0.01 M sodium phosphate, 0.01 M sodium citrate, pH 7.2, and the sample adjusted to pH 5.0 immediately prior to depurination.

In order to insure that 70°C was sufficiently below the T_m of this molecular weight DNA, the melting profile of an aliquot was examined. The T_m obtained was 79.5°C and no hyperchromicity was observed at 70°C.

Capped pyrex tubes containing 1.0 mL of DNA (1.1 mg/mL) were incubated at 70°C for 29 hrs using a Pierce "Reacti-Therm" heating module. The samples were then transferred to centrifuge tubes, the pyrex tubes washed with 500 μL (2x) of buffer, and the DNA precipitated by addition of 3.0 mL of cold 95% ethanol. The samples were kept at 0°C overnight and then centrifuged (12,000 rpm) at 2°C for 1 hr. The supernatant was transferred to a graduated conical tube, and the pellet washed with an additional 2.0 mL cold ethanol. The DNA recovered was dissolved in 10 mM sodium cacodylate, 10 mM NaCl, 1.0 mM EDTA, pH 6.0 and stored frozen.

B. *Analysis of Depurination.* Lindahl and Nyberg (4) found that > 95% of the radioactively labeled purines were recovered in ethanol-soluble form after precipitation of the DNA. For the present study, the composition of the supernatant solutions were examined by HPLC to check the amount of depurination that had occurred.

Separation of all four bases, adenine, guanine, cytosine, and thymine was achieved on a Partisil 10 μM ODS (11) column (hplc technology, ltd.) by isocratic elution with 2.5% methanol, 0.1% TFA in H_2O at a flow rate of 1.0 mL per minute.

The supernatant solutions obtained as described above were evaporated under N_2 to approximately 1.0 mL, 200 μL of 1.0% TFA added, and the volume adjusted to 2.0 mL with water. TFA, added so that the final concentration equalled that of the eluant, was included to lower the pH and insure that all the guanine, which is highly insoluble at neutral pH,

would be recovered. Also to insure that all materials were in solution, these samples were sonicated in a bath sonicator for 1.5 hrs.

The elution profile (fig. 8) was monitored at 250 nm. The amount of guanine and adenine present in the supernatant (Table II) was determined by comparing the intensities with a standard curve (fig. 9) generated from a mixture of these two purines at known concentrations. The percent depurination was then determined from the relationship between this amount and that obtained from an equal aliquot of DNA (1.0 mL of 1.1 mg/mL) which had been fully depurinated by boiling for 1.0 hr. at pH 2.85. Three 1.0 mL aliquots were analyzed separately for the extent of depurination and the results indicate that under the conditions used above an average of approximately 5% of the purines were removed (Table II).

C. *Introduction of Apurinic Sites into pBR322 Plasmid DNA.* Lindahl and Andersson (5) have also shown that the rate of depurination of double-stranded DNA can be applied to phage PM2 DNA (9800 base pairs). Under the same conditions as described above, approximately 1 apurinic site as expected is introduced per plasmid molecule after 4 min of heating at 70°C.

For the present study, pBR322 DNA (4362 base pairs) was purchased from International Biotechnologies, Inc. The sample was shown to contain >95% supercoiled molecules on 1% agarose gels. To introduce approximately 1 apurinic site per molecule an appropriate amount was first precipitated on dry ice for 30 min after addition of 2.5 volumes of cold 95% ethanol. The sample was spun at 13,750 rpm for 10 min in a microcentrifuge (Fisher Model 235A), the supernatant decanted and 100 μL of ethanol used to wash the pellet. After the second spin (5 min) the pellet

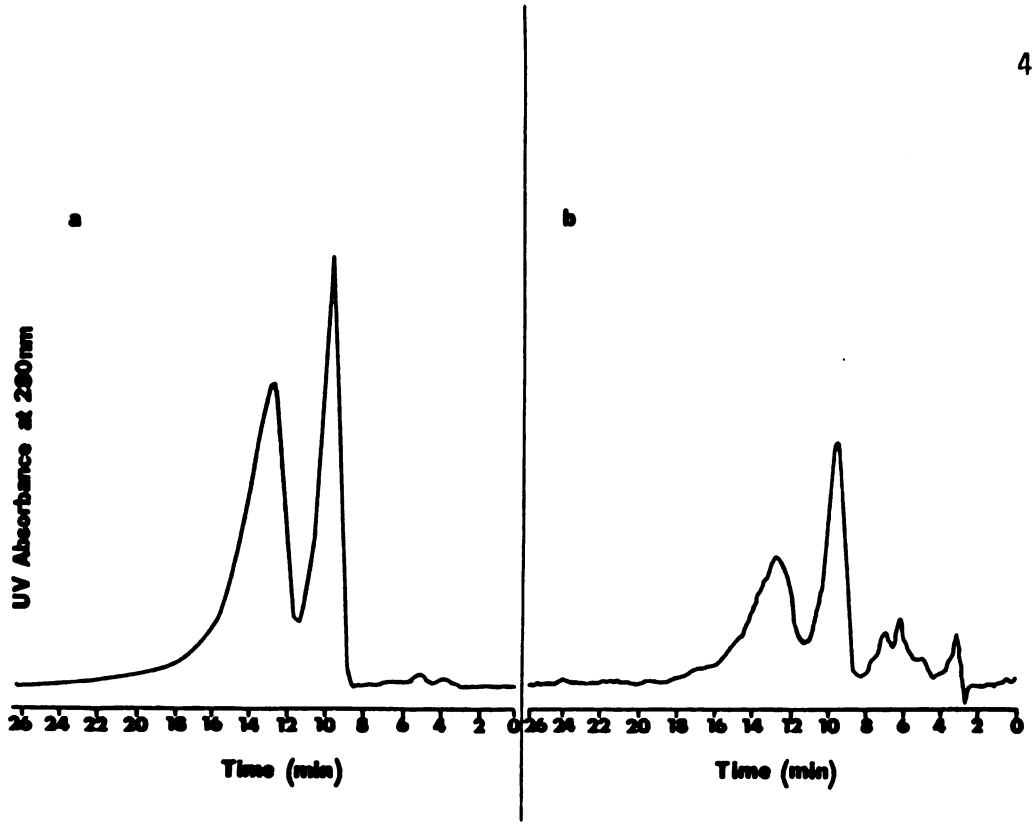

fig. 8: HPLC elution profiles used to quantitate the extent of depurination of sonicated DNA. The partisil 10 μm ODS(II) column was run isocratically at a flow rate of 1.0 mL per min with 0.1% TFA, 2.5% methanol in water as eluant. Using this solvent system, guanine and adenine had retention times of 9.6 and 12.8 min, respectively. These chromatograms were expanded to facilitate the estimation of peak areas from weighing the guanine and adenine peaks. The HPLC traces shown are from 20 μL injections of the ethanol-soluble fraction (2.0 mL volume) representing 1.16 mg of CT DNA which had been (a) heated at 100°C at pH 2.85 for 1.0 hr and (b) heated for 29.2 hrs at 70°C in 0.1 M NaCl, 0.01 M sodium phosphate, 0.01 M sodium citrate, pH 5.0. Chromatogram (a) represents totally depurinated DNA (apurinic DNA) and (b) represents partial depurination. Absorbance full scale (AFS) is 0.2 for (a) and 0.02 for (b). UV absorbing materials eluting between 2 and 8 min were also observed for an equal aliquot that had not been heated.

TABLE II. Peak intensities for standard guanine and adenine samples and those obtained from partially and totally depurinated CT DNA.

Purine base	AFS[b] x weight ($\times 10^{-4}$)	amount (μg)	% total
Standard Samples[a]			
Guanine	93.6	0.9066	100
	45.6	0.4533	50
	24.0	0.2267	25
	11.0	0.1134	12.5
	8.83	0.0907	10
	6.97	0.0680	7.5
	4.44	0.0453	5
	3.62	0.0363	4
	2.36	0.0272	3
	1.76	0.0181	2
Adenine	167.8	1.08	100
	82.9	0.54	50
	41.3	0.27	25
	19.6	0.135	12.5
	15.1	0.108	10
	11.2	0.081	7.5
	7.59	0.054	5
	5.95	0.043	4
	3.31	0.032	3
	2.28	0.022	2
Depurination Samples			
Apurinic acid[c]			
Guanine	119.5	1.16[e]	100
Adenine	190.5	1.23	100
Partial Depurination[d]			
Guanine	6.65	0.0668[f]	5.75
	7.26	0.0727	6.27
	6.2	0.0624	5.38
Adenine	8.29	0.0612	4.99
	7.58	0.0567	4.62
	6.49	0.0497	4.05

[a] For the 100% standard, 4.0 mL of 1.0 mM adenine was added to 3.0 mL of 1.0 mM guanine and the volume adjusted to 10 mL with the same solvent (0.1% TFA) so that a 20 μL injection contained 1.08 μg of adenine and 0.9066 μg of guanine. All other standard solutions were obtained from appropriate dilutions of the 100% standard with 0.1% TFA.

[b] Peak intensities were normalized by multiplying the weight in grams by the absorbance full scale (AFS).

[c,d] Obtained as given in fig. 8.

[e,f] Amounts were determined from the plots shown in fig 9.

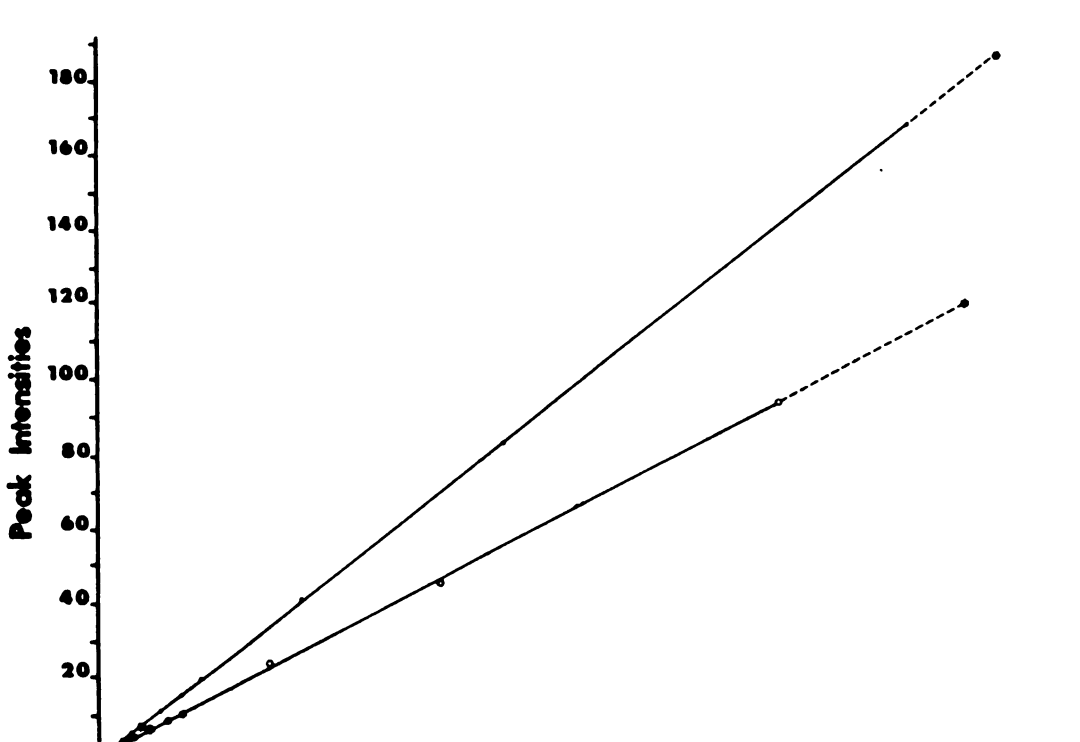

fig. 9: Plot of peak intensities obtained from HPLC (conditions given in fig. 8) versus concentration (μg) for standard solutions of guanine (o—o) and adenine (•—•) prepared as described in Table II(a). Data was fit using a linear least squares analysis. * indicates points for apurinic acid and partially depurinated DNA. For the latter this point represents the average of three measurements (see Table II).

was dried under vacumn and subsequently dissolved in 0.1 M NaCl, 0.01 M sodium phosphate, 0.01 M sodium citrate, pH 5.0 that had been pre-equilibrated at 70°C. After incubation for 8 min, the plasmid was recovered by precipitation as above. The pellet was dissolved in an appropriate buffer and used immediately.

METHODS

Sample Preparation. Concentrations of both native sonicated CT DNA and DNA modified to contain 5% depurinated sites, were determined using the extinction coefficient at 260 nm of 6600 per phosphate. For the tripeptides, the concentrations reported are those determined using 5600 as extinction coefficient at 280 nm. All NMR experiments were performed with samples dissolved in 10 mM sodium cacodylate, 10 mM NaCl, and 1.0 mM EDTA, pH 6.0. The fluorescence and T_m measurements were made in a lower salt buffer containing 1.0 mM sodium cacodylate, 1.0 mM NaCl, 0.1 mM EDTA, pH 6.0.

Fluorescence Experiments. The fluorescence studies were done on a Perkin-Elmer model MPF-2A spectrophotometer operating in the ratio mode. The sample temperature (20°C) was regulated using a circulating water bath. In order to eliminate interference in the fluorescence intensity measurements due to absorption by the nucleic acids at the excitation wavelength, a 3 x 3 mm cell was used and the sample excited at 304 nm. A 10 nm slit width was used for both emission and excitation and a 290 nm cut-off filter employed to minimize scattering. The titration curves were generated by adding a small amount of concentrated peptide (1.0 mM) to both sonicated DNA (native or modified to contain 5% apurinic sites) and the same volume (300 μL) of buffer (1.0 mM sodium cacodylate, 1.0 mM NaCl, 0.1 mM EDTA, pH 6.0).

Thermal Denaturation Studies. A Gilford System 2600 microprocessor-controlled UV-Vis Spectrophotometer equipped with a 2527 thermo-programmer was used to obtain the helix-to-coil transition curves.

^{19}F NMR. The fluorine spectra were recorded at 94.1 MHz on a Varian XL-100 equipped with a 1080 Nicolet computer. The chemical shifts were measured with respect to NaF present in a capillary tube. Upfield shifts are reported negative. Solution conditions and sample concentrations are given in the appropriate figure legends. The solvent-induced shifts (SIS) were determined from spectra acquired in 10% D_2O versus 90% D_2O. For the T_1 measurements, the 180° - τ - 90° (T1IR) sequence was used. The integrated peak intensities were analyzed using a three-parameter exponential curve fit to $A_\tau = B + C\exp(-\tau/T_1)$, where A_τ is the peak intensity after waiting a time τ and B, C, and T_1 are optimized. The nuclear Overhauser effect (NOE) values were determined by comparing the integrated peak intensities of the decoupled spectra obtained by continuous proton irradiation to those of the corresponding spectra without proton irradiation. To minimize temperature changes, these spectra were obtained by alternately collecting 12 scans without NOE and then 12 scans with NOE. This was continued until a sufficient signal-to-noise ratio was obtained.

Electrophoresis. Polyacrylamide gel electrophoresis was carried out on 13 x 12 x 0.3 cm vertical slab gels according to the method of Maniatis et. al. (6). The gels contained 8% (w/v) acrylamide (BRL) with 0.27% (w/v) N,N'-methylenebisacrylamide (BRL) and were run at 100 volts (~ 21 mamps) for approximately 4 hrs or until the tracking dye (bromophenol blue) had traveled the length of the gel. An electrode buffer consisting of tris-borate-EDTA (TBE) (0.09M tris-borate, 2.5 mM EDTA, pH 8.3) was employed. The gels were then stained with ethidium bromide and photographed.

1% agarose gels (5 x 7.5 x 0.35 cm) were run on a horizontal gel electrophoresis unit (IBI Model QSH) also using TBE as the running buffer. The electrophoresis was carried out at 100 volts (~ 35 mamps) for approximately 50 min. The gels were stained with ethidium bromide and photographed using Polaroid positive/negative 4 x 5 land film, Type 55. The negatives were scanned using a soft laser scanning densitometer (Biomed Instruments, Inc., Model SL-504).

References

1. **Steward, J. M. and Young, J. D.,** Solid-Phase Peptide Synthesis, San Francisco, W. H. Freeman, 1969.

2. **Merrifield, R. B.,** Solid-Phase Peptide Synthesis. III. An Improved Synthesis of Bradykinin, *Biochemistry*, *3*, 1385-1390, (1964).

3. **Yamashiro, D. and Li, C. H.** Synthesis of a Pentekontapeptide with High Lipolytic Activity Corresponding to the Carboxyl-Terminal Fifty Amino Acids of Ovine β-Lipotropin, *Proc. Nat. Acad. Sci. USA*, *71*, 4945-4949, (1974).

4. **Lindahl, T. and Nyberg, B.,** Rate of Depurination of Native Deoxyribonucleic Acid, *Biochemistry*, *11*, 3610-3617, (1972).

5. **Lindahl, T. and Andersson, A.,** Rate of Chain Breakage at Apurinic Sites in Double-Stranded Deoxyribonucleic Acid, *Biochemistry*, *11*, 3618-3623, (1972).

6. **Mantiatis, T., Jeffrey, A. and van deSande, H.,** Chain Length Determination of Small Double- and Single-Stranded DNA Molecules by Polyacrylamide Gel Electrophoresis, *Biochemistry*, *14*, 3787-3794, (1975).

CHAPTER III

COMPLEX FORMATION BETWEEN DIASTERIOMERIC TRYPTOPHAN-CONTAINING TRIPEPTIDES AND DOUBLE-STRANDED DNA.

INTRODUCTION

In order to study the involvement of the aromatic amino acids in protein-DNA associations, a number of investigations have focused on the binding of the tripeptide lysyl-tryptophyl-lysine to various polynucleotides (1,review). Of particular interest is whether the aromatic indole ring can stack between the nucleic acid bases. The results, to date, provide evidence supporting this type of interaction on the part of this model peptide.

In the present study, ^{19}F NMR was used as a probe to examine the complex formed by this tripeptide with double-stranded DNA. The fluorine label is on the 5 position of the tryptophan ring (fig. 1). Lys-*d*-5FTrp-Lys was studied concurrently with its diasteriomer. Previous studies with similar diasteriomeric dipeptides (2,3) suggested that these two tripeptides would form distinct complexes with DNA.

The results of the ^{19}F NMR, fluorescence, and thermal denaturation studies for these tripeptide-DNA complexes are presented and discussed in this chapter.

RESULTS

^{19}F Chemical Shifts. The shift of the tryptophyl fluorine resonance position when in the presence of native DNA provides information about the local environment of the fluorine nucleus in these complexes. The chemical shifts are measured relative to NaF present in a capillary. Upfield shifts are reported negative.

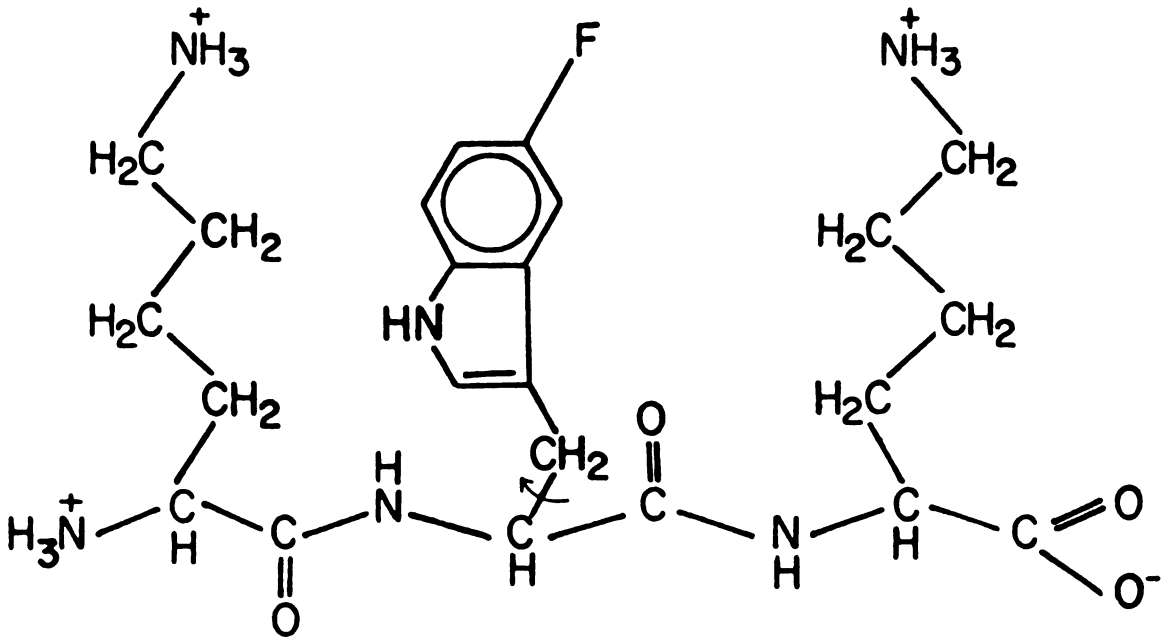

fig. 1: Structure of the tripeptide lysyl-5-fluoro-tryptophyl-lysine.

A. pH Titration of the Free Tripeptides. The associations between DNA and the Lys-5FTrp[1]-Lys tripeptides are expected to involve electrostatic interactions (4-7). The sensitivity of the indole fluorine chemical shift to effects involving the positively charged groups was measured by observing the fluorine resonance position as a function of pH for both diasteriomeric tripeptides as well as the free FTrp (fig. 2).

The titration curve for the free amino acid indicates that the fluorine chemical shift is sensitive to the titration of both the α-carboxyl and the α-amino groups. The ^{19}F resonance position shifts upfield with deprotonation. The direction of the chemical shifts are consistent with that observed in ^{1}H NMR where the α-CH proton of the amino acid being titrated shifts upfield as the pH is increased. pK_a values of 9.5 and 2.5 were obtained from the pH dependence of the fluorine chemical shifts (Table I.). These values are consistent with those reported for the α-amino (pK_a = 9.39) and the α-carboxyl (pK_a = 2.38) groups of tryptophan (8). The magnitude of the observed shifts is significantly greater than those measured in ^{1}H NMR considering the fact that the fluorine nucleus is seven bonds away from the titratable group.

When FTrp is incorporated into the tripeptides, there is still an observable upfield shift as the N-terminal amino group is titrated. The magnitude of the shift is smaller as expected. pK_a values of 7.2 and 7.6 are indicated for the *l*- and *d*-Trp peptides, respectively. In addition the ^{19}F NMR resonance position is sensitive to the ionization state of the lysyl

[1]ABBREVIATIONS: FTrp, 5-fluoro-*dl*-tryptophan; 5FTA, 5-fluorotryptamine; Tri(*l*), lysyl-5-fluoro-*l*-tryptophyl-lysine; Tri(*d*), lysyl-5-fluoro-*d*-tryptophyl-lysine; SIS, solvent-induced shift; NOE, nuclear Overhauser effect.

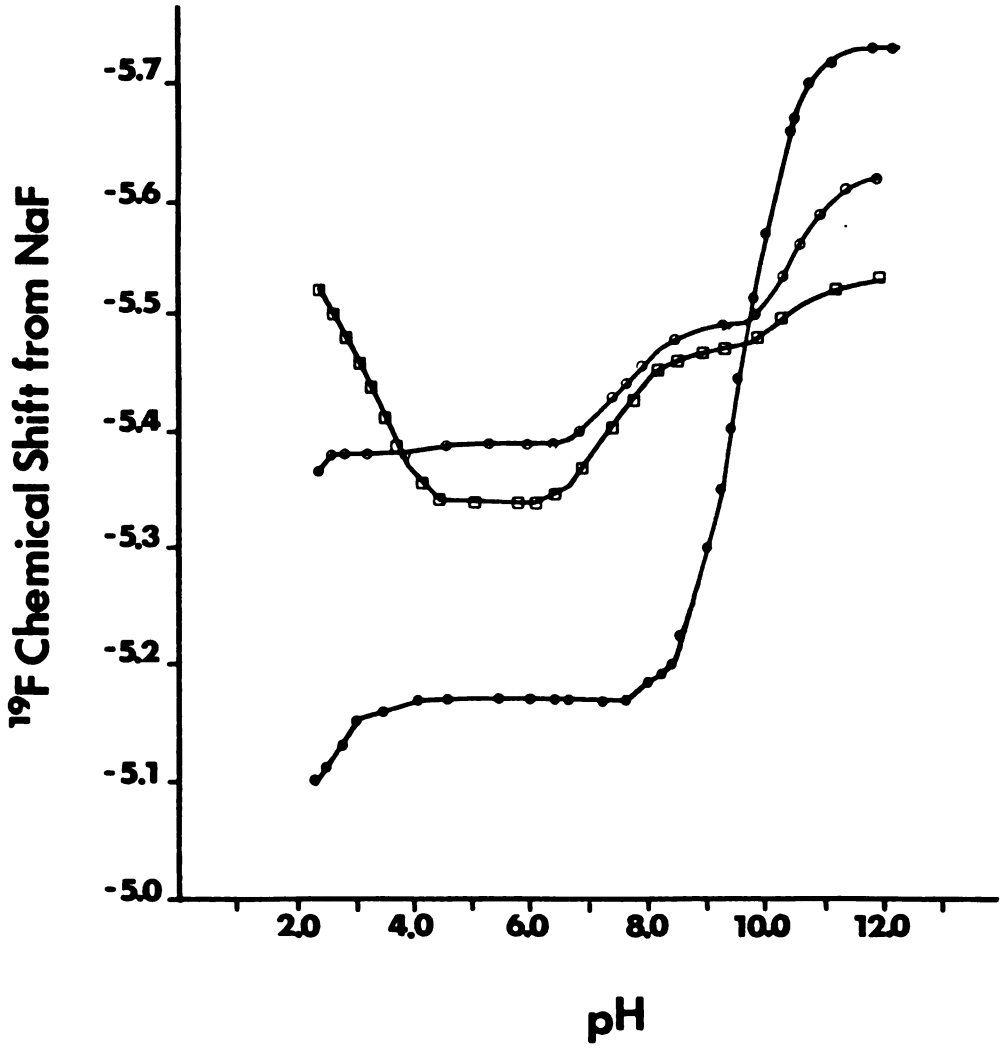

fig. 2: Fluorine chemical shifts as a function of pH for FTrp, ●—● , Tri(*l*), □—□, and Tri(*d*), ○—○. Samples contained 10% D_2O. In order to eliminate effects from changes in the ionic strength as the pH was altered, samples were prepared in 100 mM NaCl. The curves were generated by titrating a sample prepared at low pH (2.3) with one prepared at high pH (9.3). Higher pH values were obtained by adjustment with 1.0 N NaOH. The study was done at 25°C.

TABLE I. pH dependence of the ^{19}F NMR chemical shifts for 5FTRP, Tri(*l*) and Tri(*d*).

SAMPLE[a]	TITRATABLE GROUP	pK_a[b]	$\Delta\delta$(ppm)[c]
FTRP	COOH	2.5	-0.11
	NH_3^+	9.5	-0.56
Lys-*l*-FTrp-Lys	COOH	3.1	0.21
	α-NH_3^+	7.2	-0.12
	ε-NH_3^+	10.3	-0.06
Lys-*d*-FTrp-Lys	α-NH_3^+	7.6	-0.10
	ε-NH_3^+	10.4	-0.15

[a]Samples were prepared as described in fig. 2.

[b]The pK_a values were determined using the following equation:

$$\delta = \delta_{HA} - K_a(\delta - \delta_A/[H^+]) \quad \text{(ref. 9)}$$

where δ_{HA} and δ_A are the chemical shifts of the protonated and unprotonated species, respectively. δ is the observed chemical shift at a given pH. K_a values were obtained from the slopes of the δ versus $\delta - \delta_A/[H^+]$ plots.

[c]The chemical shifts for the protonated species, δ_{HA}, were obtained from the y-intercepts of the plots described in b. $\Delta\delta = \delta_A - \delta_{HA}$.

ε-amino groups. Again an upfield shift is observed for both tripeptides; reflecting a pK_a value of 10.3 and 10.4 for the *l*- and *d*-Trp peptides respectively. Based on these data, subsequent studies of the complexes were done at pH 6.0. At this pH, contributions to the chemical shift from slight variations in the sample pH are minimized. Also, at pH 6.0, the tripeptides bear the same net charge; that is, the N-terminal α-amino and ε-amino groups of the lysines are fully protonated and the C-terminal group negatively charged.

The titration curves of the two tripeptides differ significantly at low pH where the α-carboxyl group of the C-terminal lysine is titrated. For the *d*-Trp peptide a slight upfield shift is observed which is smaller than that for the free FTrp as expected. On the other hand, for the *l*-Trp peptide, the shift of the resonance position is larger and in the opposite direction, that is, downfield instead of upfield as expected. The ^1H NMR titration curve is also distinct for this tripeptide (see below).

B. Titration of Tripeptides with DNA. Both the *d*- and *l*-tryptophan-containing peptides were titrated with sonicated DNA. Differences in both the magnitude and direction of the fluorine chemical shift are observed (fig. 3; Table II.). For the *l*-Trp-containing peptide, the fluorine resonance position shifts continuously upfield as the concentration of DNA is increased until a phosphate-to-peptide ratio of 20:1 is attained. The magnitude of this upfield shift is -0.48 ppm. For the *d*-Trp-containing peptide the shift is downfield and there is no further shift after a ratio of 5:1. The total downfield shift observed for the *d*-Trp peptide is 0.13 ppm.

C. Concentration Dependence of the ^{19}F NMR Chemical Shift of 5-Fluorotryptamine (5FTA). Previous ^1H NMR studies of Lys-*l*-Trp-Lys in the

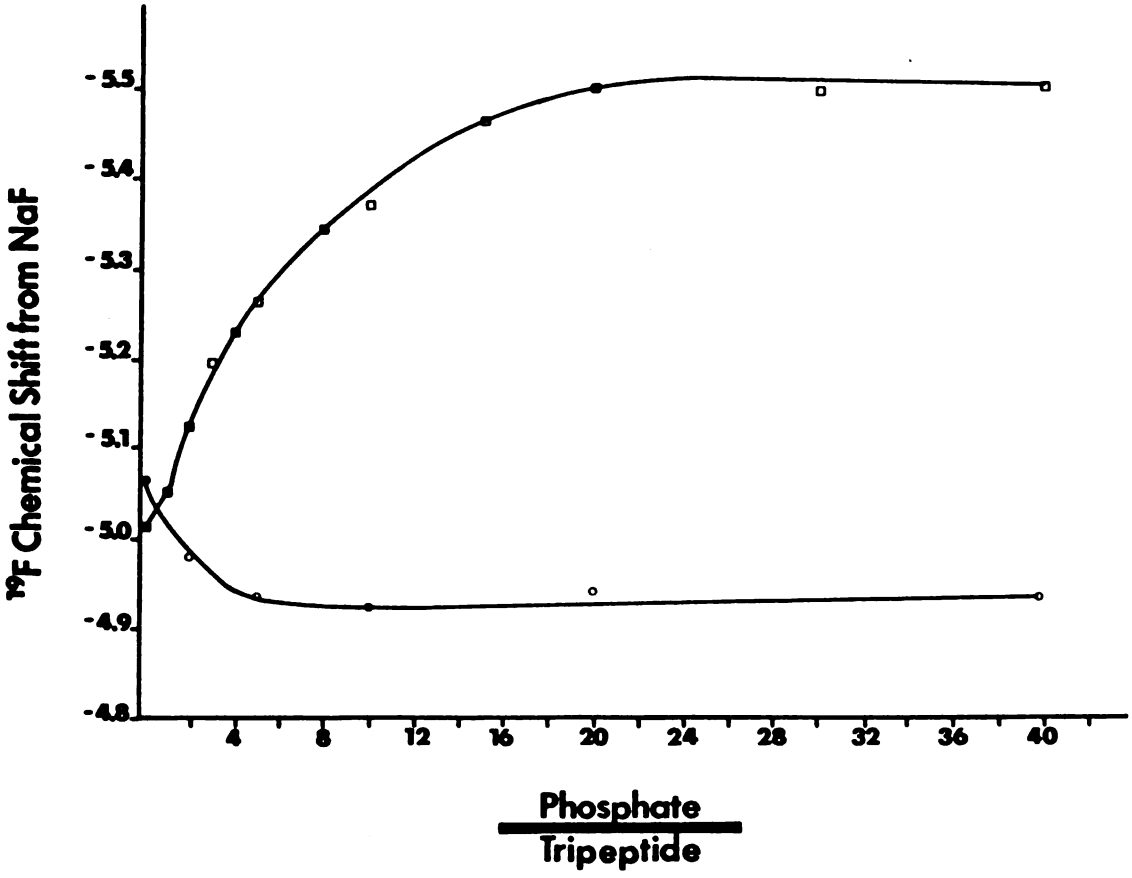

fig. 3: Plot of the ^{19}F NMR chemical shifts for both Tri(*l*), □—□, and Tri(*d*), ○—○, as a function of phosphate/tripeptide ratio. The curves were generated by titrating a solution containing 3 mM peptide with a solution 120 mM in DNA phosphates and 3 mM in peptide. Both solutions were in 10 mM sodium cacodylate; 10 mM sodium chloride; 1 mM EDTA; pH 6.0, containing 10% D_2O. The titrations were done at 37°C.

TABLE II. ^{19}F chemical shift, solvent-induced shift (SIS) and relaxation parameter values[a] for Lys-FTrp-Lys free and in its nucleic acid complexes.

SAMPLE[b]	δ[c] (ppm)	SIS[d] (ppm)	$W_{\frac{1}{2}}$ (Hz)	T_1 (sec)	NOE
Lys-*l*-FTrp-Lys 37°C	-5.01	-0.2	1	1.90±0.02	1.34±0.04
Lys-*d*-FTrp-Lys 37°C	-5.06	-0.2	1	1.85±0.01	1.33±0.05
Lys-*l*-FTrp-Lys + DNA 37°C (P/TRI = 30)	-5.49 $\Delta\delta$ (-0.48)[e]	-0.2	70	0.39±0.01	0.56±0.02
Lys-*d*-FTrp-Lys + DNA 37°C (P/TRI = 30)	-4.93 $\Delta\delta$ (0.13)[e]	-0.2	6	0.51±0.03	0.88±.01

[a] ± values represent the average deviation from the mean. T_1 values are the average of four measurements; NOE determinations are the average of five.

[b]Samples were prepared in 0.01 M NaCl, 0.01 M sodium cacodylate, 0.001 M EDTA at pH 6.0. P/TRI refers to the ratio of moles of polynucleotide phophates to Lys-FTrp-Lys.

[c]Chemical shifts were measured with respect to NaF present in a capillary tube. Upfield shifts are reported negative.

[d]The solvent-induced shift (SIS) is the chemical shift in 10%H_2O-90%^2H_2O minus that in 90%H_2O-10%^2H_2O.

[e]$\Delta\delta$ is the difference in chemical shift between the free peptide and its complex with DNA.

presence of DNA and poly(rA) have provided the most direct evidence for stacking interactions (7). The upfield shift of the C-2 aromatic indole proton resonance (see fig. 1) was attributed to ring current effects. In order to obtain evidence that ring current effects would also induce upfield shifts in the fluorine resonance position, both the fluorine and proton chemical shifts for a small indole derivative, 5-fluorotryptamine (fig. 4), were measured as a function of concentration. Tryptamine is known to self-associate and this self-association has been monitored previously using proton NMR (10). The proton NMR study was repeated with 5FTA and an upfield shift of 0.09 ppm was observed for the C-2 proton as the concentration was increased from 15 to 150 mM (pH 3.55). ^{19}F NMR spectra were obtained of the same samples and an upfield shift of the same magnitude (0.13 ppm) was observed.

D. Solvent-induced Shift. To determine the solvent accessibility of the fluorine nucleus in the tripeptide-nucleic acid complexes, the spectrum of each was taken in H_2O vs D_2O. For both complexes an upfield shift of 0.2 ppm was observed when the solvent was changed from 10% D_2O to 90% D_2O (fig. 5, Table II.). The magnitude and direction of the shift is the same as that observed for the tripeptide free in solution.

E. Ionic Strength Dependence of the Complexes. Using the method developed by Record, et. al. (11), the number of charge interactions in a given complex can be evaluated from the dependence of the observed association constant K_{obsd} on the ionic strength. Briefly, if "m" electrostatic bonds are formed with the phosphate groups of the polymer, then $m\psi Na^+$ ions will be released. "ψ" is the fraction of counterions, here Na^+, bound per phosphate. Record et. al. have determined this to be equal to

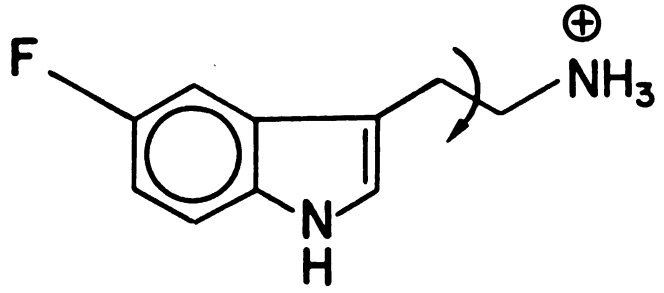

fig. 4: Structure of 5-fluorotryptamine. Both the proton and fluorine NMR spectra of the 150 mM solution in D_2O, pH 3.55 and appropriate dilutions were obtained at 25°C.

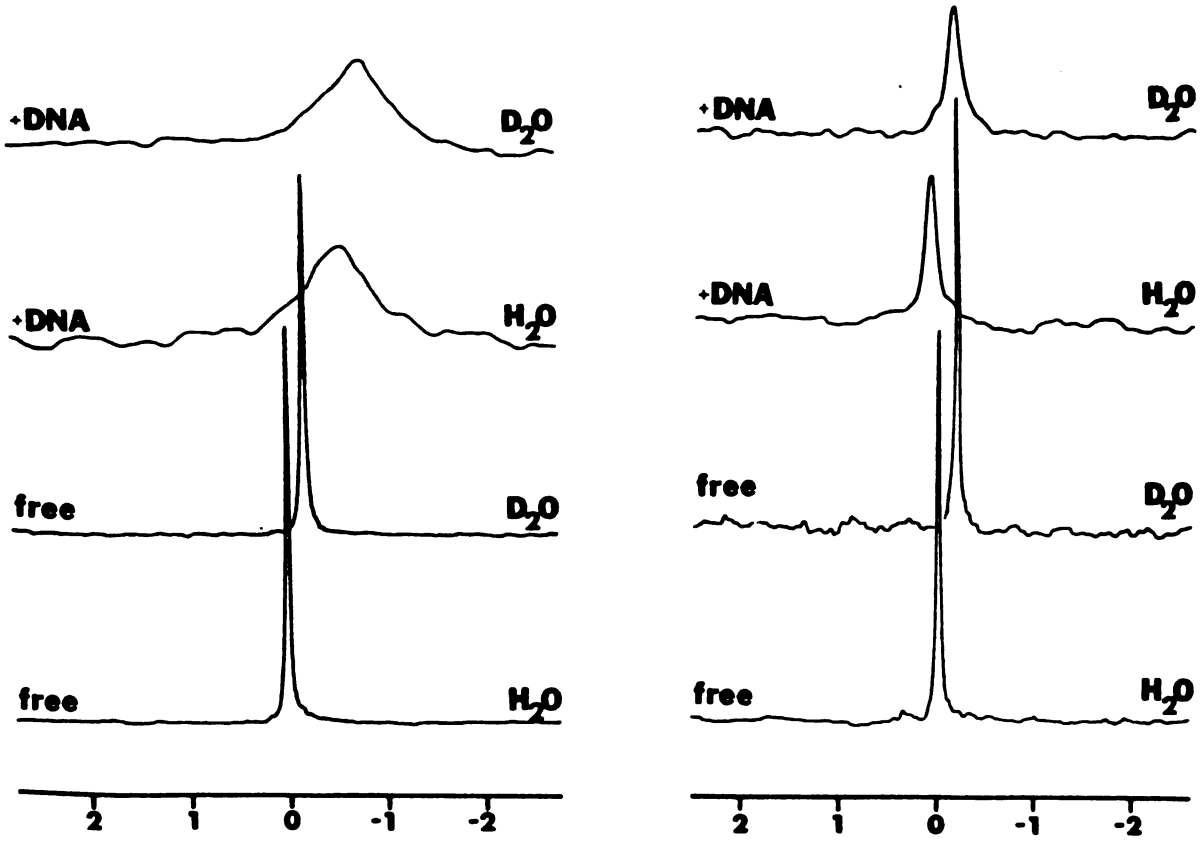

fig. 5: ^{19}F NMR spectra (37°C) indicating the solvent-induced shift found for both diasteriomers of Lys-5FTrp-Lys free and in the presence of double-stranded DNA. Spectra obtained with Tri(*l*) are shown on the right and those obtained with Tri(*d*) are on the left. Spectra were obtained in 10% H_2O - 90% D_2O (D_2O) and in 90% H_2O - 10% D_2O (H_2O). Samples conditions are as given in Table II.

0.88 for double-stranded DNA (11). The binding reaction can be written as:

$$L + P \overset{K_o}{\leftrightarrows} LP + m\psi Na^+ \qquad (1)$$

where L, P, and LP represent ligand, polymer, and complex respectively. The corresponding association constant is:

$$K_o = [LP][Na^+]^{m\psi}/[P][L] \qquad (2)$$

The measured (observed) binding constant is given by:

$$K_{obsd} = [PL]/[P][L] \qquad (3)$$

and it follows that

$$K_{obsd} = K_o[Na^+]^{-m\psi} \qquad (4)$$

or

$$log\ K_{obsd} = \log K_o - m\psi \log[Na^+] \qquad (5)$$

From the slope of a plot of log K_{obsd} versus -log[Na^+] an estimate of the number of ion pairs formed between DNA and the peptide can be obtained.

In this study, ^{19}F NMR was used to monitor the complexes as a function of ionic strength. The change in chemical shift as a function of [Na^+] is shown in fig. 6. The titration curves demonstrate that the association between DNA and each tripeptide involves some contribution from electrostatic interactions. For both tripeptide complexes, the ^{19}F resonance position returns to that of the tripeptide free in solution at high ionic strength. The chemical shift of the free *d*-Trp-containing peptide is sensitive to salt concentration at low ionic strength; therefore, the shifts of the complex with this tripeptide have been corrected accordingly.

Values for K_{obsd} at each ionic strength were estimated from the ^{19}F

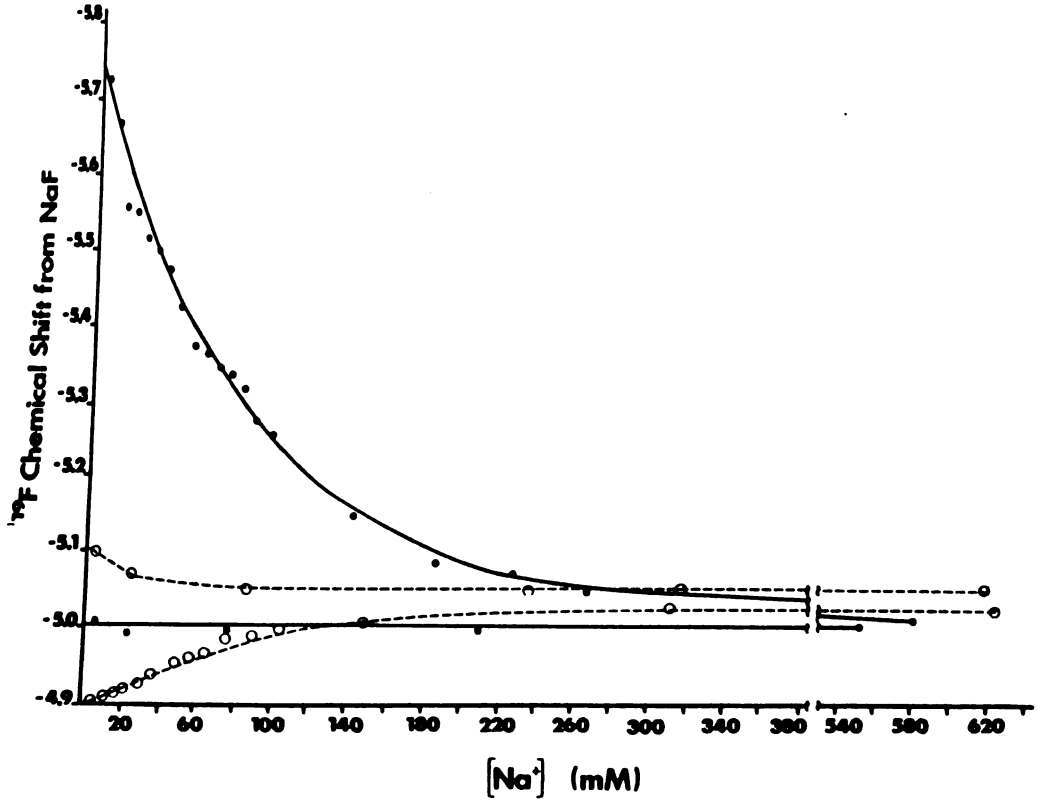

fig. 6: Plot of ^{19}F NMR chemical shifts as a function of ionic strength for Tri(*l*), ●—●, and Tri(*d*), ○---○, free in solution and and Tri(*l*), ●—●, and Tri(*d*), ○---○, *in the presence* of DNA. For both complexes, a small amount of a concentrated *salt solution* (1.8 M) was added to the complex (18 mM phosphate/0.6 mM pep*tide; ratio* phosphate/tripeptide = 30:1) initially containing 3.3 mM added Na^+, pH 6.4. The study was done at 37°C.

chemical shift using:

$$K_{obsd} = C_b/P_oC_f = (1/P_o)\ \{(\delta - \delta_f)/(\delta_b - \delta)\} \qquad (6)$$

where P_o is the concentration of DNA, C_f and C_b are the concentrations of free and bound tripeptide, respectively, δ is the chemical shift measured at each ionic strength, and δ_f and δ_b are the chemical shifts observed at the lowest (totally free peptide) and the highest (totally bound peptide) ionic strengths, respectively.

The slopes of the log K_{obsd} versus -log $[Na^+]$ plots (fig. 7) from equation (5) give 1.9 and 1.6 as the number of electrostatic bonds formed in the *d*-Trp- and *l*-Trp- containing peptide-DNA complexes, respectively.

F. Temperature Dependence of the Complexes. ^{19}F NMR was used to monitor the chemical shift of the complexed peptides as a function of temperature. The melting curves obtained are shown in fig. 8. The fluorine resonance position of both NaF and the tripeptides was found to be sensitive to temperature; hence, the chemical shifts of the complexes were corrected accordingly. The fluorine peak for the *l*-Trp peptide complex moves downfield and that of its diasteriomer moves upfield as the temperature is increased. The chemical shift of both complexed peptides returns to that found for the free tripeptides as the complex dissociates with increasing temperature.

^{19}F NMR Relaxation Measurements. In order to assess the relative mobilities of the aromatic moiety of the tripeptide when bound to DNA, several relaxation parameters were measured.

A. Linewidth, T_1, and NOE Values of the Tripeptides Free and Complexed to DNA. The linewidth, T_1, and NOE values obtained for the two tri-

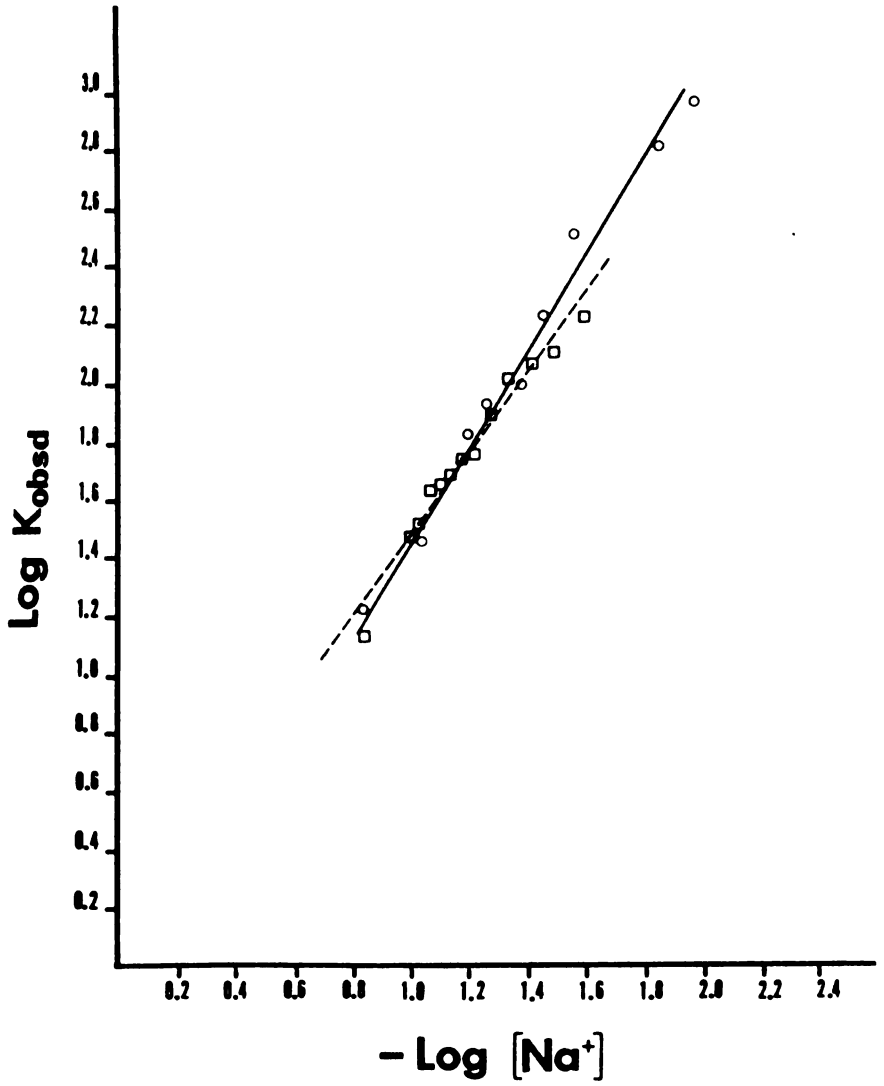

Fig. 7: Log-log plots of K_{obsd} versus $[Na^+]$ (equation (5)) for the interaction of *Tri(l)*, □—□, and Tri(*d*), ○—○, with DNA. The values of "m" obtained from the *slopes* ($= m\psi$) are 1.9 and 1.6 for the Tri(*d*)- and Tri(*l*)-DNA complexes, respectively.

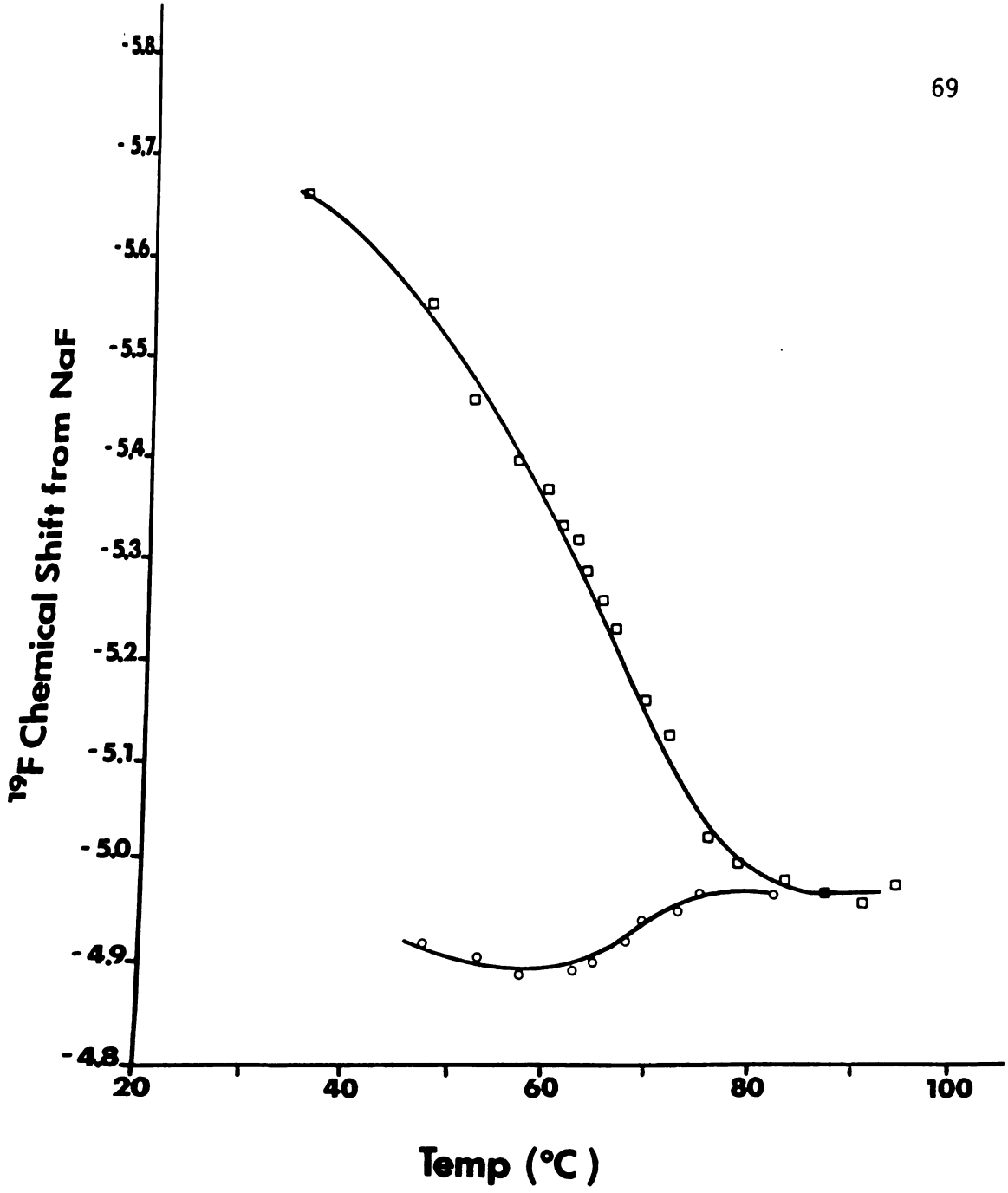

fig. 8: ^{19}F chemical shifts as a function of temperature for DNA complexed with *Tri(l)*, □—□, and Tri(*d*), ○—○. Samples were prepared in 10 mM sodium cacodylate, 10 mM NaCl, 1.0 mM EDTA, pH 6.0 at a DNA phosphate/tripeptide ratio of 30:1 (18 mM/0.6 mM). Spectra of each tripeptide free in solution were also recorded. The chemical shifts of the complexes were corrected for the shift with temperature observed for the free peptides.

peptides, both free in solution and in the presence of DNA are given in Table II. For the complexes, the phosphate-to-tripeptide ratio was 30:1. All studies were done at 37°C. For the *l*-Trp-containing peptide, the linewidth observed in the presence of DNA increases significantly from that found for the free tripeptide while there is only a slight increase in the case of its diasteriomer. The T_1 values decrease significantly for both tripeptides when comparing the free with the bound state as expected for a small ligand binding to a large polymer. There is no significant difference in these values for the two complexes. The NOE also decreases when the two tripeptides are in the presence of DNA; the value measured for the *l*-Trp peptide is less than that observed for the *d*-Trp peptide.

The relationship of the ^{19}F NMR relaxation parameters to molecular motions are shown for a two-correlation time model (21,26) in fig. 9. Curves illustrating the theoretical dependence of the ^{19}F T_1 and NOE on the internal motion correlation time τ_i were calculated for several overall motion correlation times τ_o.

B. Temperature Dependence of the Linewidth. The increase in linewidth with decreasing temperature was monitored for both tripeptides, free and complexed to DNA (Table III.). The linewidth of the *l*-Trp peptide complex increases from 70 to 144 Hz as the temperature is decreased from 37 to 20°C while for an equivalent temperature change, the linewidth increase of the *d*-Trp peptide complex and the free peptides are only ~5 Hz and ~1 Hz, respectively.

Proton NMR Studies

A. pH Titration of the Free Tripeptides. In order to insure that the ^{19}F chemical shifts observed as a function of pH for the free tripeptides

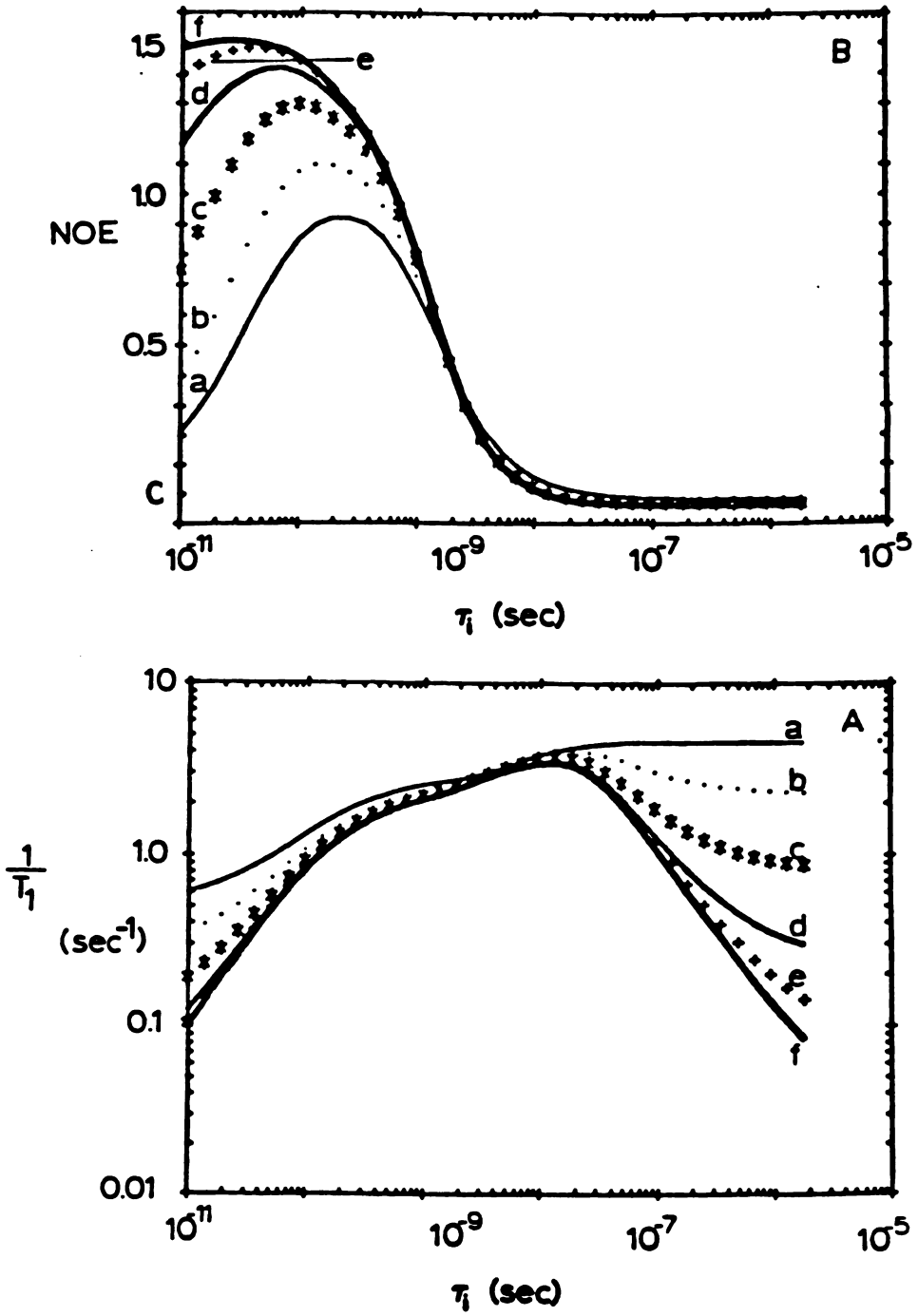

fig. 9: Theoretical curves for the spin-lattice relaxation time (T_1) and nuclear Overhauser effect (NOE) calculated assuming a two-correlation time model (26). The plots show the dependence of these relaxation parameters on the internal correlation time τ_i for a series of overall correlation times τ_o. The values for the overall correlation times are (a) 3×10^{-8} s, (b) 10^{-7} s, (c) 3×10^{-7} s, (d) 10^{-6} s, (e) 3×10^{-6} s, (f) 10^{-5} s.

TABLE III. Linewidth as a function of temperature for the tripeptides free and complexed to DNA.

Temperature (°C)	Linewidth[a] (Hz)			
	Tri(*l*)	Tri(*d*)	Tri(*l*) + DNA	Tri(*d*) + DNA
20.1	2	2	144	11
25.2	2	2	116	10
30.2		2	112	7
37.3	1	1	70	6

[a] Values are corrected for the applied line broadening.

corresponded to the assigned titratable groups, the proton NMR chemical shifts were also measured as a function of pH. pH titration curves for the titratable protons of both Tri(*l*) and Tri(*d*) are shown in fig. 10. The pK_a values obtained from these curves agree with those found using ^{19}F NMR (Table IV.).

Fluorescence Data. Quenching of the tryptophan fluorescence has been observed for Lys-*l*-Trp-Lys in the presence of various polynucleotides (4-6, 12-17). The fluorescence quenching data has been used to determine the binding parameters. In order to insure that the fluorine label does not influence the binding characteristics of the *l*-Trp-containing peptide and to compare the relative affinities of the two diasteriomers for native DNA, titration curves were generated (fig. 11) for each of the tripeptides using fluorescence.

A. Quantitative Analysis of the Fluorescence Data. Fluorescence intensities were measured at different peptide concentrations in the presence (I_c) and in the absence (I_f) of sonicated double-stranded DNA. These measurements were performed at several DNA concentrations (195 and 97 μM). Both the peptide and DNA concentrations were corrected for dilution.

The binding parameters were obtained from the fluorescence titrations by the following method. The measured intensity, I_c, can be expressed as:

$$I_c = I_f P_f + I_b P_b$$

where P_f and P_b are the populations of tripeptide free and bound, respectively, and I_b is the intensity for the fully bound state. Since

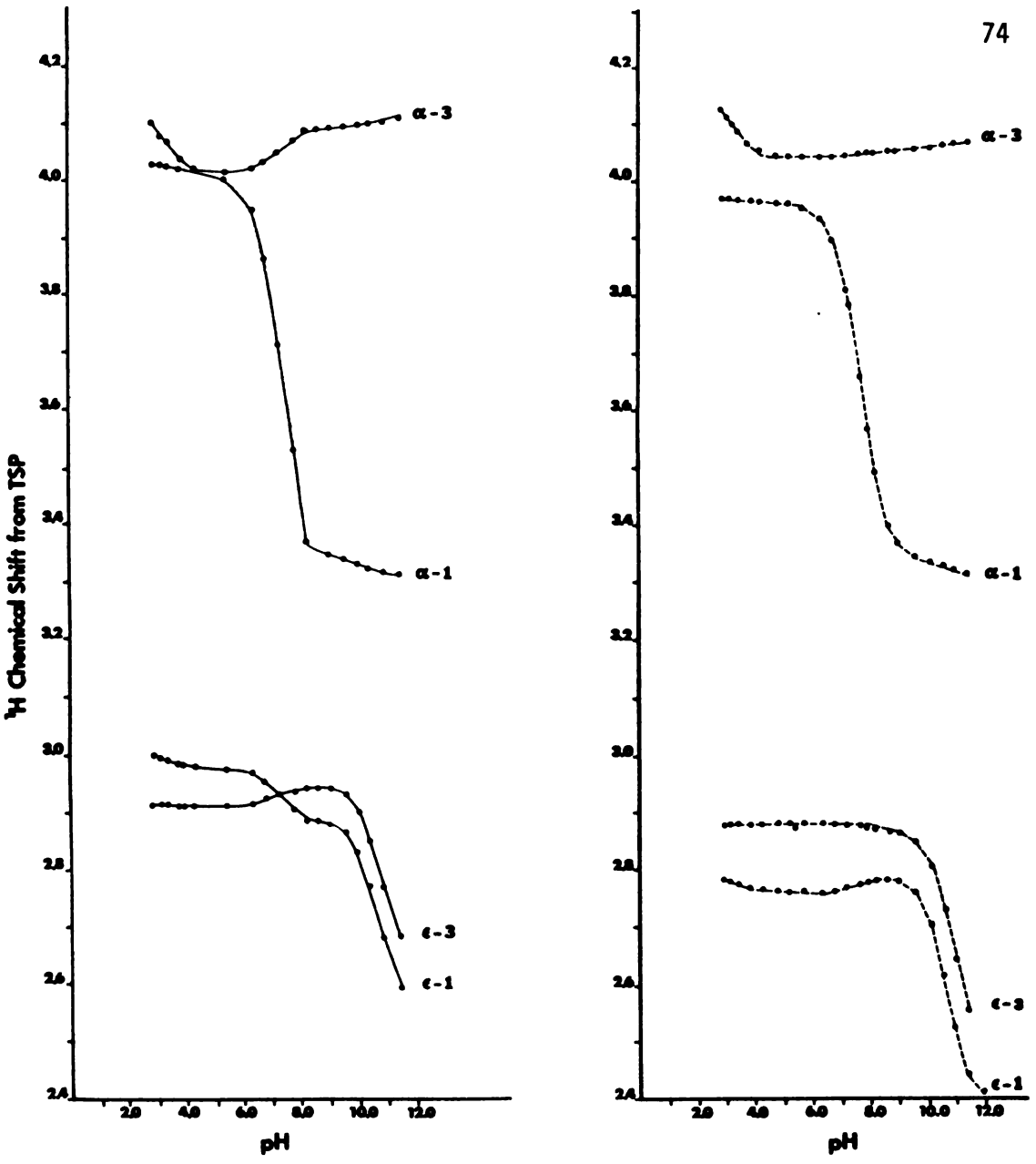

fig. 10: Plots of the proton chemical shifts as a function of pH for Tri(*l*), left, and Tri(*d*), right. The 240 MHz spectra were recorded at 25°C in D_2O. The curves were generated by titrating a peptide solution at pH 2.9 with one at pH 11.9. All shifts are relative to 3-(trimethylsilyl)tetradeutero sodium propionate (TSP). The peptides are numbered starting at the N-terminal; the N-terminal lysine is number one, the tryptophan number two, and the C-terminal lysine number three.

TABLE IV. pH dependence of the proton chemical shifts for Tri(*l*) and Tri(*d*).

SAMPLE[a]	TITRATABLE GROUP	pK_a[b]
Lys-*l*-FTrp-Lys	COOH (α-3)	3.3
	NH_3^+ (α-1)	7.2
	NH_3^+ (ε-1)	10.6
	NH_3^+ (ε-3)	10.8
Lys-*d*-FTrp-Lys	COOH (α-3)	3.0
	NH_3^+ (α-1)	7.6
	NH_3^+ (ε-1)	10.9
	NH_3^+ (ε-3)	10.7

[a]Samples were prepared as described in fig. 10.

[b]The pK_a values were determined as described in Table II. except that

$$\delta = \delta_A - 1/K_A\{ (\delta - \delta_{HA})[H^+]\} \quad \text{(ref. 9)}$$

was used when appropriate. δ_{HA} and δ_A are the chemical shifts of the protonated and unprotonated species, respectively. δ is the observed chemical shift at a given pH.

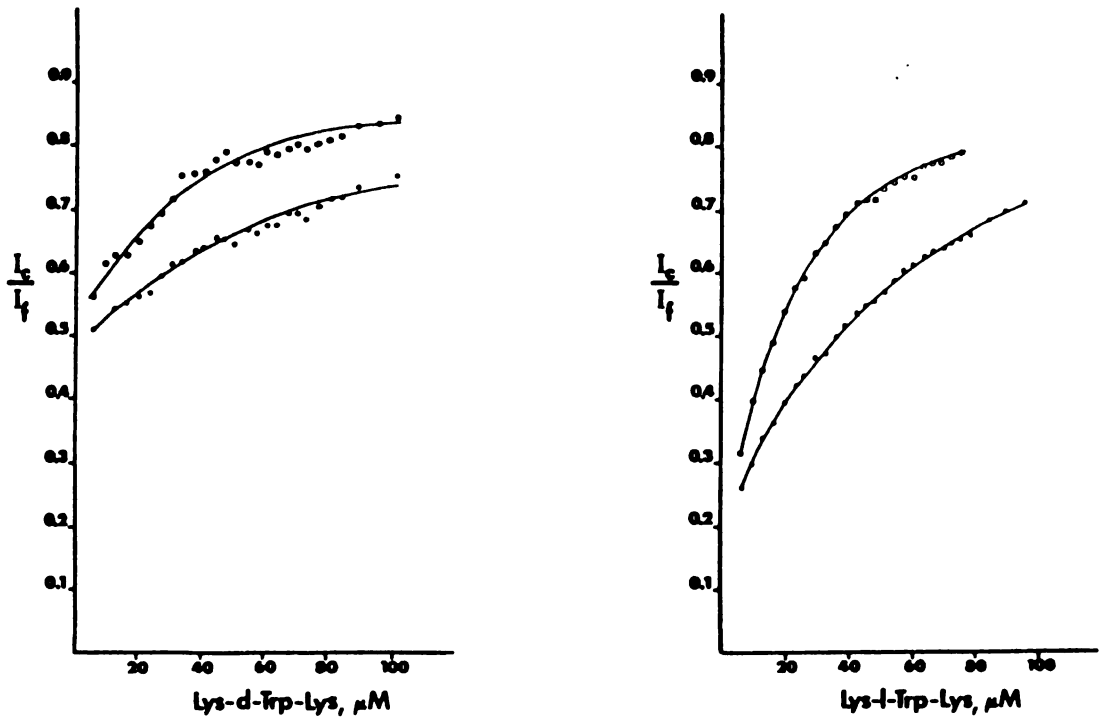

fig. 11: Fluorescence titration of double-stranded DNA with Tri(*d*), curves shown at the left, and Tri(*l*), right. The relative fluorescence change, I_c/I_f, as a function of tripeptide concentration at two different DNA concentrations, 195 μM (●—●) and 97 μM (○—○), is shown for each peptide.

$P_f + P_b = 1$ and

$C_b/C_t = P_b$; $C_f/C_t = P_f$

where C_t is the total concentration of tripeptide, and C_b and C_f are the tripeptide concentrations bound and free, respectively, it follows that

$$I_c = I_f(1 - C_b/C_t) + I_b(C_b/C_t)$$

which can be rearranged to give:

$$C_b = (1 - I_c/I_f/1 - I_b/I_f)C_t$$

The binding density ν, defined as C_b/P_o can then be expressed in terms of the fluorescence intensities:

$$\nu = C_b/P_o = \frac{C_t(1 - I_c/I_f)}{P_o(1 - I_b/I_f)}$$

In the present study, I_b/I_f was determined by measuring the fluorescence intensity at a high DNA concentration (~400 μM DNA/6 μM peptide) where all tripeptide was assumed to be bound. The value of I_b/I_f measured for Tri(*l*) in this manner was 0.24 and that for Tri(*d*) was 0.48. These same samples were then diluted with the appropriate amount of tripeptide (6 μM solution) to obtain the initial solutions for the titration with tripeptide.

The experimental data were analyzed using the equation developed by McGhee and von Hippel (18) to describe the binding of non-interacting ligands to a homogeneous one-dimensional lattice. The equation for this "excluded binding" model is given by:

$$\nu/C_f = K(1 - n\nu)(1 - n\nu/(1 - (n - 1)\nu))^{n-1} \qquad (7)$$

where "n" is the number of phosphates covered by one ligand, and "K" is the association constant. This equation corrects for non-linear (convex

downward) Scatchard plots which result from n ≥2; that is, the restriction of binding sites by neighbor exclusion.

Using this equation and plotting ν/C_f versus ν, a value for K is obtained from the y-intercept and a value for 1/n from the x-intercept. For the present study, a non-linear least squares fitting routine was used to obtain values for K from the fluorescence measurements. The best fit of the data is shown in fig. 12. The values obtained for the association constants were 7.7 x 10^4 M^{-1} and 6.2 x 10^4 M^{-1} for the *l*- and *d*-Trp peptides, respectively.

Thermal Denaturation Data. The relative affinities of these diasteriomeric tripeptides for native versus single-stranded DNA can be evaluated from the variations in the DNA melting temperature induced by the binding of these tripeptides. An increase in T_m (temperature at which the helix to coil transition is 50% complete) is expected if the DNA helix is stabilized by bound peptide while a lowering of the T_m would suggest a preferential binding to single-stranded DNA.

In order to minimize non-specific binding, these studies were done at low degrees of saturation. The tripeptide-DNA complexes were prepared at peptide/DNA phosphate ratios of 0.2 (100 μM peptide/500 μM DNA) and 0.1 (100 μM peptide/976 μM DNA). The melting transitions were monitored at 295 nm (fig. 13). For both diasteriomeric tripeptides an increase in the thermal stabilization of the DNA helix was observed (Table V.). The rise in T_m due to binding of the *d*-Trp containing peptide is 4°C less than that found for the *l*-Trp peptide at both ratios.

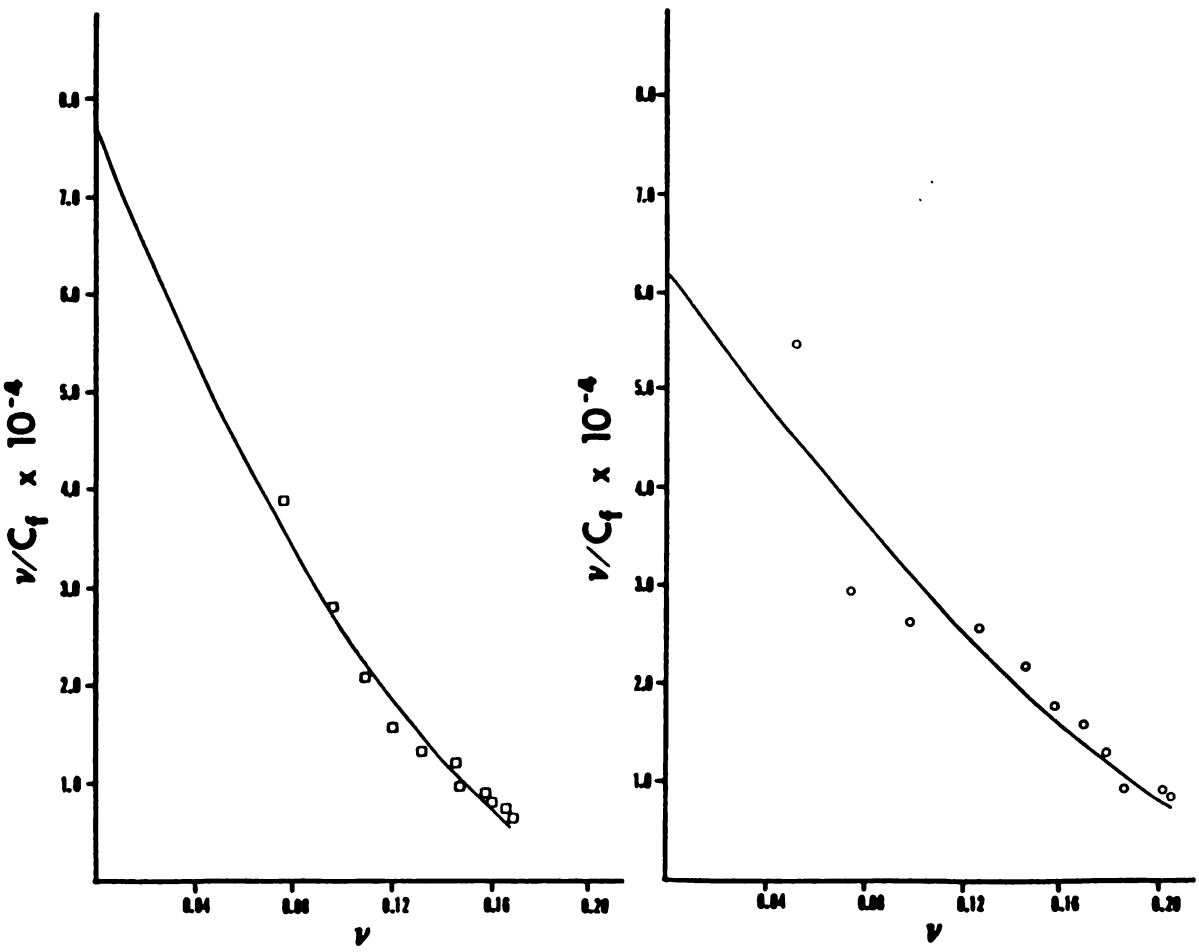

fig. 12: Scatchard plots for the binding of Tri(*l*), right, and Tri(*d*), left, to sonicated calf thymus DNA (97 μM). The curves represent the best fit of the fluorescence titration data according to the "excluded" binding model of McGhee and von Hippel (eqn. 7). The values obtained for the association constants are 7.7 x 10^4 M^{-1} with n = 4.1, and 6.2 x 10^4 M^{-1} with n = 3.2 for the *l*- and *d*-Trp peptides, respectively.

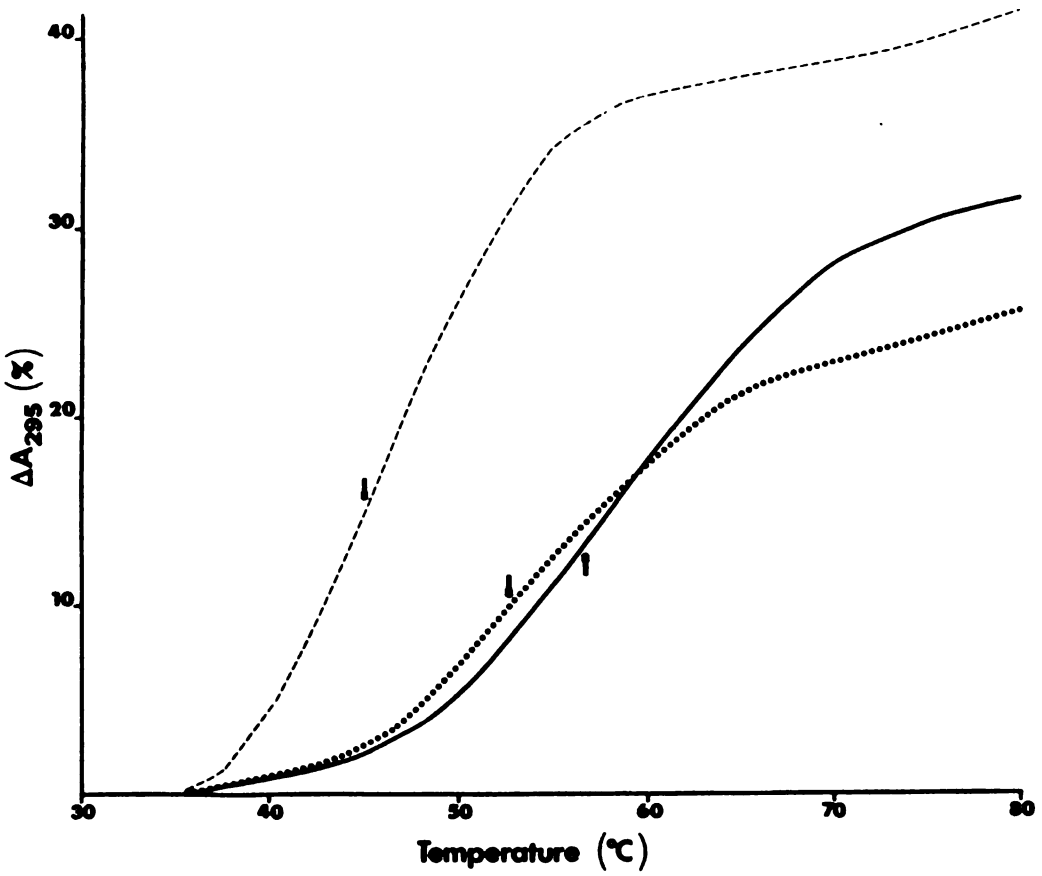

fig. 13: Thermal denaturation profiles of DNA, ———, and its complexes with Tri(*l*), ——— , and Tri(*d*), •••••, in 1.0 mM sodium cacodylate, 1.0 mM NaCl, and 0.1 mM EDTA, pH 6.0. The samples were prepared at a peptide/DNA phosphate ratio of 0.1 (100 μM peptide/976 μM DNA). The temperature was raised by 0.5°C/min. and the hyperchromicity monitored at 295 nm. The midpoint of each curve (peak of the derivative curve) is indicated by an arrow.

TABLE V. Rise in melting temperature of DNA due to the binding of Tri(*l*) and Tri(*d*).

[DNA] (M)	[Tri(*l*)] (M)	[Tri(*d*)] (M)	T_m[a] (°C)	ΔT_m[b] (°C)
5.0×10^{-4}			47.25	
5.0×10^{-4}	1.0×10^{-4}		63.75	16.5
5.0×10^{-4}		1.0×10^{-4}	59.25	12.0
9.8×10^{-4}			45.0	
9.8×10^{-4}	1.0×10^{-4}		56.75	11.75
9.8×10^{-4}		1.0×10^{-4}	52.75	7.45

[a] T_m values were determined from the derivative curves of the melting profiles.
[b] $\Delta T_m = T_m$complex - T_mDNA.

DISCUSSION

The ^{19}F NMR results presented here demonstrate that the diasteriomeric tripeptides, Lys-*l*-Trp-Lys and Lys-*d*-Trp-Lys, form distinct complexes with double-stranded DNA.

For both complexes, the lysyl residues are involved in electrostatic binding to the nucleic acid phosphates. The fluorine resonance position observed for each of the complexes returns to that found for the free tripeptides as the ionic strength of the solution is increased. Evidence that the binding of the *l*-Trp peptide to DNA involves an electrostatic contribution has been reported previously (4-7). The data presented here indicate that the *d*-Trp peptide is also electrostatically bound to DNA.

Analysis of the ionic strength dependence of the fluorine chemical shift for the complexes leads to an estimate of the number of ion pairs formed. The results indicate that for both peptides ~two positive charges participate in ion pair formation. The number of electrostatic bonds for the *l*-Trp-DNA complex has not been evaluated previously. However, from an identical analysis of the data available for the poly(rA) complex (19), Record et al. (11) found that this complex included three charge interactions. Since double-stranded DNA is less flexible than single-stranded poly(rA), the participation of fewer positive charges is reasonable.

Although both peptide complexes involve the same number of charge interactions, the ^{19}F NMR data indicate that changing the chirality about the α-carbon bond of the aromatic residue places the fluorine nucleus on the indole ring in different environments when these diasteriomers are complexed to DNA. For the *l*-Trp-containing peptide in its DNA complex, the fluorine resonance position shifts upfield from that found for the free

tripeptide. In proton NMR studies of aromatic molecules, upfield shifts of the proton resonances are observed if these molecules are associated through stacking interactions (20). These upfield shifts are a consequence of the ring current anisotropy of neighboring aromatic moieties. In the present study, ring current effects also induced an upfield shift of the fluorine resonance position for 5FTA which self-associates through stacking. The upfield shift observed for the *l*-Trp peptide complex, then, could be interpreted in terms of ring current effects, suggesting that the *l*-Trp ring is positioned in close proximity to the nucleic acid bases. Also, the magnitude of the upfield shift (-0.48 ppm) is too large to be totally accounted for in terms of changes occuring with the positively charged groups. A smaller upfield shift of -0.18 ppm was observed in the pH titration study. This interpretation of the fluorine chemical shift is consistent with the results of a previous proton NMR study (7) of the *l*-Trp peptide-DNA complex. An upfield shift of the C-2 indole proton was observed and attributed to ring current effects of the DNA bases.

The ^{19}F NMR relaxation measurements provide further information on the differences between the DNA complexes formed by these two diasteriomeric tripeptides. The relaxation parameters reflect the relative mobilities of the indole ring when in the presence of DNA. If the *l*-Trp ring is partially stacked with the bases of the DNA, the mobility of the indole ring should be restricted, perhaps more than that of the *d*-Trp. For the *l*-Trp-containing peptide, a substantial increase in linewidth from 1 to 70 Hz is observed upon complex formation, accompanied by a decrease in both the NOE and T_1 values. In contrast, for its diasteriomer, much less increase in the linewidth (from 1 to 6 Hz) is observed upon binding to DNA, while the NOE and T_1 values also decrease.

A broadening of the fluorine resonance line is expected upon binding due to the imposed restriction in tumbling. The significant difference in the values observed for the two complexes may be due partially to a constraint of the *l*-Trp ring when it is bound to DNA. However, the linewidth could conceivably represent a sum of contributions from several factors. Contributions from chemical exchange processes are reflected in the temperature dependence of the linewidth. The rate of change in the line-broadening with decreasing temperature is essentially the same for both peptide complexes. The activation energy estimated from this data (~7 kcal) is higher than that expected from the simple decrease in overall correlation time of the DNA over this temperature range (29). This suggests a partial contribution to the linewidth from chemical exchange. Since the temperature dependence of the linewidth is the same for both complexes, the marked increase of the *l*-Trp peptide complex over that observed for the *d*-Trp complex is apparently due to a considerable decrease in the mobility of the *l*-Trp indole ring when complexed to DNA.

Although the T_1 values are markedly decreased when both peptides are bound, the *l*-Trp peptide more so than the *d*-Trp peptide, the variation in values is not as striking as with the linewidths. A substantial decrease in T_1 is expected for a small ligand bound to a large polymer which has a much longer correlation time. The fact that the values for the complexes are similar is not inconsistent with the idea that the relative mobilities of the aromatic rings are different for the diasteriomeric tripeptide-DNA complexes. The T_1 for fluorine has a broad minimum that can cover a range of correlation times (see fig. 9). Therefore, although comparison of the T_1 values measured for the free tripeptides with those for these peptides in the presence of DNA indicate complex formation, the T_1 appears

to be relatively insensitive in the region that could distinguish the two complexes. The NOE, on the other hand decreases rapidly in this range of correlation times (see fig. 9). The lower NOE value observed for the *l*-Trp containing peptide is consistent with the idea that the mobility of the *l*-Trp indole ring is restricted to a greater extent that the *d*-Trp ring when complexed to DNA; the somewhat lower T_1 value also supports this notion.

Values for the relative binding affinities of both tripeptides to DNA were obtained from an analysis of the fluorescence titration data. The fluorescence intensity of the tryptophan is quenched for both peptides. Under conditions where nearly all of the peptide should be bound (6 μM Tri/400 μM DNA phosphate), a decrease in fluorescence intensity of approximately 74% is observed for the *l*-Trp peptide. In previous fluorescence studies of the DNA complex with the unfluorinated *l*-Trp peptide, quenching was also observed (4,5,6,15-17,19). However, only approximately 30% quenching was reported (16) at low degrees of saturation (13.5 μM Tri(*l*)/700 μM DNA). Although direct comparison with this data is not possible because of slight differences in the experimental conditions (ie. study was done at 10°C and correction for inner filter effect was necessary), the extent of quenching is significantly less than that observed for the fluorinated analog. This discrepancy could indicate that the fluorine label influences the binding characteristics of this tripeptide or that the fluorine merely enhances the mechanism(s) by which the tryptophan is quenched. Comparison of the binding constants suggests the latter explanation. Using the "excluded" binding model of McGhee and von Hippel to evaluate the fluorescence data, Record et al.(15) reported a binding constant of 8.0×10^4 M^{-1} for the *l*-Trp peptide with DNA. This is in good agreement with the value obtained here for the fluorinated derivative (7.7

x 10^4 M^{-1}) using the same experimental conditions and method of analysis.

For the *d*-Trp-containing tripeptide, the tryptophan fluorescence was also quenched upon binding. The amount of quenching (~52%) is substantially less than that found for its diasteriomer. In previous investigations, the quenching of the *l*-Trp peptide in the presence of various polynucleotides has been attributed to the stacking of the indole ring with the nucleic acid bases (22). However, for the fluorinated analog the fluorine appears to have an effect on the amount of quenching. Thus the quenching observed for the *d*-Trp peptide, and subsequently used to obtain the binding constant, may not be due to stacking. A binding constant of 6.2 x 10^4 M^{-1} was determined from the fluorescence data obtained for the *d*-Trp peptide. This value is comparable to that found for its diasteriomer.

In previous studies by Helene and coworkers, the fluorescence data for the unfluorinated tripeptide was analyzed assuming two types of bound peptide molecules (4,5,15-17,19). This assumption is supported by fluorescence decay time measurements determined for the tripeptide free and in the presence of several polynucleotides, including DNA (16,17). Analysis of their data according to the following binding process:

$$\textit{l}\text{-Trp peptide} + \text{DNA} \overset{K_1}{\rightleftharpoons} \text{Complex(I)} \overset{K_2}{\rightleftharpoons} \text{Complex(II)}$$

leads to values of K_1 = 7.3 x 10^4 M^{-1} and K_2 = 0.36. Both complexes involve electrostatic interactions. Complex(II) includes an additional stacking of the tryptophan with the nucleic acid bases. K_1 measures the electrostatic contribution; K_2 is the ratio of concentrations of stacked to unstacked molecules. It can be seen that the contribution of K_2 to the overall bind-

ing constant, $K = K_1(1 + K_2)$, is small. Since the fluorescence decay parameters for the two fluorinated tripeptides are not available, no assumptions concerning the number of complexes could be made in the present investigation. However, for both of these tripeptides, the major contribution to the binding constant should also result from the electrostatic interactions. Thus, that the *l*-Trp peptide complex may involve an additional interaction besides electrostatic binding as suggested by the ^{19}F NMR data, is not incompatible with the similarity in binding affinities.

The variations in the melting temperature of DNA induced by the binding of these tripeptides also suggests that the diasteriomers form distinct DNA complexes. From the UV absorbance measurements, both peptides were found to increase the T_m of the helix to coil transition of calf thymus DNA. This behavior is expected since the electrostatic potential of double-stranded DNA is higher than that of single strands, and both peptides are bound electrostatically. The differences in the complexes formed are reflected in the fact that the *l*-Trp peptide is more effective in stabilizing the DNA helix relative to the random coil structure than its diasteriomer. This suggests that the *l*-Trp peptide prefers the double-stranded form more than its diasteriomer. The small (4°C), but significant, difference in the melting temperatures for the two complexes, is not detectable within the accuracy of the melting curves obtained using fluorine NMR.

Our observations of the complexes formed by these two diasteriomeric peptides support the findings of Gabbay et. al. (2,3). In an investigation of Lys-*l*-Phe-amide- and Lys-*d*-Phe-amide-DNA complexes, evidence for the partial insertion of the *l*-Phe ring between the bases was

obtained while this was not observed for the *d*-Phe ring. On the basis of these data, it was proposed that the positive charges of the lysine residues were stereospecifically bound to the DNA and therefore dictated the direction in which the aromatic ring would point: either in towards the helix or out away from it. The ^{19}F NMR data of the present study suggests that the *l*-Trp indole ring also interacts to some extent with the nucleic acid bases. The upfield shift and the decrease in mobility of the *l*-Trp residue in the presence of DNA relative to its diasteriomer suggests that the two complexes differ in the position of the aromatic ring with respect to the helix as proposed by Gabbay.

Extensive studies of the nucleic acid complexes formed by oligopeptides containing aromatic amino acids have lead to the proposed "partial insertion" model (2,3,23,24). According to this model, the *l*-aromatic amino acid is stacked between two consecutive bases on the same DNA strand. The insertion of the aromatic residue would result in a slight bending of the helix. This model differs from that found for the classical intercalators which involves the unstacking of two base pairs with concommitant unwinding of the DNA helix (25). Comparison of the ^{19}F NMR data for several fluorinated intercalators (26,27) obtained previously in our laboratory with that presented here for these tryptophan-peptides also suggests that the indole ring is bound to DNA in a mode distinct from that found for the classical intercalators. This difference was also indicated by the ^{19}F NMR results obtained for 5FTA in its complex with DNA (21). For drugs which are bound by intercalation, the ^{19}F NMR chemical shift induced upon binding can have contributions from several sources. Among these, ring current effects which cause an upfield shift and solvent effects, where transfer from an aqueous to a non-polar environment

usually causes a downfield shift (28), are expected to dominate. A large downfield shift of the fluorine resonance (1.6 ppm) was observed when both fluoroquine and fluoroquinacrine were associated with DNA (26,27). For these complexes, no solvent-induced shift was observed which is appropriate for a fluorine nucleus not interacting with the solvent. The ^{19}F NMR data for these drugs is consistent with the intercalative mode of binding; that is, that the fluorine nucleus is positioned in the hydrophobic area between base pairs which is inaccessible to solvent. For the *l*-Trp-containing peptide, on the other hand, the direction of the chemical shift for the complex is upfield relative to that found for the free tripeptide and the full solvent-induced shift is observed. The data obtained for the *l*-Trp peptide indicate that the mode of binding to DNA is different than that found for the intercalating drugs. The fluorine of the indole ring is exposed to solvent and therefore is not in an hydrophobic region; however, the upfield shift suggests that there is some overlap of the aromatic ring with the nucleic acid bases.

In conclusion, the results of the present study indicate that the aromatic indole ring of the tripeptide lysyl-5-fluoro-*l*-tryptophyl-lysine is involved in a stacking interaction when bound to double-stranded DNA. The data are consistent with the idea that the tryptophyl ring is not intercalated in the classical sense but partially inserted between the bases of one strand of the double helix. Changing the chirality of the aromatic residue modifies the mode of binding. Although Lys-*d*-Trp-Lys participates in the same number of electrostatic bonds and exhibits the same affinity for double-stranded DNA, the *d*-Trp peptide-DNA complex is easily discriminated by ^{19}F NMR. The *d*-Trp indole ring does not appear to associate with the nucleic acid bases of DNA.

References

1. **Helene, C. and Maurizot, J. C.,** Interactions of Oligopeptides with Nucleic Acids, *CRC Critical Rev. Biochem., 10,* 213-258, (1981).

2. **Adawadkar, P., Wilson, w. d., Brey, W. and Gabbay, E. J.,** Stereospecific Interaction of Dipeptide Amides with DNA. Evidence for Partial Intercalation and Bending of the Helix, *J. Am. Chem. Soc., 97,* 1959-1961, (1975).

3. **Gabbay, E. J., Adawadkar, P. D. and Wilson, W. D.,** Stereospecific Binding of Diastereomeric Peptides to Salmon Sperm DNA, *Biochemistry, 15,* 146-151, (1976).

4. **Toulme, J. J., Charlier, M. and Helene, C.,** Specific Recognition of Single-Stranded Regions in Untraviolet-irradiated and Heat-denatured DNA by Tryptophan-containing Peptides, *Proc. Nat. Acad. Sci. USA, 71,* 3185-3188, (1974).

5. **Toulme, J. J. and Helene, C.,** Specific Recognition of Single-Stranded Nucleic Acids. Interaction of Tryptophan-containing Peptides with Native, Denatured and Ultraviolet-irradiated DNA, *J. Biol. Chem., 252,* 244-249, (1977).

6. **Helene, C. and Dimicoli, J. L.,** Interaction of Oligopeptides containing Aromatic Amino Acids with Nucleic Acids. Fluorescence and Proton Magnetic Resonance Studies, *FEBS Lett., 26,* 6-10, (1972).

7. **Dimicoli, J. L. and Helene, C.,** Interactions of Aromatic Residues of Proteins with Nucleic Acids. I. Proton Magnetic Resonance Studies of the Binding of Tryptophan-containing Peptides to Poly(adenylic acid) and Deoxyribonucleic Acid, *Biochemistry, 13,* 714-723, (1974).

8. **Greenstein, J. P. and Winitz, M.**, Amino Acids as Dipolar Ions, *In Chemistry of the Amino Acids*, John Wiley and Sons, Inc., N.Y., vol. 1, Chap. 4, 486, (1961).

9. **Giralt, E., Viladrich, R. and Pedroso, E.**, Determination of Acid Dissociation Constants of Histidine-Containing Peptides by Proton Magnetic Resonance Spectroscopy, *Organic Magnetic Resonance*, *21*, 208-213, (1983).

10. **Dimicoli, J. L. and Helene, C.**, Complex Formation between Purine and Indole Derivatives in Aqueous Solutions. Proton Magnetic Resonance Studies, *J. Amer. Chem. Soc.*, *95*, 1036-1044, (1973).

11. **Record, T. M., Lohman, T. M. and de Haseth, P.**, Ion Effects on Ligand-Nucleic Acid Interactions, *J. Mol. Biol.*, *107*, 145-158, (1976).

12. **Maurizot, J. C., Boubault, G. and Helene, C.**, Interaction of Aromatic Residues of Proteins with Nucleic Acids. Binding of Oligopeptides to Copolynucleotides of Adenine and Cytosine, *Biochemistry*, *17*, 2096-2101, (1978).

13. **Helene, C., Toulme, J. J. and Le Doan, T.**, A Spectroscopic Probe of Stacking Interactions between Nucleic Acid Bases and Tryptophan Residues of Proteins, *Nucl. Acids Res.*, *7*, 1945-1953, (1979).

14. **Porschke, D.**, Structure and Dynamics of a Tryptophane Peptide-Polynucleotide Complex, *Nucl. Acids Res.*, *8*, 1591-1612, (1980).

15. **Porschke, D. and Ronnenberg, J.**, The Reaction of Aromatic Peptides with Double Helical DNA. Quantitative Characterization of a Two Step Reaction Scheme, *Biophys. Chem.*, *13*, 283-290, (1981).

16. **Montenay-Garestier, T., Brochon, J. C. and Helene, C.**, Complex Formation between Tryptophan-Containing Peptides and Nucleic Acids: Fluorescence Decay Studies using Synchrotron Radiation, *Intern. J. Quant. Chem.*, *20*, 41-48, (1981).

17. **Montenay-Garestier, T., Fidy, J., Brochon, J. C. and Helene, C.,** Dynamics of Peptide-nucleic acid Complexes. Fluorescence Polarization Studies, *Biochimie, 63*, 937-940, (1981).

18. **McGee, J. D. and von Hippel, P. H.,** Theorectical Aspects of DNA-Protein Interactions: Co-operative and Non-co-operative Binding of Large Ligands to a One-dimensional Homogeneous Lattice, *J. Mol. Biol., 86*, 469-489, (1974).

19. **Brun, F., Toulme, J. J., and Helene, C.,** Interactions of Aromatic Residues of Proteins with Nucleic Acids. Fluorescence Studies of the Binding of Oligopeptides Containin Tryptophan and Tyrosine Residues to Polynucleotides, *Biochemistry, 14*, 558-563, (1975).

20. **Giessner-Prettre, C. and Pullman, B.,** Intermolecular Nuclear Shielding Values for Protons or Purines and Flavins, *J. theor. Biol, 27*, 87-95, (1970).

21. **Mirau, P. A., Shafer, R. H. and James, T. L.,** Binding of 5-Fluorotryptamine to Polynucleotides as a Model for Protein-Nucleic Acid Interactions: Fluorine-19 Nuclear Magnetic Resonance, Absorption, and Fluorescence Studies, *Biochemistry, 21*, 615-620, (1982).

22. **Helene, C.,** Mechanisms of Quenching of Aromatic Amino Acid Fluorescence in Protein-Nucleic Acid Complexes, *In Excited States in Organic Chemistry and Biochemistry*, (eds. B. Pulmman and N. Goldblum), Reidel Press, 65-78, (1977).

23. **Gabbay, E. J., Sanford, K. and Baxter, C.S.,** Specific Interaction of Peptides with Nucleic Acids, *Biochemistry, 11*, 3429-3435, (1972).

24. **Gabbay, E. J., Sanford, K., Baxter, C. S. and Kapicak, L.,** Specific Interaction of Peptides with Nucleic Acids. Evidence for a "Selective Bookmark" Recognition Hypothesis, *Biochemistry, 12*, 4021-4029, (1973).

25. **Lerman, L. S.**, Structural Considerations in the Interaction of DNA and Acridines, *J. Mol. Biol.*, *3*, 18-30, (1961).

26. **Bolton, P. H., Mirau, P. A., Shafer, R. H. and James, T. L.**, Interaction of the Antimalarial Drug Fluoroquine with DNA, tRNA, and Poly(A): ^{19}F NMR Chemical-Shift and Relaxation , Optical Absorption, and Fluorescence Studies, *Biopolymers*, *20*, 435-449, (1981).

27. **Mirau, P. A., Shafer, R. H., James, T. L. and Bolton, P. H.**, Fluoroquinacrine Binding to Nucleic Acids: Investigation of the ^{19}F-NMR, Optical, and Fluorescence Properties in the Presence of DNA, Poly(A), and tRNA, *Biopolymers*, *21*, 909-921, (1982).

28. **Sykes, B. D. and Weiner, J. H.**, Biosynthesis and ^{19}F NMR Characterization of Fluoroamino Acid Containing Proteins, *In Magnetic Resonance in Biology* (ed. J. S. Cohen), Wiley-Interscience, 171-197, (1980).

29. **Bolton, P. H. and James, T. L.**, Molecular Motions in RNA and DNA Investigated by Phosphorus-31 and Carbon-13 NMR Relaxation, *J. Phys. Chem.*, *83*, 3359-3366, (1979).

CHAPTER IV

COMPLEX FORMATION BETWEEN DIASTERIOMERIC TRYPTOPHAN-CONTAINING TRIPEPTIDES AND APURINIC DNA.

INTRODUCTION

The results of a recent binding study (1), followed by fluorescence spectroscopy, indicated that the affinity of the tripeptide, Lys-*l*-Trp-Lys, for double-stranded DNA, increased after the introduction of apurinic sites. The binding affinity was shown to increase in proportion to the level of depurination. It was proposed that the aromatic amino acid, by substituting for the missing purine, was responsible for the selection and preferential binding at the apurinic sites. This interpretation suggests the possibility that aromatic amino acids could play an important role in DNA repair mechanisms. The in vivo repair of some forms of damaged DNA requires the selective recognition of apurinic sites (2,review). These sites are created by the enzymatic removal of damaged purines, and are subsequently located by Ap endonucleases which catalyze the cleavage of the phosphate backbone at this site.

The potential of this simple tripeptide as a model for the study of DNA repair enzymes is substantiated further by recent experimental evidence that this peptide is also capable of promoting strand breakage of apurinic DNA (3,4,5). Thus this tripeptide not only appears to locate apurinic sites as is done by the apurinic endonucleases but also mimics the catalytic activity of these repair enzymes. The ability of this peptide to facilitate cleavage, also appears to be linked to the presence of the aromatic residue, tryptophan. It has been proposed that the tryptophan binds at the apurinic site and positions the lysyl amino group(s), responsible for chain breakage, in close proximity to the reactive group at the apurinic site (4).

The data presented in Chapter III demonstrate that Lys-*d*-Trp-Lys forms a complex with double-stranded DNA which is distinct from that of

Lys-*l*-Trp-Lys. The tryptophan moieties are in different environments which are easily discriminated by ^{19}F NMR since the fluorine chemical shift is a sensitive indicator of differences in the local environment of the fluorine nucleus. If the tryptophan is bound in an unique manner at apurinic sites as compared to native DNA, this should also be reflected in the fluorine chemical shift. In addition, differences in the complexes formed by the two diasteriomers can also be observed. If the tryptophan ring plays an important role in the cleavage of apurinic DNA, any differences in the position of the indole ring manifested by ^{19}F NMR studies should also cause significant differences in their relative nicking activities.

This chapter contains the ^{19}F NMR and fluorescence results obtained for the complexes formed with apurinic DNA. In addition, the ability of both of these tripeptides to cleave DNA at apurinic sites has been examined.

RESULTS

^{19}F NMR Studies. The *l*-Trp peptide has been shown to cleave DNA at apurinic sites. All studies of the nicking activity have been done using supercoiled plasmid DNA. Cleavage of linear DNA has not been observed (personal communication, Claude Helene). The ^{19}F NMR studies were done at 37°C in order to be able to compare these data with those obtained with native DNA.

A. Titration of the Tripeptides with Apurinic DNA. The *d*- and *l*-tryptophan-containing diasteriomers of Lys-5FTrp-Lys were titrated with DNA modified to contain ~5% apurinic sites. The changes in the ^{19}F chem-

ical shift observed as a function of phosphate-to-tripeptide ratio are shown in fig. 1. The fluorine resonance position of the *l*-Trp peptide shifts upfield as the concentration of apurinic DNA increases. At a ratio of 25:1, the magnitude of the upfield shift is -0.41 ppm. The direction of the fluorine chemical shift of the *d*-Trp peptide complex is also upfield. However, at the same ratio (25:1) a shift of only -0.06 ppm is observed.

B. Temperature Dependence of the Linewidth. The observed linewidth for both of these tripeptides increases as the concentration of depurinated DNA is raised. The increase in linewidth for the *l*-Trp peptide complex (16 Hz) is greater that that for its diasteriomer (4 Hz). In order to determine possible contributions from chemical exchange processes, the linewidth was monitored as a function of temperature for both tripeptide-apurinic DNA complexes (Table I). The signal for the *l*-Trp peptide complex is broadened to a greater extent than that of the *d*-Trp peptide complex as the temperature is decreased from 37 to 20°C.

Fluorescence Data. The affinities of both of these tripeptides for apurinic DNA were determined using fluorescence spectroscopy. The extent of quenching observed as a function of tripeptide concentration is shown in fig. 2. The data were obtained under the same experimental conditions and analyzed by the same methods as used for the native DNA complexes. These procedures are described in chapter III. These measurements were performed at several apurinic DNA concentrations (99 and 197 μM). I_b/I_f ratios, were 0.21 and 0.35 for the *l*- and *d*-Trp peptides, respectively. Association constants of 5.3 x 10^4 M^{-1} and 7.0 x 10^4 M^{-1} for the *l*-Trp and *d*-Trp peptides, respectively, were obtained by fitting the data to

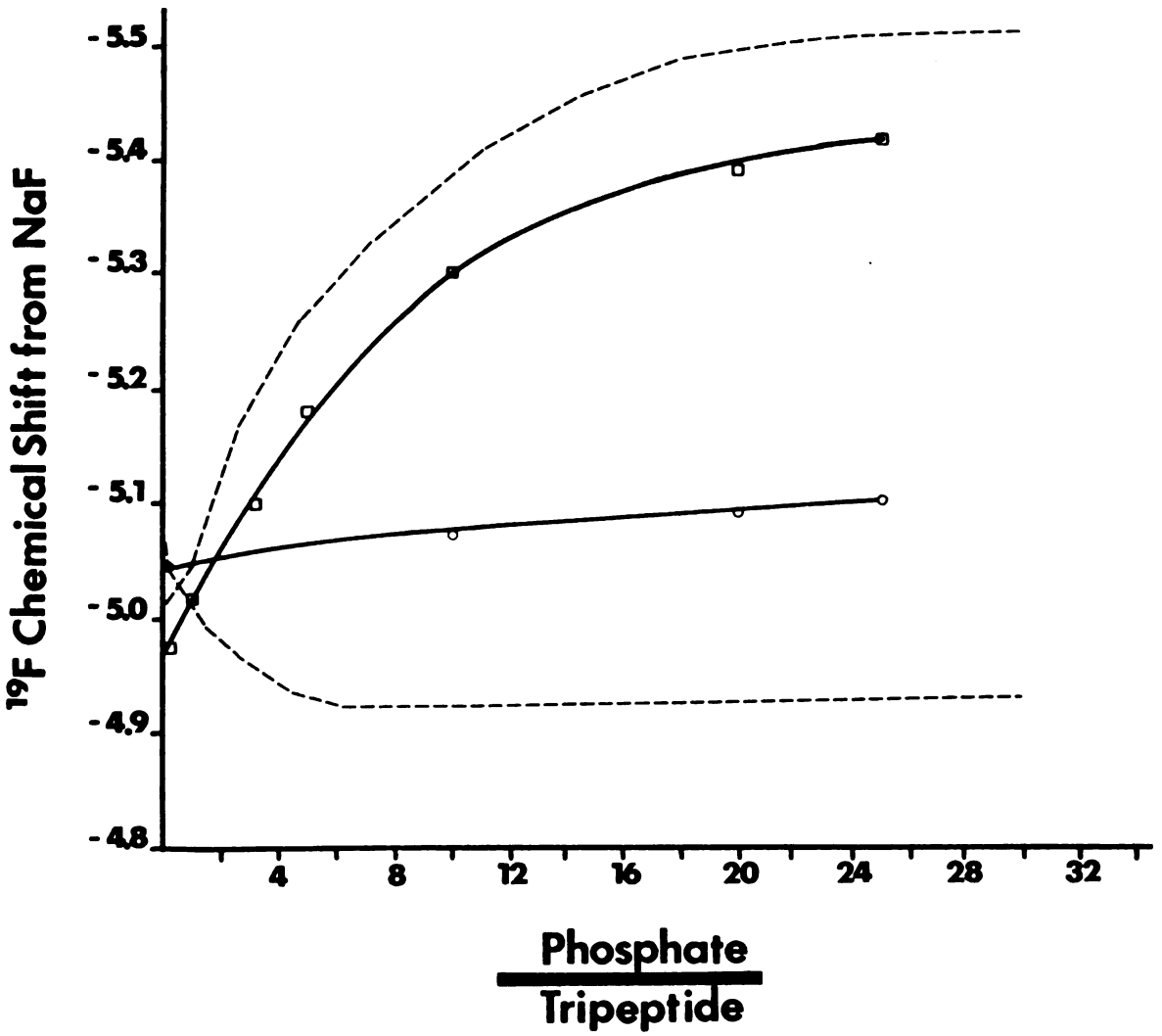

fig. 1: Plot of the ^{19}F NMR chemical shifts for both Tri(*l*), □—□, and Tri(*d*), ○—○, as a function of phosphate/tripeptide ratio. Solid curves were obtained using DNA modified to contain ~5% apurinic sites. For comparison the dashed curves obtained with native DNA are included. The curves were generated by titrating a solution containing 3 mM peptide with a solution 75 mM in DNA phosphates and 3 mM in peptide. Both solutions were in 10 mM sodium cacodylate; 10 mM sodium chloride; 1 mM EDTA; pH 6.0, containing 10% D_2O. The titrations were done at 37°C.

TABLE I. Linewidth as a function of temperature for the tripeptides free and complexed to 5% depurinated DNA.

Temperature (°C)	Linewidth[a] (Hz)			
	Tri(*l*)	Tri(*d*)	Tri(*l*) + Ap-DNA	Tri(*d*) + Ap-DNA
20.1	2	2	40	11
25.2	2	2	36	8
30.2		2	20	6
37.3	1	1	17	5

[a] Values are corrected for the applied line broadening.

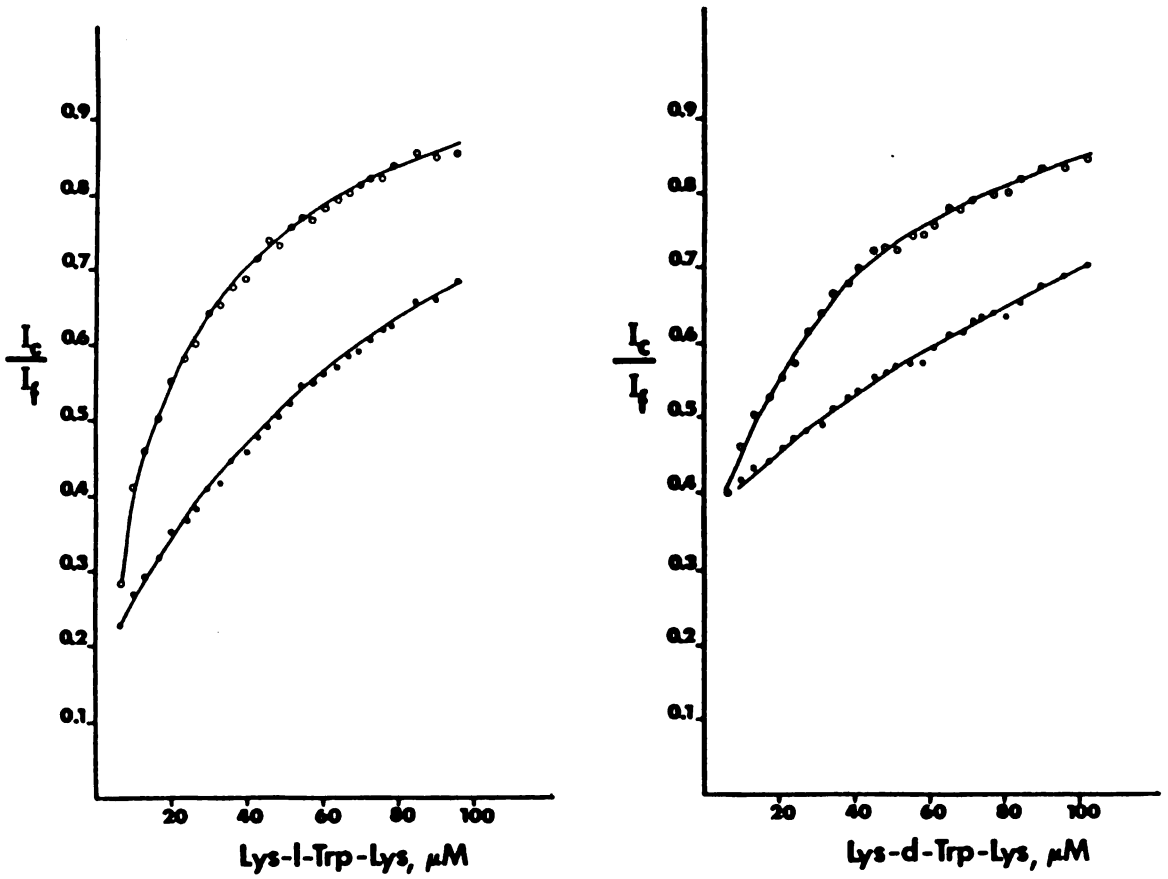

fig. 2: Fluorescence titration of 5% depurinated DNA with Tri(*l*), curves shown at the left, and Tri(*d*), right. The relative fluorescence change, I_c/I_f, as a function of tripeptide concentration at two different DNA concentrations, 197 μM (●—●) and 99 μM (○—○), is shown for each peptide where I_c and I_f are the intensities measured in the presence and absence of apurinic DNA, respectively.

the McGhee and von Hippel equation (eqn 7, chapter III). The best fit of the data for each tripeptide is shown in fig. 3.

Nicking Activity of Both Diasteriomeric Tripeptides. The ability of these tripeptides to cleave DNA at apurinic sites was examined using agarose gel electrophoresis. Single-strand cleavage of plasmid DNA, converts the supercoiled to the relaxed form. For plasmid pBR322 DNA, these two forms are well-separated on 1% agarose gels, the supercoiled form migrating in front of the nicked form.

Plasmid pBR322 DNA was prepared to contain an average of one apurinic site per molecule. The plasmid DNA pellet, recovered by precipitation with 95% ethanol, was dissolved in 1.0 mM sodium cacodylate, 1.0 mM NaCl, 0.2 mM EDTA, pH 6.0. This DNA (200 μM in 10 μl) was incubated at 37°C with 10 μl of 100 μM Tri(*l*) or Tri(*d*). The control was run with 10 μl added buffer. Aliquots (2 μl; 0.13 μg) were removed at 10 min intervals from zero to 60 min and placed on ice. The samples were loaded on 1% agarose gels which were subsequently stained with ethidium bromide and photographed. The negatives were scanned and the relative amounts of nicked and supercoiled plasmid molecules determined from the area under the appropriate peaks. Neither tripeptide introduces nicks into native pBR322 DNA (fig. 4). Both tripeptides promote cleavage of pBR322 DNA which contains apurinic sites. The rate at which nicks are introduced is the same for both diasteriomers.

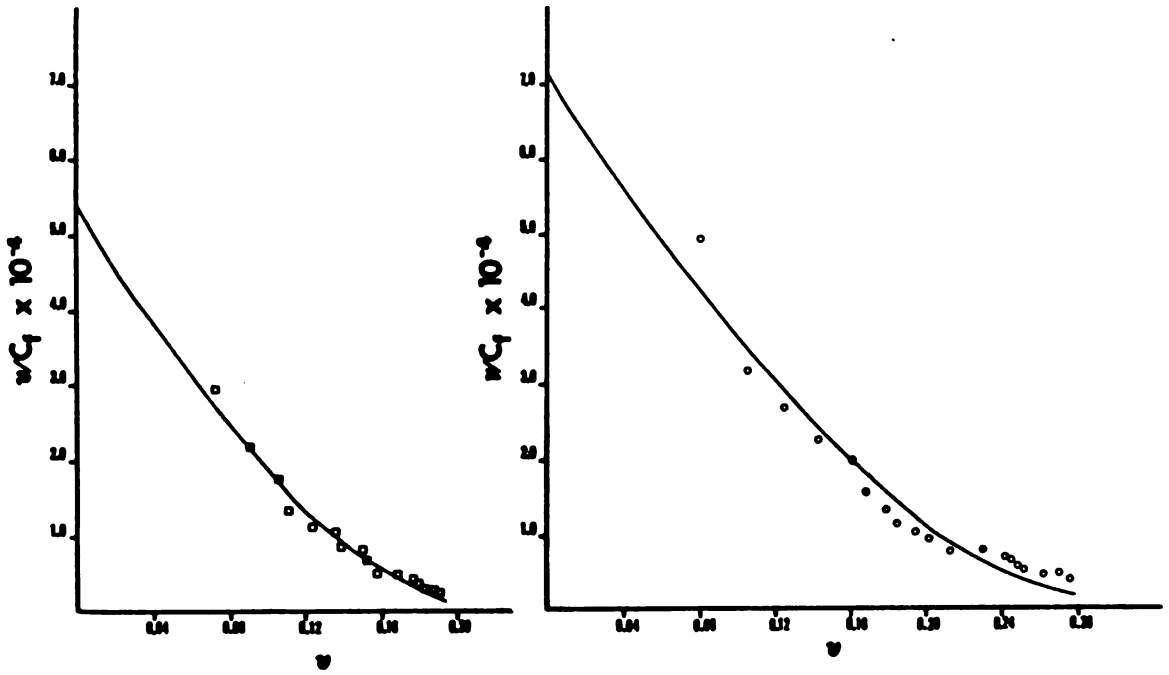

fig. 3: Scatchard plots for the binding of Tri(*l*), left, and Tri(*d*), right, to 5% depurinated DNA (99 μM). The curves represent the best fit of the fluorescence titration data according to the "excluded" binding model of McGhee and von Hippel (eqn. 7, Chap. III). The values obtained for the association constants are 5.3 x 10^4 M^{-1} with n = 4.1, and 7.0 x 10^4 M^{-1} with n = 3.1 for the *l*- and *d*-Trp peptides, respectively.

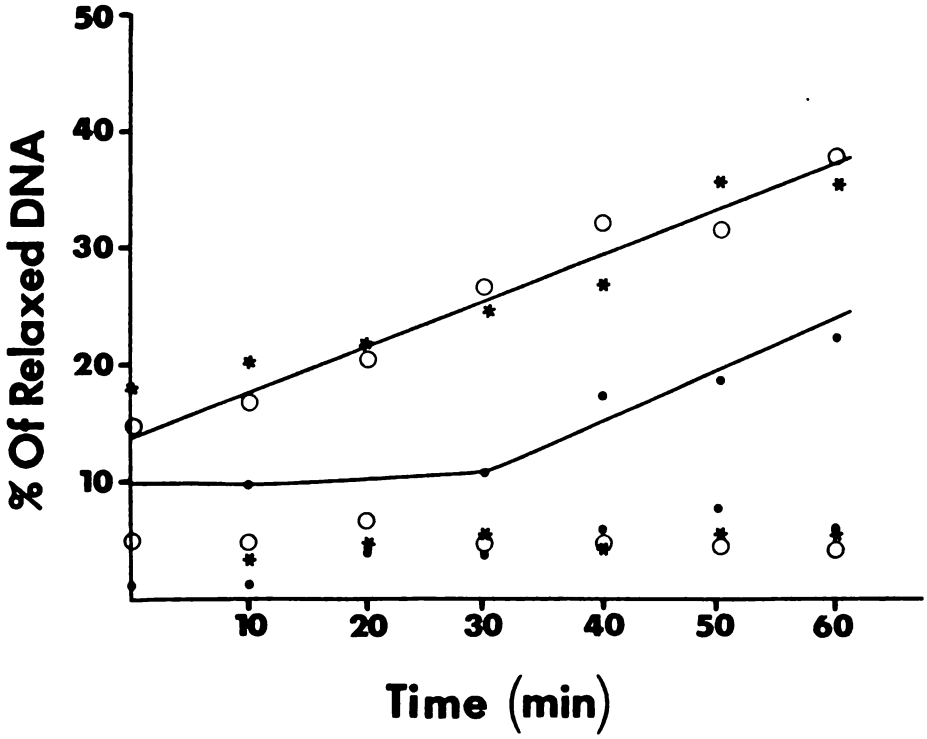

fig. 4: Chain nicking of pBR322 DNA containing an average of one apurinic site per molecule alone, ●—●, and on incubation with Tri(*l*),○—○, and Tri(*d*), ✱—✱. Data points obtained for native pBR322 alone (●), and in the presence of Tri(*l*), (○), and Tri(*d*), (✱) under the same conditions were obtained as controlls. The conversion of supercoiled plasmid to the relaxed form was monitored on 1% agarose gels. Negatives of the ethidium bromide-stained gels were scanned. The peaks were cut out and weighed; the % relaxed was determined from the area of relaxed/area of relaxed + supercoiled.

DISCUSSION

The ^{19}F NMR data presented here suggest that both peptides, Lys-*l*-Trp-Lys and Lys-*d*-Trp-Lys, form complexes with depurinated DNA which are distinct from those formed with native DNA. With depurinated DNA an additional type of binding site (apurinic site) has been introduced. The differences observed in the ^{19}F NMR parameters when these peptides are in the presence of apurinic versus native DNA could be due to molecules bound exclusively to apurinic sites or molecules bound at both apurinic and native sites. Since a single peak is observed in the presence of depurinated DNA, these peptides would have to be in fast exchange between the various sites if the measurements reflect an average of molecules bound to both sites. However, the relative binding affinities of the *l*-Trp peptide to apurinic and native sites have been studied previously (1). Based on fluorescence titration data obtained at various levels of depurination, Helene and coworkers have deduced that the affinity of this tripeptide for an apurinic site is approximately two orders of magnitude higher than that for a native site (1). Given that Lys-Trp-Lys binds strongly and preferentially to apurinic sites, it is reasonable to assume that the ^{19}F NMR results can be attributed to distinct modes of binding at the apurinic site.

When 5% of the purine bases are removed from native DNA, differences in both the ^{19}F NMR chemical shift and linewidth measurements are observed. There is a deshielding of the *l*-Trp peptide (0.08 ppm downfield shift) in the apurinic site versus the native site. In contrast, the *d*-Trp peptide is more shielded (0.19 ppm upfield shift) in the apurinic site than in the native site. However, as reflected in the linewidth meas-

urements, only the *l*-Trp peptide complex experiences a change in its dynamic state between the native and apurinic sites. The increase in the observed linewidth is considerably less in the presence of depurinated DNA as compared to native (17 Hz vs 70 Hz). While the change in the chemical shift for the *d*-Trp peptide is substantial (0.19 ppm), the linewidth is not altered by the introduction of apurinic sites. The temperature dependence of the linewidth observed for both peptides is essentially the same with depurinated DNA as with native DNA, suggesting that,to the extent that exchange contributes, all linewidths contain the same contribution. The data indicate that the indole ring of the *l*-Trp peptide is more constrained than that of its diasteriomer in the presence of apurinic DNA. In addition, the mobility of the *l*-Trp ring is less restricted at the apurinic site where a cavity has been created by removal of a purine, than at the native site.

The overall binding affinities of these tripeptides for apurinic DNA, calculated from the fluorescence data, are not significantly different than those obtained with native DNA. In addition, no significant difference between the binding affinities of these two diasteriomers is observed before or after depurination. Helene and coworkers, also using the results of fluorescence data, have reported overall association constants for the *l*-Trp peptide of 1.6 x 10^4 M^{-1} and 1.0 x 10^5 M^{-1} for native and apurinic DNA (5%) at 4°, respectively (1). The data, obtained at low degrees of saturation, were analyzed assuming the formation of two types of complexes, as discussed in chapter III. The difference in affinities is less than an order of magnitude which is not necessarily within the accuracy of the Scatchard analysis used for the fluorinated analog. In their study the strong binding of the tripeptide at apurinic sites over native sites was

based on the analysis of data obtained at different levels of depurination (0.3% to 5%). In the present study only 5% depurinated DNA was used. The binding constants of 5.3 x 10^4 M^{-1} and 7.0 x 10^4 M^{-1} for the *l*-Trp and *d*-Trp complexes, respectively, are an average for peptides bound at native sites and peptides bound at apurinic sites.

The degree of quenching of the tryptophan fluorescence observed for the *d*-Trp peptide is greater in the presence of apurinic DNA than native DNA at low degrees of saturation (65% versus 52%). This could be due to a different mode of binding at the apurinic site and is consistent with the ^{19}F NMR data. Any differences between the modes of binding of the *l*-Trp peptide are not reflected in the percent of quenching; the fluorescence is quenched to the same extent with both DNA's (76% versus 79%).

When either of these tripeptides is incubated with plasmid DNA containing apurinic sites, no measurable difference in the rate of cleavage of the DNA backbone is observed. Previous studies comparing the nicking ability of several tripeptides have shown that those containing either tryptophan or tyrosine between two lysines are most active (3,4,5). It has been suggested that the aromatic amino acid is important to both the recognition of and cleavage at apurinic sites. The ^{19}F NMR results conclusively show that each diasteriomer has a distinct mode of binding to depurinated DNA. The fluorine chemical shift for the complexes indicates that the fluorine nuclei reside in different local environments and the differential linebroadening demonstrates that the motional properties of these peptides within or between their binding sites on apurinic DNA are significantly different. However, neither the change in local environment nor the change in mobility affects the rate of cleavage suggesting that

neither the precise positioning of the indole ring nor significant changes in its mobility are crucial to the nicking activity. However, both the ^{19}F NMR parameters and the relative binding affinities should be followed as a function of the level of depurination. This would allow a more precise characterization and separation of the effects due to binding at apurinic versus native sites in DNA.

References

1. **Behmoaras, T., Toulme, J. J. and Helene, C.,** Specific Recognition of Apurinic Sites in DNA by a Tryptophan-containing Peptide, *Proc. Nat. Acad. Sci. USA, 78,* 926-930, (1981).

2. **Lindahl, T.,** DNA Glycosylases, Endonucleases for Apurinic/Apyrimidinic Sites, and Base Excision-Repair, *Progr. Nucleic Acid Res. molec. Biol., 22,* 135-192, (1979).

3. **Behmoaras, T., Toulme, J. J. and Helene, C.,** Reconnaissance it coupure des sites apuriniques dans l'ADN par le tripeptide lysyl-tryptophyl-lysine, *C. R. Acad. Sc. Paris, 293,* 5-8, (1981).

4. **Behmoaras, T., Toulme, J. J. and Helene, C.,** A Tryptophan-containing Peptide Recognizes and Cleaves DNA at Apurinic Sites, *Nature, 292,* 858-859, (1981).

5. **Pierre, J. and Laval, J.,** Specific Nicking of DNA at Apurinic Sites by Peptides Containing Aromatic Residues, *J. Biol. Chem., 256,* 10217-10220, (1981).